UNIVERSITY OF CALIFORNIA
RIVERSIDE

Effects of Crude Oil and Phenanthrene on Cholesterol Biosynthesis and Its Relationship to Developmental Toxicity in Larval Fish

A Dissertation submitted in partial satisfaction
of the requirements for the degree of

Doctor of Philosophy

in

Environmental Toxicology

by

Victoria Lane Brown McGruer

June 2021

Dissertation Committee:

Dr. Daniel Schlenk, Chairperson
Dr. David C. Volz
Dr. Morris Maduro

The Dissertation of Victoria Lane Brown McGruer is approved:

_____

_____

_____

Committee Chairperson

University of California, Riverside

Acknowledgments

I am indebted to my friends, family, and advisors without whom this dissertation would not have been possible. First and foremost, my PhD advisor Dr. Daniel Schenk. Over the past four years, Dr. Schlenk has provided invaluable mentorship and support. His door or "virtual" door has always been open to discuss research and next steps while simultaneously allowing me to develop independence as a scientist. I truly appreciate his time and advice, as well as the research and networking opportunities he has fostered.

I would also like to thank my committee members, Dr. Morris Maduro and Dr. David Volz, for their time, advice, and support in helping me progress through graduate school. Dr. Volz has always been there for one-on-one meetings, and I appreciate him opening his lab to collaborate on this dissertation. Dr. Volz truly cares about mentorship and is always trying to set all students up for success. I also want to thank my qualifying exam committee members Dr. Samantha Ying and Dr. Sachiko Haga-Yamanaka, for their time and research advice. Additionally, thank you to our collaborators at the University of Miami, Dr. Martin Grosell, and his current and former lab members, including Dr. Christina Pasparakis, as well as Dr. Andrew Esbaugh and Dr. Alexis Khursigara at the University of Texas, for their contributions to this work.

Over the past few years, there have been many lab members who have helped advance this dissertation. Dr. Justin Greer and Dr. Jason Magnuson were always available for a "quick question" and were instrumental in getting me through the challenging parts of graduate school. Dr. Marissa Giroux, Dr. Scott Coffin, Dr. Luísa Bertotto, Dr. Nicolette Andrzejczyk, Gary Harraka, and Phil Tanabe have always created

a welcoming lab environment. They helped to train me, answer questions, and were open to talk at any time, without their support and friendship, this work would not have been possible. I would also like to recognize current and former Volz lab members Dr. Subham Dasgupta, Dr. Sara Vliet, Constance Mitchell, Dr. Aalekhya Reddam, Vanessa Cheng, Sarah Avilla-Barnard, and Jenna Wiegand for their contributions to this work as collaborators and support as friends.

Finally, I would like to thank my friends and family for their unwavering support. I have been incredibly fortunate to have made many close friends throughout graduate school. Aalekhya Reddam, Miranda Aiken, and Sophia Parks, I would not have completed this dissertation without you. You have brought me so much happiness over the past four years, thank you! I would especially like to thank my partner, Win, who has supported me through all the highs and lows of the past four years. Together we have found ourselves hiking endlessly in the Box Springs, peering up at the Milky Way on Mt. Whitney, and watching the moonlight reflect on the walls of Yosemite as we climbed into the night. I cherish these memories with you. Finally, I am infinitely grateful for my mom and dad for their constant encouragement, love, and support. I would not have made it here without you. No matter how far apart we are, you have always been there for me and a phone call away. I also want to express my gratitude to my brother, Colin, my stepfather, Martin, and my grandmother, Ilene, for their love and support.

This research was supported by UCR's Graduate Division and the UCR Dissertation Year Program Award. Additional support was provided by a grant from The Gulf of Mexico Research Initiative (Relationship of Effects of Cardiac Outcomes in Fish

for Validation of Ecological Risk II [RECOVER II]; SA-1520). Funding for attendance to numerous conferences was provided by the UCR Graduate Student Association Travel Grant, Society of Environmental Toxicology and Chemistry North America Student Travel Award, and the International Symposium on Pollutant Responses in Marine Organisms Student Travel Award.

Copyright Acknowledgements

The text and figures in Chapter 2, in part or in full, are a reprint of the material as it appears in "*Deepwater Horizon* crude oil exposure alters cholesterol biosynthesis with implications for developmental cardiotoxicity in larval mahi-mahi (*Coryphaena hippurus*)" published in Comparative Biochemistry and Physiology, Part C, Vol. 220, Pages 31-35, June 2019. The co-authors Dr. Christina Pasparakis and Dr. Justin B. Greer, helped in setting up experiments and analyzing data. The co-authors Dr. John D. Stieglitz and Dr. Daniel D. Benetti, helped in setting up experiments. The co-author Dr. Martin Grosell helped supervise this research. The co-author Dr. Daniel Schlenk directed and supervised this research. All authors edited, revised, and approved the final version of the manuscript.

The text and figures in Chapter 3, in part or in full, are a reprint of the material as it appears in "Effects of Phenanthrene Exposure on Cholesterol Homeostasis and Cardiotoxicity in Zebrafish Embryos" published in Environmental Toxicology and Chemistry, Vol. 40, Pages 1586-1595, January 2021. The co-author Philip Tanabe helped in setting up experiments and analyzing data. The co-authors Dr. Sara M.F. Vliet, Dr. Subham Dasgupta, and Dr. David C. Volz helped in method development and analysis procedures. The co-author Le Qian helped in analyzing data. The co-author Dr. Daniel Schlenk directed and supervised this research. All authors edited, revised, and approved the final version of the manuscript.

The text and figures in Chapter 4, in part or in full, are currently under review for publication as "Exposure to *Deepwater Horizon* crude oil increases free cholesterol in larval red drum (*Sciaenops ocellatus*)" in Aquatic Toxicology. This work was submitted for publication on May 21th, 2021.

Dedication

To my parents, Deb Brown and Nick McGruer, for your unconditional support. I love you endlessly.

ABSTRACT OF THE DISSERTATION

Effects of Crude Oil and Phenanthrene on Cholesterol Biosynthesis and Its Relationship to Developmental Toxicity in Larval Fish

by

Victoria Lane Brown McGruer

Doctor of Philosophy, Graduate Program in Environmental Toxicology
University of California, Riverside, June 2021
Dr. Daniel Schlenk, Chairperson

Polycyclic aromatic hydrocarbons (PAHs) are pervasive pollutants globally, and exposure has been linked to developmental toxicity in the early life stages of many species. Oil spill disasters such as *Deepwater Horizon* can result in a large and concentrated release of PAHs directly into aquatic ecosystems. Previous studies have demonstrated that exposure to crude oil or phenanthrene (a reference PAH found in oil) produces an array of gross morphological abnormalities in developing fish embryos, including edema and craniofacial defects. However, our understanding of the molecular mechanisms that lead to these phenotypes is still limited. Recently, studies utilizing transcriptomic analyses in several oil-exposed marine fish species including red drum (*Sciaenops ocellatus*) and mahi-mahi (*Coryphaena hippurus*) found significant changes in the abundance of transcripts involved in cholesterol biosynthesis. Given the vital role of cholesterol in embryonic development, we hypothesized that disruption of these metabolic pathways following exposure to crude oil or phenanthrene alone may contribute to abnormal development of fish embryos. Aim 1 is the first study in any fish

species to investigate the impact of crude oil exposure on cholesterol concentrations in fish embryos. Here we found that exposure to the highest tested High Energy Water Accommodated Fraction (HEWAF) concentration ∑PAH 8.3 μg L^{-1} significantly reduced total cholesterol in mahi-mahi larval homogenates. Aim 2 built upon our initial findings and assessed the role of cholesterol on phenanthrene-induced cardiotoxicity in zebrafish (*Danio rerio*). While free cholesterol concentrations in the larval body were not affected in zebrafish exposed to phenanthrene, treatment with cholesterol prior to phenanthrene exposure significantly mitigated phenanthrene-induced bradycardia. This suggests that cholesterol may play a role in advancing PAH-driven cardiotoxicity. In aim 3, we investigated the effects of crude oil on embryos of the Gulf native species, red drum. Here we found that while expression of several key genes in the synthesis pathway were not affected, red drum larvae displayed significant increases in free cholesterol, detected by whole-mount staining (∑PAH 4.71-16.15 μg L^{-1}). Overall, our findings demonstrate that cholesterol in developing fish embryos can be impacted by crude oil exposure. Future work should investigate the mechanisms underlying changes to cholesterol homeostasis.

Table of Contents

Chapter 1: Introduction 1
1.1 Environmental impacts of petroleum 1
1.2 Polycyclic aromatic hydrocarbon toxicity 2
1.3 Oil- and PAH-induced developmental toxicity 4
1.4 Cardiotoxicity 8
1.5 Transcriptomic predictions 11
1.6 Cholesterol biosynthesis as a potential target 13
1.7 Overview of research aims and hypotheses 17
Chapter 2: Deepwater Horizon crude oil exposure alters cholesterol biosynthesis with implications for developmental cardiotoxicity in larval mahi-mahi (*Coryphaena hippurus*) 20
2.1 Abstract 20
2.2 Introduction 21
2.3 Materials and methods 23
2.4 Results 28
2.5 Discussion 31
2.6 Conclusion 35
Chapter 3: Effects of phenanthrene exposure on cholesterol homeostasis and cardiotoxicity in zebrafish embryos 36
3.1 Abstract 36
3.2 Introduction 37
3.3 Methods 40
3.4 Results 47
3.5 Discussion 57
Chapter 4: Exposure to *Deepwater Horizon* crude oil increases free cholesterol in larval red drum (*Sciaenops ocellatus*) 65
4.1 Abstract 65
4.2 Introduction 65
4.3 Methods 68

4.4 Results 73
4.5 Discussion 79
Chapter 5: Summary and conclusions 84
5.1 Summary 84
5.2 Hypothetical adverse outcome pathway 91
5.3 Concluding remarks 95
References 97
Appendix A – Chapter 2 supplemental information 112
Appendix B – Chapter 3 supplemental information 115
Appendix C – Chapter 4 supplemental information 121

List of Figures

Chapter 2

Figure 2-1: Mahi-mahi survival 30
Figure 2-2: Mahi-mahi total cholesterol 30
Figure 2-3: Mahi-mahi gene expression 31

Chapter 3

Figure 3-1: Zebrafish survival, heart rate, pericardial area 49
Figure 3-2: Zebrafish gene expression 51
Figure 3-3: Zebrafish filipin staining time course 53
Figure 3-4: Effects of cholesterol pretreatment on heart rate 54
Figure 3-5: Effects of cholesterol pretreatment on filipin staining 55
Figure 3-6: Zebrafish yolk area 57

Chapter 4

Figure 4-1: Red drum survival 75
Figure 4-2: Red drum pericardial area 75
Figure 4-3: Red drum gene expression 76
Figure 4-4: Red drum total cholesterol 77
Figure 4-5: Red drum filipin staining 78

Chapter 5

Figure 5-1: Hypothetical adverse outcome pathway 94

Appendix A

Figure A-1: HEWAF composition December 2017 exposures 113
Figure A-2: HEWAF composition January 2018 exposures 114

Appendix B

Figure B-1: Region of interest for phenotypic and filipin measurements in zebrafish 116
Figure B-2: Representative images filipin staining 24-48 hpf 117
Figure B-3: Representative images filipin staining 72 hpf 118
Figure B-4: Representative images filipin staining cholesterol pretreatment 119

Figure B-5: Diagram of cholesterol biosynthesis pathway.....120

Appendix C

Figure C-1: Region of interest for pericardial area measurements in red drum 122
Figure C-2: Region of interest for filipin measurements in red drum 122
Figure C-3: HEWAF composition for red drum exposures.....123

List of Tables

Chapter 1

Table 1-1: Oil effect concentrations - select species 7

Chapter 2

Table 2-1: Mahi-mahi primer sequences for qPCR 28

Appendix A

Table A-1: ∑PAH data and geometric means - mahi exposures 112
Table A-2: Mahi exposures water quality parameters 112

Appendix B

Table B-1: Zebrafish primer sequences for qPCR.....115
Table B-2: Phenanthrene concentrations exposures with embryos 115
Table B-3: Phenanthrene concentrations exposures without embryos 116

Appendix C

Table C-1: Red drum primer sequences for qPCR 121
Table C-2: Red drum exposures water quality parameters..... 124-125

List of Acronyms

DWH	Deepwater Horizon
PAH	Polycyclic aromatic hydrocarbon
∑PAH	Sum concentration of select polycyclic aromatic hydrocarbons
Ppm	Parts per million
Ppb	Parts per billion
LC_{50}	50% lethal concentration
HEWAF	High Energy Water Accommodated Fraction
EC_{50}	Half-maximal effective concentration
IC_{50}	Half-maximal inhibitory concentration
LOEC	Lowest Observed Effect Concentration
EC	Excitation-contraction
AP	Action potential
SR	Sarcoplasmic reticulum
SERCA	SR Ca^{2+} ATPase
NCX	Sodium-calcium exchanger
I_{kr}	Delayed rectifier K^+ channel current
AOP	Adverse outcome pathway
mRNA	Messenger ribonucleic acid
HMG-CoA	3-hydroxy-3-methylglutaryl-coenzyme A
hpf	Hours post-fertilization

I_{CaL}	L-type Ca^{2+} current
MβCD	methyl-β-cyclodextrin
hERG1	voltage-gated potassium channels Kv11.1
qPCR	quantitative polymerase chain reaction or real-time PCR
Fdft1	farnesyl-diphosphate farnesyltransferase 1
UMEH	University of Miami Experimental Hatchery
UV	Ultraviolet
OFS	Oil from the surface
RSMAS	Rosenstiel School of Marine and Atmospheric Science
SREBP	sterol regulatory element-binding protein
SCAP	sterol regulatory element-binding protein cleavage-activating protein
ef-α	elongation factor 1-alpha
ANOVA	Analysis of variance
SEM	Standard error of the mean
HSD	Honest significant difference
SRE	Sterol regulatory element
t-tubules	Transverse tubules
DMSO	Dimethyl sulfoxide
PFA	Paraformaldehyde
PBS	Phosphate-buffered saline
PBST	1X PBS containing 0.1% Tween-20
SD	Standard deviation

miRNA	microRNA
Ppt	Parts per trillion
IACUC	Institutional Animal Care and Use Committee
GC/MS−SIM	Gas chromatography/mass spectrometry−selective ion monitoring
cDNA	Complementary DNA
SQLE	Squalene epoxidase
a.u.	Arbitrary units
WAF	Water accommodated fraction
OMR	Optomotor response
ND	Not detected
ROI	Region of Interest
Phe	Phenanthrene
Atorv	Atorvastatin
HMGCS	3-hydroxy-3-methylglutaryl-CoA synthase
LSS	lanosterol synthase
DHCR24	24-dehydrocholesterol reductase
LDM	Lanosterol 14-demethylase
DHCR7	7-dehydrocholesterol reductase

Chapter 1: Introduction

1.1 Environmental impacts of petroleum

Over the past 50 years, 44 major oil spills (> 420,000 gallons) have affected U.S. waters. (NOAA, 2017). As exploration for oil continues offshore, drilling operations are moving into deep and ultradeep environments, which brings new challenges and risks (Skogdalen and Vinnem, 2012). The 2010 *Deepwater Horizon* (*DWH*) oil spill, to date the largest marine spill in US history, is an example and realization of this risk. Over 87 days, more than 134 million gallons of oil were released into the Gulf of Mexico, covering 400 square miles of seafloor, and oiling more than 1,300 miles of shoreline. Oil was discharged at depth and rose through the water column to produce a slick on the surface of the Gulf that cumulatively covered over 43,300 square miles, approximately the size of the state of Virginia. Shoreline, marsh, pelagic, and benthic habitats were oiled during this time, killing an estimated 2 to 5 trillion larval fish and threatening the many species that live in these regions (Trustees, 2016). Together, impacts to and recovery of Gulf fisheries were of particular concern.

While the damage assessment and initial restoration efforts following the *DWH* oil spill were immediate, restoration, monitoring, and research efforts continue to this day. Global oil demand persists, and inevitably oil pollution from run-off and accidental spills continues. By increasing our understanding of how ecosystems and resources are

impacted by oil pollution, we can better inform risk assessments and disaster responses for future events.

1.2 Polycyclic aromatic hydrocarbon toxicity

Crude oil is comprised of a complex mixture of organic and inorganic compounds, including aliphatic hydrocarbons, polycyclic aromatic hydrocarbons (PAHs), and heterocyclics, and other trace components (Bayona et al., 2015). Thousands of compounds have been identified in crude oils, and oil from distinct sources can vary significantly in composition (Wang et al., 2006). However, toxicologically, PAHs are the most studied fraction of crude oil, and understanding PAH-induced toxicity has been a primary focus of understanding crude oil toxicity for many years (Marty et al., 1997). Oil released from the *DWH* Macondo well contained 3.9% PAHs by weight (Reddy et al., 2012), and a field assessment following the spill found ∑PAHs (sum of 43 individual PAHs) ranged from < 0.01 to 77 µg/L in water samples taken at 1m and 10m depth. (Bejarano et al., 2013).

Studies over the past 20+ years have demonstrated that crude oil toxicity in fish is associated with exposure to water-soluble PAHs. Pacific herring embryos exposed to dissolved PAHs with proportionally low concentrations of mononuclear aromatics and alkanes displayed abnormal development (Carls et al., 1999). Additionally, zebrafish (*Danio rerio*) embryo exposure to individual 2-4 ring non-alkylated PAH compounds abundant in crude oil revealed that the three-ring compounds dibenzothiophene or

phenanthrene produce a phenotype characteristic of embryos exposed to crude oil. Mixture studies further revealed that toxicity increases specifically with the percentage of tricyclic compounds, implicating phenanthrene as the driver of oil-induced developmental toxicity in fish (Incardona et al., 2004).

Oil composition can change in the environment through time via weathering processes such as evaporation, dissolution, biodegradation, and photooxidation (Wang et al., 2006). This changing chemical profile can likewise alter oil-induced toxicity. While some spills occur at the surface, oil from the Macondo well was released at a depth of approximately 1500 m. As oil migrated up through the water column, water-soluble hydrocarbons dissolved into the water column, and further weathering occurred at the surface (Reddy et al., 2012). However, the effects of weathering on toxicity have been shown to vary between species. Mahi-mahi (*Coryphaena hippurus*) and Pacific herring (*Clupea pallasi*) are much more sensitive to oil that has undergone weathering processes compared to un-weathered oil (Carls et al., 1999; Esbaugh et al., 2016). By contrast, red drum (*Sciaenops ocellatus*) were similarly sensitive to weathered and un-weathered oil (Khursigara et al., 2017). Taken together, exploring the toxicity of both the entire crude oil mixture, as well as individual components of oil is essential to understanding how organisms are affected by exposure.

1.3 Oil- and PAH-induced developmental toxicity

Research following significant oil spills before *DWH* provided a general understanding of species and stage sensitivity. The 1989 Exxon Valdez spill prompted traditional toxicity testing on adult and juvenile fish. Results demonstrated that pelagic species were the most sensitive, with LC_{50} values in the 1-3 mg L^{-1} (ppm) range. These were relatively high concentrations compared with environmental observations (Reviewed by Incardona and Scholz, 2018). However, subsequent field collections of early life stage fish such as Pacific herring (*Clupea pallasi*) larvae revealed a high incidence of morphological abnormalities associated with oiled shorelines (Hose et al., 1996). Follow-up laboratory experiments were then able to reproduce this phenotype by exposing herring embryos to oiled gravel columns with environmentally relevant effects concentrations in the ∑PAHs 0.7-7.6 µg L^{-1} (ppb) range (Carls et al., 1999). Since then, a common toxicity phenotype has been described in fish embryos across many species exposed to crude oil. This phenotype is characterized by pericardial and yolk sac edema, craniofacial defects, reductions in heart rate (bradycardia), and cardiac arrhythmias (Incardona and Scholz, 2018).

Developing embryos are especially vulnerable to toxicant exposure because they are rapidly forming organ systems that define function for the remainder of the organism's life. While post-metamorphosis fish (juveniles and adults) are susceptible to oil exposure, they have additional lines of defense. Scales provide dermal protection, and thus exposure to oil constituents is primarily via the gills or ingestion. Once PAHs reach the

bloodstream, they can be metabolically detoxified in the fully developed liver. By comparison, fish embryos are much smaller in size and thus able to rapidly accumulate relatively high tissue PAH concentrations and have a reduced metabolic capacity for detoxification (Incardona and Scholz, 2018).

Marine embryos are buoyant, with species- and population-specific distribution within the water column (Sundby and Kristiansen, 2015). A large portion of *DWH* crude oil rose to the surface waters, producing surface slicks (Ryerson et al., 2012). Localization in the upper water column increases the risk of exposure to oil slicks (Incardona et al., 2014). Exposure to large oil droplets and slicks may be lethal to fish embryos through smothering and hypoxia (Carls et al., 2008). However, the route of toxicity induced by smaller particles present in dispersed oil appears to depend on the composition of the embryonic chorion. For example, oil droplets were found to attach to Atlantic haddock (*Melanogrammus aeglefinus*) embryos leading to an increased PAH body burden relative to Atlantic cod (*Gadus morhua*) to which oil particles did not adhere to the chorion (Sørensen et al., 2017). However, more work is needed to understand how oil fouling of the chorion varies across species. Oil has not been observed to bind with the chorion of zebrafish, red drum, or mahi-mahi (Carls et al., 2008; Morris et al., 2018). In the absence of direct oil particle interaction, embryos are susceptible to the dissolved fraction of oil. However, particulate oil may act as a reservoir for the continuous supply of dissolved PAHs (Carls et al., 2008).

ΣPAH (sum of 50 individual PAHs) concentrations that cause acute embryo lethality vary by species, but in mahi-mahi and red drum the estimated 50% lethal concentration (LC_{50}) values range from 8.8 to 45.8 μg L^{-1} depending on the oil type (summarized in Table 1-1). However, sublethal embryonic oil exposure can lead to delayed mortality in the larval and juvenile stages (Heintz et al., 2000) or cause malformations that can impair function in adults which are otherwise visually unaffected (Hicken et al., 2011; Incardona et al., 2015; Mager et al., 2014).

Field collection of live embryos following the *DWH* oil spill was not possible. However, laboratory studies assessed the developmental sensitivity of fish native to the Gulf of Mexico to oil collected from the *DWH* source well (source oil) and skimmed from the surface (slick oil). Exposure solutions were generated by mixing oil into water, producing a High Energy Water Accommodated Fraction (HEWAF). ∑PAHs (sum of 50 individual PAHs) concentrations were determined to calculate effect concentrations including half-maximal effective concentrations (EC_{50}), half-maximal inhibitory concentrations (IC_{50}), and LC_{50} values for bluefin tuna (*Thunnus thynnus*), yellowfin tuna (*Thunnus albacares*), zebrafish, amberjack (*Seriola dumerili*), mahi-mahi, and red drum. These effects are summarized in table 1-1. While these effect values are not directly comparable due to differences in testing conditions and developmental stage, this summary gives a relative estimate of ∑PAH concentrations that produce relevant biological effects.

Table 1-1 LC_{50}, EC_{50}, IC_{50}, and Lowest Observed Effect Concentration (LOEC) values ∑PAH (μg L^{-1}) for select species at varying stages (hours post-fertilization (hpf)) exposed to weathered (slick) oil HEWAF, artificially weathered oil HEWAF, or un-weathered (source) oil HEWAF.

Species (life stage)	**Oil type**	**LC_{50}**	**EC_{50} (Pericardial edema)**	**IC_{50} (Heart Rate)**	**LOEC (Atrial contract-ility)**	**EC_{50} (Cardiac Output)**	**Reference**
Bluefin tuna (hatching stage)	Artificially weathered HEWAF		0.9	8.5			(Incardona et al., 2014)
Yellowfin tuna (hatching stage)	Slick oil HEWAF		2.5	7.5			(Incardona et al., 2014)
Zebrafish (48 hpf)	Slick oil HEWAF		LOEC = 34				(Incardona et al., 2013)
Mahi-mahi (Edema = 48 hpf, Lethality = 96 hpf)	Source oil HEWAF	45.8	7.3		15.2		(Esbaugh et al., 2016)
	Slick oil HEWAF	8.8	>5.1		2.6		(Esbaugh et al., 2016)
Red drum (48 hpf)	Source oil HEWAF	21.3					(Khursigara et al., 2017)
	Slick oil HEWAF	19.1	2.4			2.2	(Khursigara et al., 2017)

1.4 Cardiotoxicity

The embryonic heart is one of the first functional organs in the developing vertebrate embryo, and the early stages of heart development are similar across fish species (Glickman and Yelon, 2002; Perrichon et al., 2019). Exposure to crude oil or the tricyclic PAH phenanthrene impairs heart function resulting in pericardial edema, bradycardia, and cardiac arrhythmias – abnormalities indicative of cardiotoxicity. Zebrafish embryos exposed to relatively high doses of crude oil or phenanthrene produced a phenotype indistinguishable from cardiac loss-of-function mutants. Therefore, craniofacial and spinal defects that arise in embryos exposed to crude oil or phenanthrene alone have been hypothesized to be secondary to cardiac malfunction and loss of circulation (Incardona et al., 2004). However, some outcomes of crude oil exposure appear not to be secondary to abnormal cardiac development (reviewed by Grosell and Pasparakis, 2021).

Recent studies have further explored the mechanisms underlying crude oil-induced cardiotoxicity. Brette et al. (2014 and 2017) demonstrated that crude oil or phenanthrene alone alters the processes that link electrical excitation to the contraction of the cardiomyocyte, termed excitation-contraction (EC) coupling in isolated tuna and mackerel cardiomyocytes. Cardiac processes in tuna cardiomyocytes are similar to mammalian systems. Under normal conditions, EC coupling in teleost cardiomyocytes is stimulated by action potentials (APs) generated by pacemaker cells (Stoyek et al., 2015) and further controlled by autonomic and hormonal modulation (Farrell and Smith, 2017). These APs stimulate the opening of L-type voltage-gated calcium channels, allowing an

influx of Ca^{2+} across the cell membrane. Ca^{2+} then binds to type-2 ryanodine receptors, located in the adjacent sarcoplasmic reticulum (SR) membrane, subsequently stimulating the release of SR calcium stores. This rise in cytoplasmic Ca^{2+} activates the myofilaments and triggers heart contraction. Following contraction, this process needs to be rapidly reset. Return of Ca^{2+} stores to the SR occurs through the SR Ca^{2+} ATPase (SERCA), and Ca^{2+} is eliminated from the cell through the sodium-calcium exchanger (NCX). The declining concentrations of cytosolic Ca^{2+} allow for dissociation of Ca^{2+} from the myofilaments and muscle relaxation. Additionally, repolarization of the cell relies on voltage-gated sodium (Na^{+}), Ca^{2+}, and potassium (K^{+}) channels. The coordination of these processes returns the cell to a resting state and ready for the next action potential (Bers, 2002).

Exposure to crude oil or phenanthrene has been shown to disrupt EC-coupling in several fish species (Abramochkin et al., 2021; Ainerua et al., 2020; Brette et al., 2017, 2014; Heuer et al., 2019). Initially, Brette et al. (2014) exposed bluefin and yellowfin tuna cardiomyocytes to several types of *DWH* crude oil of different stages of weathering. Following up on this work, Brette et al. (2017) conducted a very similar experiment using individual PAHs. In each of these studies, it was observed that crude oil or phenanthrene alone simultaneously decreased the Ca^{2+} transient amplitude and increased the duration of the action potential. Using pharmacological methods to determine the mechanisms of these effects, they found that the prolongation of the action potential occurred by inhibiting K^{+} efflux from the cell. K^{+} efflux occurs primarily through the delayed rectifier K^{+} channel current (I_{kr}), which is key to cell repolarization (Jeevaratnam et al., 2018).

Next, they demonstrated that Ca^{2+} flux into the cell was reduced through SERCA and that this likely reduced Ca^{2+} stores from the SR, further impairing contractility (Brette et al., 2017, 2014). More recently, mahi-mahi cardiomyocytes exposed to crude oil displayed similar increases in action potential duration and I_{Kr} reduction. These alterations were then linked to a measured reduction in sarcomere shortening, an index of cardiomyocyte contractility (Heuer et al., 2019). Reduced contractility likely underlies impairment of cardiac function in oil exposed adult mahi-mahi (Nelson et al., 2016) as well as in life stages ranging from the developing embryo to adult in several other species (Incardona et al., 2015, 2014; Khursigara et al., 2017) following oil exposure.

Studies in multiple species relate embryonic PAH exposure to changes in heart morphology and/or reduced swimming performance. In zebrafish, sublethal exposure to low PAH concentrations for 48 h following fertilization resulted in reduced swimming performance and significant changes to ventricular shape following ten months of growth in clean water (Hicken et al., 2011). Similarly, herring and pink salmon embryos demonstrated these same impacts after 7-8 months of growth in clean water following exposure (Incardona et al., 2015). Mahi-mahi exposed as embryos until 48 hours post-fertilization (hpf) also demonstrate reduced critical swimming velocities after a shorter (25 day) recovery, although ventricular shape was not assessed (Mager et al., 2014). These results highlight the long-term and likely permanent effects of embryonic oil exposure. Swimming performance is generally thought to play a role in ecological success because of its role in feeding and other essential functions. Ecosystem modeling has shown that feeding and respiratory function are drivers of population growth (Megrey

et al., 2007). Therefore, reduced swimming performance may have higher-level consequences on the population.

While further studies are needed to substantiate the link between cardiac impacts and population-level effects, we also require a greater understanding of the molecular interactions between tricyclic PAHs and biomolecules that produce these downstream effects. In ecotoxicology, an Adverse Outcome Pathway (AOP) is a conceptual framework that links existing knowledge about a direct molecular interaction (molecular initiating event) to an adverse outcome at higher levels of biological organization (Ankley et al., 2010). Ultimately, by understanding the effects of a chemical on the molecular, cellular, and organismal levels, we can develop predictive power and infer how populations, communities, and ecosystems may be impacted (Schirmer et al., 2010). For PAH-induced developmental toxicity, the mechanisms underlying ion channel disruption and subsequent altered cardiac morphology are unclear. Understanding this interaction would directly tie exposure to higher-level impacts needed to understand risk and contribute to understanding species-specific vulnerability and thus ecological risks associated with exposure to oil or PAHs from other sources.

1.5 Transcriptomic predictions

Over the past few years, several studies have employed transcriptomic analyses to assess the messenger (m)RNA expression profile of fish embryos exposed to crude oil. Transcriptomic analyses allow for a broad look at the organismal response to toxicant

exposure which can reduce bias when hypothesizing about potential toxicity mechanisms. When studies assessing oil toxicity were compared, cholesterol biosynthesis was consistently one of the top impacted pathways. Cholesterol related pathways were predicted to be enhanced in red drum (Xu et al., 2017), mahi-mahi (Xu et al., 2017), Atlantic haddock (Sørhus et al., 2017), and sheepshead minnow (Jones et al., 2020) embryos and larvae exposed to crude oil. While it is difficult to compare between species due to developmental differences, cholesterol biosynthesis was downregulated in Atlantic cod (Olsvik et al., 2012) and trended toward inhibition in Gulf killifish (Jones et al., 2020) embryos and larvae. In adult female fathead minnow (*Pimephales promelas*) exposed to phenanthrene alone, cholesterol metabolism was the only pathway disrupted in the liver at every dose and timepoint tested (Loughery et al., 2018). Additionally, cholesterol biosynthesis was found to be significantly suppressed in the livers of adult southern flounder (*Paralichthys lethostigma*) chronically exposed to *DWH* oiled sediments (Rodgers et al., 2021). Together these studies indicate that the PAH component of oil may be responsible for disruption of the cholesterol pathway and that this dysregulation may persist across life stages.

Due to the critical role cholesterol plays in early embryo development, including cardiac development, and observing this pattern of cholesterol dysregulation across species, we identified cholesterol dysregulation as a potential mechanism underlying oil-induced developmental toxicity. In subsequent chapters, we investigate whether these transcriptional predictions translate into changes to cholesterol concentrations in developing embryos. We then ask if cholesterol dysregulation could underlie the

cardiotoxic changes we see in developing fish embryos through disruption to ion channel function or other key developmental pathways.

1.6 Cholesterol biosynthesis as a potential target

Cholesterol is a critical component of eukaryotic cells, and under normal conditions cholesterol levels and synthesis are under significant regulation. Comprising 10-45 mol% of total lipids in the plasma membrane, cholesterol is a key regulator of membrane thickness, fluidity, and permeability (Yeagle, 1985). Eukaryotic membranes can display immense differences in cholesterol content between distinct cell types and intracellular organelles. Variation in cholesterol content between discrete membranes is thought to have evolved to assist in the performance of different functions (Subczynski et al., 2017). Cholesterol-enriched membranes coordinate many cellular processes, including signal transduction (Incardona and Eaton, 2000), recycling of membrane proteins, and ion channel function (Balijepalli et al., 2007). Cholesterol is also a precursor for forming other biologically essential molecules, including steroid hormones (Payne and Hales, 2004). Therefore, the dysregulation of cholesterol, resulting in either an abnormal increase or decrease in cholesterol concentration, can disrupt biological function and has been implicated in the generation of disease in both fish and mammals (Barros et al., 2018; Law et al., 2003; Maerz et al., 2019).

Zebrafish embryos have been used as a model organism for studying cholesterol-related diseases, and the results have demonstrated that appropriate regulation of cholesterol is essential for fish embryo development during organogenesis (Barros et al., 2018; Maerz

et al., 2019). Teleost fish are lecithotrophic, relying entirely on maternal yolk deposits throughout embryo development until exogenous feeding commences. Though yolk composition varies between species (Tocher and Sargent, 1984), cholesterol is the most abundant lipid in the zebrafish yolk, making up 40% of total lipids (Fraher et al., 2016). However, fish embryos rely on both cholesterol transported from the maternally deposited yolk as well as endogenous cholesterol synthesis (Signore et al., 2016).

Several studies have investigated the effects of drugs that inhibit endogenous cholesterol production, giving insight into the importance of cholesterol to embryo development (Campos et al., 2016; Maerz et al., 2019; Thorpe et al., 2004). Cholesterol-lowering statins are a class of drug which inhibit 3-hydroxy-3-methylglutaryl-coenzyme A (HMG-CoA) reductase, an enzyme that catalyzes the rate-limiting step in the cholesterol biosynthetic pathway (Brown and Goldstein, 2009). Exposing zebrafish embryos following fertilization until 48 hpf to Atorvastatin (Maerz et al., 2019) or Simvastatin (Barros et al., 2018) resulted in a cardiotoxicity phenotype, presenting as heart looping defects, pericardial edema, and bradycardia. Statin-exposed embryos also developed body curvature (Barros et al., 2018; Maerz et al., 2019) and smaller heads and eyes (Maerz et al., 2019). Statin-induced body curvature, bradycardia, and pericardial edema were all partially rescued by co-exposure with water-soluble cholesterol, indicating that cholesterol reduction was at least partially responsible for these effects (Maerz et al., 2019). Interestingly, this phenotype is very similar to what is observed in fish embryos exposed to crude oil, though many toxicants can produce these malformations.

If cholesterol homeostasis is disrupted in fish exposed to crude oil or phenanthrene, several mechanisms could result in maldevelopment. The first is through the disruption of signaling pathways, including hedgehog signaling. Hedgehog signaling is involved in embryo development by regulating patterning and cell proliferation. Hedgehog proteins require cholesterol modifications for their activity (Blassberg and Jacob, 2017), and reduction of cellular sterols has been correlated with reduced hedgehog signaling (Cooper et al., 2003). Atorvastatin treatment has been shown to reduce hedgehog signaling resulting in heart malformations in zebrafish embryos (Maerz et al., 2019).

Besides impacting cardiac morphogenesis through cholesterol-dependent signaling pathways, cholesterol dysregulation could also impair ion channel function in the heart more directly, subsequently causing downstream developmental effects. Extensive research demonstrates the influence of cholesterol on ion-channel function either by interacting with ion channel subunits directly (reviewed by Levitan et al., 2014) or indirectly by altering the fluidity of the surrounding membrane (reviewed by Levitan et al., 2010). As discussed previously, studies examining fish cardiomyocytes identified K^+ efflux from the cell through the delayed rectifier K^+ channel current (I_{kr}) and reduced extracellular Ca^{2+} influx via the L-type Ca^{2+} current (I_{CaL}) as targets of oil or phenanthrene exposure.

Several studies have evaluated the effects of membrane cholesterol levels on I_{CaL}. However, the I_{CaL} response depends on the cell type. One of the first studies to consider these effects looked at rabbit portal vein myocytes, noting that dietary

hypercholesterolemia increased I_{CaL} in isolated myocytes. These findings agree with a study demonstrating that cholesterol extraction by methyl-β-cyclodextrin (MβCD) subsequently reduced I_{CaL} in mice skeletal muscle cells (Pouvreau et al., 2004). Interestingly, the opposite effect was found with cholesterol addition having an inhibitory effect in conduit coronary arteries from male miniature swine (Bowles et al., 2004). In swine, I_{CaL} suppression in the coronary arteries was reversed by MβCD-induced cholesterol depletion, indicating this effect was due to elevated cholesterol in the membrane. When researchers conducted the same test on myocytes isolated from the arterioles of the same pigs, however, cholesterol had no effect. Together these studies indicate that the effect of cholesterol on L-type Ca^{2+} channels is highly organism and tissue-dependent.

I_{kr} is produced in humans by the voltage-gated potassium channels Kv11.1 (hERG1) (Balijepalli et al., 2007), and ERG channels are conserved in function across vertebrates (Langheinrich et al., 2003). The interaction of Kv1.1 with cholesterol is less studied, but it has been shown that Kv11.1 channels in canine ventricular myocytes and HEK293 cells localize to cholesterol-enriched regions of the membrane. Membrane cholesterol depletion in these cells by MβCD accelerated the deactivation rate of I_{Kr}, with the opposite effect observed with cholesterol addition (Balijepalli et al., 2007). However, the pathological significance of Kv11.1 regulation by cholesterol has not been shown (Chun et al., 2013).

Under specific conditions and cell types, changes to cholesterol levels in the cell membrane can influence I_{Cal} and I_{Kr}. Additionally, many other ion channels important to heart function have been shown to be affected by changes in cholesterol levels, either by changing membrane properties or directly interacting with the channel (Levitan et al., 2014, 2010). The effect of membrane cholesterol levels on ion channels is difficult to predict. Channels in the same subfamily can show variable responses to changes in membrane cholesterol (Levitan et al., 2010). Given this variability, differences in channel response to cholesterol between mammals and fish are certainly possible. Each heartbeat requires a coordinated response by many ion channels in the heart, which potentially have different sensitivities to changes in membrane cholesterol. Heart form and function progress together. Disruption of atrial contraction alone has been shown to disrupt subsequent morphogenesis (Singleman and Holtzman, 2012). Though speculative, ion channel dysfunction is an interesting and potentially consequential effect of cholesterol dysregulation.

1.7 Overview of research aims and hypotheses

This research aims to improve our understanding of the mechanisms underlying crude oil and PAH-induced developmental toxicity in fish. As discussed in the sections above, transcriptional analyses have consistently found disruption to cholesterol biosynthesis to be one of the top impacted pathways in early life stage fish exposed to crude oil. The following chapters investigate whether transcriptome-based predictions of cholesterol disruption translate into disruption to cholesterol levels in crude oil or phenanthrene

exposed early life stage fish. Additionally, we seek to understand the biological consequences of altered cholesterol homeostasis on cardiac morphogenesis and function. By describing these processes, we hope to improve our understanding of the impacts of oil and PAHs on subcellular, cellular, and organismal levels of biological organization. Through extrapolation, our knowledge of these processes can contribute to the foundation for which population and ecosystem-wide assessments are made before or following a pollution event. The scope and hypotheses assessed within each chapter are described below.

Within chapter 2, we examine the impacts of environmentally relevant concentrations of *DWH* crude oil on cholesterol levels in mahi-mahi larvae. Mahi-mahi are native to the gulf, and previous studies have predicted changes to the cholesterol biosynthetic pathway in mahi at 96 hpf (Xu et al., 2016). This study links these previously predicted changes to alterations of key genes in the pathway via real-time PCR (qPCR) and total cholesterol levels in larval homogenates.

Chapter 3 builds on our findings of cholesterol disruption in chapter 2 in the model organism, zebrafish. In this study, we expose zebrafish embryos to the model tricyclic PAH, phenanthrene, and assess transcriptional changes within the cholesterol synthesis pathway, as well as optimize a whole-mount stain for free cholesterol to determine the concentration and distribution of free cholesterol within the embryo. Finally, we assess the relevance of cholesterol to phenanthrene-induced bradycardia and ask whether the changes we see could be due to perturbations in yolk utilization.

Chapter 4 asks whether the results gained from our zebrafish study in chapter 3 are relevant to the early development of the Gulf native species red drum. In this experiment, 72 hpf red drum embryos were exposed to oil collected from the *DWH* surface slick. Transcriptional responses in the cholesterol synthesis pathway were assessed, and morphology was quantified as a phenotypic anchor. Whole-mount staining of cholesterol optimized in chapter 2 was employed to assess free cholesterol, and total cholesterol was again determined in whole-larval homogenates. Through this work, we can make interspecies comparisons to the mahi-mahi embryos investigated in chapter 1.

Overall, our findings address open questions surrounding the relevance of cholesterol biosynthesis to oil-induced developmental toxicity and open avenues for future research investigating mechanisms underlying crude oil toxicity.

Chapter 2: Deepwater Horizon crude oil exposure alters cholesterol biosynthesis with implications for developmental cardiotoxicity in larval mahi-mahi (*Coryphaena hippurus*)

2.1 Abstract

During the spring and summer of 2010, the *Deepwater Horizon* (*DWH*) oil well released over three million barrels of crude oil into the Gulf of Mexico. As the oil dispersed it contaminated ecosystems that support numerous Gulf species including mahi-mahi (*Coryphaena hippurus*). The timing of the spill, and the location of the surface slick, coincided with the spawning of many species in the region, raising concerns over embryonic and larval exposure. Numerous abnormalities due to crude oil exposure have been documented in fish early life stages, including cardiotoxicity; however, knowledge of the molecular mechanisms that cause these phenotypes is still limited. Several transcriptomic studies have presented cholesterol biosynthesis as one of the top enriched pathways following PAH exposure. In this study, we exposed mahi-mahi embryos to DWH oil collected from the surface slick. At exposures ranging from ∑PAH 1.69 μg/L to ∑PAH 5.99 μg/L, the resulting larvae demonstrated significant increases in farnesyl-diphosphate farnesyltransferase 1 (*fdft1*) and an upward trend in 3-hydroxy-3-methylglutaryl-coenzyme A reductase (*hmgcr*) expression, genes that encode key enzymes in the cholesterol biosynthetic pathway. In addition to the increased expression of genes in the cholesterol biosynthetic pathway, a significant decrease in total cholesterol was observed in larval homogenates at ∑PAH 8.3 μg/L. These data confirm

earlier transcriptomic studies and show that oil may diminish cholesterol and adversely impact numerous cellular functions due to altered membrane stability.

2.2 Introduction

The *Deepwater Horizon (DWH)* spill in 2010 was the largest in US history, releasing 3.19 million barrels over the course of 87 days into the Gulf of Mexico (Crone and Tolstoy, 2010; Trustees, 2016). Oil was discharged at depth and rose through the water column to produce a slick on the surface of the Gulf, covering 15,300 mile^2 at its maximum (Trustees, 2016). At the surface, low molecular weight hydrocarbons are removed through evaporative processes, leaving a greater proportion of higher molecular weight compounds, including tricyclic PAHs such as phenanthrenes, which have been shown to increase toxicity (Carls and Meador, 2009; Esbaugh et al., 2016; Incardona et al., 2004). The *DWH* surface slick overlapped regionally and temporally with the spawning of many pelagic fish, including mahi-mahi raising concern that the 2010 spawn was impacted by slick oil exposure during the vulnerable embryonic and larval developmental stages (Gibbs and Collette, 1959; Palko et al., 1982; Rooker et al., 2012). A field assessment following the *DWH* spill analyzed water samples taken at 1m and 10m depths for ∑PAHs (sum of 43 individual PAHs) and found that concentrations ranged from <0.01 to 77 μg/L (Bejarano et al., 2013). Mahi-mahi embryos remain in the upper regions of the water column throughout development and were likely exposed to ∑PAH concentrations within the above range (Pasparakis et al., 2017).

Many fish species are sensitive to oil exposure during early life stages, and the developing heart is particularly vulnerable (Incardona et al., 2011; Jung et al., 2013). Cardiotoxic phenotypes include arrhythmia, bradycardia, pericardial edema, and reduced cardiac output, which have been correlated with reduced swimming performance in later life (Incardona et al., 2014, 2005, 2004; Jung et al., 2013; Mager et al., 2014; Pasparakis et al., 2016). Previous studies investigating the molecular mechanisms that cause these phenotypes have demonstrated that crude oil disrupts excitation-contraction (EC) coupling pathways in cardiomyocytes (Brette et al., 2014). More recently, work by Brette et al. (2017) established that signal transduction in phenanthrene exposed cardiomyocytes is impaired due to obstruction of ion flux.

To examine the molecular changes that occur following PAH exposure, several studies have employed transcriptomic approaches. Transcriptomics has allowed for the prediction of pathway enhancement through quantification of transcript expression, providing valuable, unbiased predictions for the development of future experimental hypotheses. Recently, several studies have conducted transcriptomic and subsequent pathway analyses on oil exposed mahi-mahi (Xu et al. 2017), red drum (Xu et al. 2017), Atlantic haddock (Sørhus et al., 2017), and phenanthrene exposed fathead minnows (Loughery et al., 2018). Each of these studies identified the cholesterol biosynthetic pathway as one of the top enriched processes.

Cholesterol is essential to maintaining membrane fluidity in all eukaryotic cells and is especially critical for upholding the structural integrity of cell membranes, including

those of cardiomyocytes (Zhu et al., 2016). In this study, we used oil exposed mahi-mahi larvae to identify changes in the cholesterol biosynthetic pathway which may contribute to known cardiotoxic phenotypes caused by *DWH* crude oil. Using qPCR we targeted genes involved in endogenous cholesterol biosynthesis, corroborated past RNA sequencing work, and propose a potential mechanism by which crude oil may induce cardiotoxicity that could apply across species.

2.3 Materials and methods

2.3.1 Experimental animals

The mahi-mahi broodstock used in this experiment were caught off the coast of Miami, FL using hook and line angling techniques and subsequently transferred to the University of Miami Experimental Hatchery (UMEH). Broodstock were acclimated in 80 m^3 fiberglass maturation tanks equipped with recirculating aquaculture systems for control of water quality and temperature and maintained in captivity for approximately 10 weeks. This is a relatively short time span in terms of holding duration, and egg quality and larval performance of captive mahi held for this duration have previously been examined with detailed results available in Kloeblen et al. (2018). Additional details on capture, transport, transfer durations, and spawning of mahi-mahi in captivity can be found in Stieglitz et al. (2017).

All embryos used in this experiment were collected using standard UMEH methods (Stieglitz et al., 2017). A prophylactic formalin treatment (100 ppm for 1 h) was

administered to the embryos, followed by a 0.5 h rinse using filtered, UV-sterilized seawater with a minimum of 300% water volume in the treatment vessel. Fertilization rate and embryo quality from each spawn was assessed microscopically. Spawns with a low fertilization rate (< 85%) or frequent developmental abnormalities (> 5%) were not used.

2.3.2 Preparation of water accommodated fractions

Naturally weathered oil from the surface (OFS) was used to prepare all HEWAFs (high-energy water-accommodated fractions) for this experiment. OFS was collected from Gulf of Mexico surface waters by British Petroleum skimming operations for testing purposes and was transferred under chain of custody to the University of Miami (sample ID: OFS-20100719-Juniper-001 A0087M). HEWAFs were prepared on the day of use with a loading rate of 1 g of oil per 1 L of 1 μm filtered UV-sterilized seawater. The mixture was then blended at low speed in a Waring CB15 blender for 30 s and immediately transferred to a glass separatory funnel and left to settle for 1 h. The lower 90% of the fluid was then drained, designated as 100% HEWAF, and diluted to nominal concentrations of 0.5%, 1%, 2% HEWAF with UV-sterilized seawater.

2.3.3 Embryonic exposures

Embryos were transported from UMEH to the University of Miami Rosenstiel School of Marine and Atmospheric Science (RSMAS) and transferred at around 3–6 h post-fertilization (hpf) to 1 L glass beakers containing UV-sterilized seawater for controls or

either 0.5%, 1%, or 2% HEWAF dilutions for treatment exposures with approximately 30 embryos per beaker. Exposures took place in an environmental chamber with temperature and light control (photoperiod: 12 L: 12 D; temperature: 25 °C). Temperature, pH, dissolved oxygen, salinity and ammonia were monitored daily. Temperature and DO were measured using a ProODO handheld optical DO probe and meter (YSI, Inc., Yellow Springs, OH) and pH was measured using a pH meter (Hach, Loveland, CO) fitted with a combination glass electrode. The pH and DO probes were calibrated daily. Salinity was measured using a refractometer, and total ammonia was determined using a micro-modified colorimetric assay (Ivančič and Degobbis, 1984). At 96 hpf, larvae from each replicate beaker were collected, snap-frozen in liquid nitrogen, and stored at −80 °C for later analysis. Samples were immediately shipped on dry ice to the University of California, Riverside.

2.3.4 Water chemistry analysis

Water samples for total sum-PAH (∑PAH) analysis were collected immediately before and immediately after the 96 h exposure period and are reported as the geometric mean of these values to account for the depletion of PAHs over time. Samples were collected in 250 mL amber bottles, stored at 4 °C, and shipped overnight on ice to ALS environmental (Kelso, WA) for analysis by gas chromatography/mass spectrometry-selective ion monitoring (GC/MS-SIM; based on EPA method 8270D). Reported ∑PAH values represent the sum of 50 PAH analytes selected by the EPA based on individual

toxicity and concentration. A summary of water quality parameters and ∑PAH concentrations are provided in Appendix A (Tables A1 and A2).

2.3.5 Total cholesterol quantification

Total cholesterol was determined in whole fish homogenates using the "Total Cholesterol Assay Kit (Colorimetric)" from Cell Biolabs, Inc. (San Diego, CA) following the manufacturer's "tissue lysates" protocol. Three biological replicates were analyzed per treatment. The samples were first homogenized with a Kontes Pellet Pestle Cordless Motor (Sigma-Aldrich, St. Louis, Missouri) in 200 µL of a chloroform:isopropanol:Triton x-100 (7:11:0.1) mixture. Standard curves were then prepared according to the manufacturer's protocol and used to calculate total cholesterol (µM) in each sample. Total cholesterol was subsequently normalized to the protein concentration (µg mL^{-1}) in each sample, determined using a Pierce™ BCA Protein Assay Kit (Thermo Scientific, Rockford, IL).

2.3.6 RNA isolation and Real-Time PCR (qPCR)

To describe the relative expression of genes in the cholesterol biosynthetic pathway either four or five biological replicates, each replicate consisting of approximately 10 embryos, were collected per treatment for qPCR analysis. Total RNA was extracted using the RNeasy Mini Kit from Qiagen (Valencia, CA). For each sample, RNA quality and quantity were determined using a Nanodrop (model ND-1000) and samples were stored at −80 °C until further processing. cDNA synthesis was conducted with the Promega

Reverse Transcription System kit (Madison, WI) using 1 μg of RNA following the manufacturer's protocol. cDNA was stored at −20 °C until qPCR was performed.

qPCR reactions were carried out using SsoAdvanced™ Universal SYBR® Green Supermix (Bio-Rad, Hercules, CA) on the BioRad CFX Connect instrument (Hercules, CA). Thermocycling conditions used for qPCR analysis of all genes were as follows: 95 °C for 5 min, followed by 40 cycles of 95 °C for 10 s and 55 °C for 30 s. Three technical replicates were performed for each biological replicate. Following amplification, qPCR products were separated on a 1.2% agarose gel to confirm product specificity. Data were normalized using elongation factor 1-alpha (ef-α) (Diamante et al. 2017), and mRNA levels were determined according to the $2^{-\Delta\Delta CT}$ method (Livak and Schmittgen, 2001).

Primers for ef-α were chosen based on sequences previously described in Xu et al. (2016). Primers for 3-hydroxy-3-methylglutaryl-coenzyme A reductase (*hmgcr*), farnesyl-diphosphate farnesyltransferase 1 (*fdft1*), and the sterol regulatory element-binding protein (SREBP) cleavage-activating protein (*scap*) were designed and target verified by NCBI Primer-BLAST. All primers were tested for specificity using melt curve analysis and 1.2% agarose gel electrophoresis. Primer efficiencies were estimated using PCR Miner and are listed in Table 2-1 (Zhao and Fernald, 2005).

Table 2-1 Primer sequences and estimated efficiencies

Gene name	Primer sequence	Average Efficiency (%)
hmgcr forward	5’ GGATCGCAGAACCCTCATCC 3’	86
hmgcr reverse	5’ CCTGGTCAGGTAGAAGTGCC 3’	
fdft1 forward	5’ CAACTTCTGCGCCATTCCAC 3’	87
fdft1 reverse	5’ TCTGCACGGCTCTCATGTTG 3’	
scap forward	5’ CGAAACTCCAAAGAAGGCCC 3’	87.3
scap reverse	5’ AGCGATCAGGTTTCCTCTCAG 3’	
ef-α forward	5’ CTACATCAAGAAGATCGGCTACAA 3’	84.2
ef-α reverse	5’ CGACAGGGACAGTTCCAATAC 3’	

2.3.7 Statistical analysis

Differences in survival, total cholesterol, and relative gene expression were tested for normality ($p > 0.05$) using a Shapiro-Wilk test. One-way analysis of variance (ANOVA) was subsequently used to evaluate statistical differences between treatment and control groups. A Tukey's post-hoc was then run to compare significance between treatment groups if $p < 0.05$. All statistical analyses were conducted in R studio.

2.4 Results

The highest exposure concentration (∑PAH 8.3 µg/L) resulted in significant decreases in survival and limited use for gene expression studies (Fig. 2-1). Exposure to ∑PAH 8.3 µg/L also produced a significant decrease in total cholesterol normalized to total protein

to 0.88 ± 0.34(μM/(μg/mL)) in whole fish homogenates compared with the seawater control 1.55 ± 0.1 (μM/(μg/mL)) (Fig. 2-2).

To assess whether decreases in total cholesterol corresponded with changes in gene expression in the cholesterol biosynthetic pathway, relative expression of *hmgcr*, *fdft1*, and *scap* were quantified by qPCR at exposure levels of ∑PAH 1.69, 2.62, and 5.99 μg/L. Expression of *fdft1* was significantly increased at ∑PAH concentrations of 2.62 μg/L and 5.99 μg/L by a fold change of 1.8 and 2.1 relative to the seawater control, respectively (Fig. 2-3A). Expression of *hmgcr* was slightly increased, though not significantly, in the oil exposed samples relative to the seawater control (Fig. 2-3B). The expression of *scap*, an mRNA that encodes the SREBP cleavage-activating protein and is involved in sensing sterol presence in the cell membrane was not significantly changed by increasing ∑PAH exposure (Fig. 2-3C).

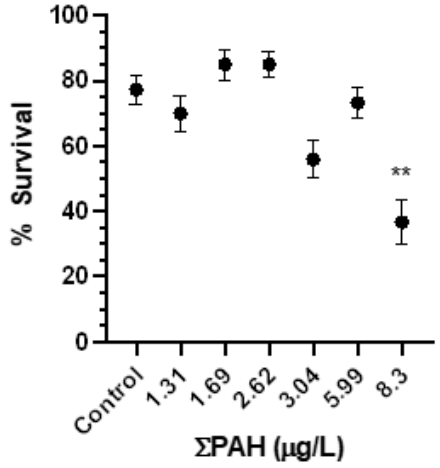

Figure 2-1 Average survival across replicate beakers for seawater control and slick oil treatments at the end of the 96 hpf exposures. Error bars represent ±SEM. Data was analyzed by one-way ANOVA followed by Tukey's HSD multiple comparisons test. Asterisks (**) represent the significant difference ($p < 0.01$). Control n =19, ∑PAH 1.3 n = 5, ∑PAH 1.69 n = 10, ∑PAH 2.62 n = 10, ∑PAH 3.04 n= 4, ∑PAH 5.99 n = 10, ∑PAH 8.3 n= 3.

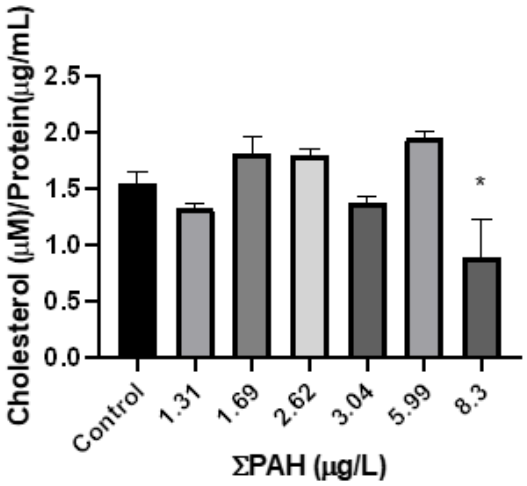

Figure 2-2 Average total cholesterol normalized to total protein across replicate beakers for seawater control and slick oil treatments. Error bars represent ±SEM. Data was analyzed by one-way ANOVA followed by Tukey's HSD multiple comparisons test. Asterisks (*) represent the significant difference ($p < 0.05$). Control n = 9, ∑PAH 1.3 n = 3, ∑PAH 1.69 n = 5, ∑PAH 2.62 n = 5, ∑PAH 3.04 n= 4, ∑PAH 5.99 n = 5, ∑PAH 8.3 n= 3.

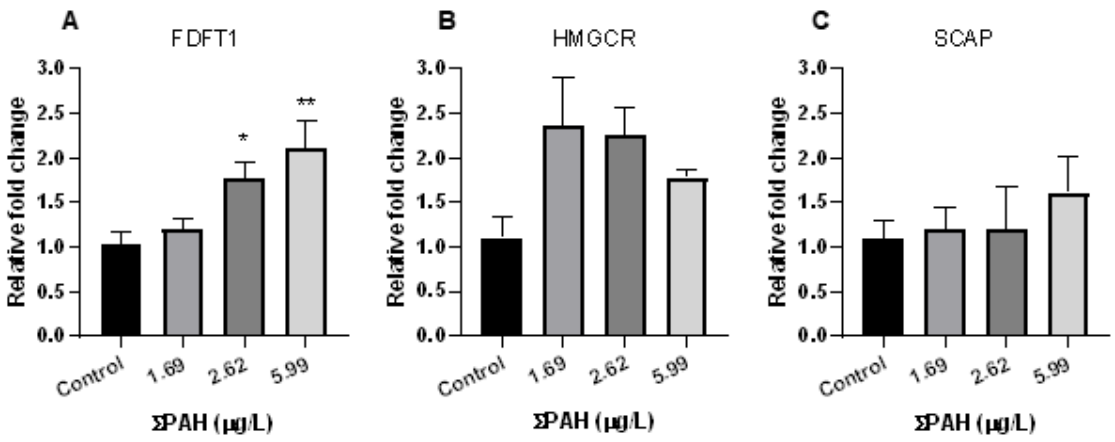

Figure 2-3 Average gene expression responses in 96 hpf mahi-mahi exposed to seawater control, and 1.69 – 5.99 µg/L ∑PAH, across replicate beakers for seawater control and slick oil treatments. Values are presented as relative fold change. (A) Relative farnesyl-diphosphate farnesyltransferase 1 (*fdft1*) expression. (B) Relative HMG-CoA reductase (*hmgcr*) expression. (C) Relative SREBP cleavage-activating protein (*scap*) expression. Data were analyzed by one-way ANOVA followed by Tukey's HSD multiple comparisons test. Error bars represent ±SEM. Asterisks (*) represent the significant difference ($p < 0.05$), (**) represent the significant difference ($p < 0.01$). Control n = 5, ∑PAH 1.69 n = 5, ∑PAH 2.62 n = 4, ∑PAH 5.99 n = 4.

2.5 Discussion

Cholesterol biosynthesis is highly conserved across vertebrates and tightly regulated in response to membrane cholesterol concentrations (Horton et al., 2002; Osborne and Espenshade, 2009; Van Der Wulp et al., 2013). The SREBP cleavage-activating protein (Scap) limits cholesterol biosynthesis in the presence of cholesterol. However, when cholesterol levels are low, the sterol regulatory element-binding protein (SREBP)/Scap complex moves to the Golgi where the SREBP is cleaved and transported to the nucleus. The cleaved SREBP, acting as a transcription factor, subsequently binds the sterol regulatory element (SRE), ultimately leading to the production of HMG-CoA reductase, the rate-limiting enzyme in the cholesterol biosynthetic pathway through the transcription

of *hmgcr* (Brown and Goldstein, 2009). Downstream of *hmgcr*, farnesyl-diphosphate farnesyltransferase 1 catalyzes the first committed step of cholesterol biosynthesis (Trapani et al., 2011). In this study, exposure to high energy water accommodation fractions of ∑PAH 1.69–5.99 μg/L caused a significant increase in *fdft1*, consistent with the prediction that the cholesterol pathway would be enhanced from the transcriptomic study using oil exposed mahi-mahi (Xu et al. 2017) (Fig. 2-3A). Additionally, we did not observe any changes to *scap*, suggesting cholesterol is being detected through the normal mechanism, described above. Because *scap* expression was not altered, we suspect that the observed induction of the cholesterol biosynthetic pathway is being prompted by a lack of cholesterol in the larvae, likely due to reduced transport or presence of cholesterol in the yolk. With less cholesterol binding to Scap, the SRE is bound, and the biosynthetic pathways are upregulated.

Consistent with this response, exposure to oil (∑PAH 8.3 μg/L), caused a significant decrease in total cholesterol in larval homogenates. Xu et al. (2017b), reported significant enhancement of the cholesterol biosynthetic pathway in 96 hpf mahi-mahi exposed to oil (∑PAH 13 ± 4 μg/L), a much higher concentration than the exposures in this study. We therefore suspect that at higher concentrations we would continue to see an increase in the expression of these genes. While several transcriptomics studies have predicted that cholesterol biosynthesis is enhanced with oil exposure across species (Sørhus et al., 2017; Xu et al., 2017), this is the first study that we are aware of that has shown an actual reduction of cholesterol in larval fish exposed to crude oil.

The observed decreases in cholesterol in oil exposed mahi-mahi could play a major role in the established toxicity phenotypes observed with oil exposure in fish, particularly in the development of cardiotoxicity. Under normal conditions, EC coupling in cardiomyocytes is stimulated by action potentials (APs) which are propagated across the heart from the pacemaker region (Laurent et al., 1983). These APs stimulate the opening of L-type voltage-gated calcium channels, allowing an influx of Ca^{2+} across the cell membrane. Ca^{2+} then binds to type-2 ryanodine receptors, located in the adjacent sarcoplasmic reticulum (SR) membrane, subsequently stimulating the release of SR calcium stores and triggering heart contraction (Bers, 2002). Critical to organism function and survival, the maintenance of this process is heavily dependent on the cellular integrity of the cardiomyocyte plasma membrane. In mammalian cardiac ventricular myocytes Ca^{2+} influx predominately occurs in the transverse tubules (t-tubules), which present themselves as infoldings of the cardiomyocyte cell membrane (Brette and Orchard, 2003). Membrane cholesterol depletion in cardiomyocytes isolated from C57BL/6J mice has been shown to decrease T-tubule integrity and significantly reduce the amplitude of Ca^{2+} transients (Zhu et al., 2016). While fish myocytes do not possess T-tubules (Shiels and White, 2005), cholesterol still plays a critical role in teleost plasma membranes (Crockett, 1998) and numerous studies, across species, have shown that membrane cholesterol is an essential regulator of ion channel function (reviewed by Levitan et al. (2010)).

Given EC coupling is conserved across vertebrates (Horton et al., 2002; Osborne and Espenshade, 2009), we suspect that cholesterol plays an essential role in maintaining

cardiomyocyte structure and function in fish. Cardiomyocytes isolated from juvenile bluefin and yellowfin tunas exposed to crude oil display disruption to EC-coupling. Brette et al. (2017, 2014), further explored disruption to coupling and found that several channels involved in ion movement throughout the EC cycle were adversely affected by oil exposure leading to decreased Ca^{2+} transients entering the cell, slow reuptake of Ca^{2+} into the SR via the SR Ca^{2+} ATPase (SERCA), and significant reduction of the delayed rectifier K^+ channel current (I_{kr}).

Given these studies, it is likely that the observed arrhythmias, and bradycardia are linked to changes in ion channel function (Reviewed in Incardona and Scholz (2018)). Low membrane cholesterol levels provide a possible mechanism for the disruption of multiple ion channels within the cardiomyocyte, as found by Brette et al. (2017). Cholesterol is a key regulator of eukaryotic membrane fluidity but the effect it has on the membrane varies with temperature and lipid composition. Cholesterol increases membrane fluidity at temperatures below 37 °C by preventing the interaction and stacking of fatty acyl chains in membrane lipids (Lodish et al., 2000). Because mahi-mahi embryos are commonly found in waters ranging in temperature between 25 and 30 °C, we predict that the reductions in cholesterol observed in this study could result in reduced membrane fluidity in the developing embryos (Ditty et al., 1994). The transmembrane helices of key transport proteins have been shown to undergo major perpendicular movement during the reaction cycle, requiring flexibility within the bilayer (Norimatsu et al., 2017). Diminished cholesterol levels due to crude oil exposure could therefore cause the membrane to become more rigid and prevent ion channels from completing the reaction

cycle. These channels are nearly identical across vertebrates, and a mechanism such as cholesterol disruption may explain the cardiotoxic response to crude oil which is common across numerous fish species.

2.6 Conclusion

In this study we evaluated the induction of genes in mahi-mahi in the cholesterol biosynthetic pathway and observed decreases in total cholesterol levels with increasing ∑PAH exposure which has previously been linked to developmental cardiotoxicity in mahi-mahi. These findings corroborate previous transcriptomic studies which highlighted cholesterol biosynthesis in several fish species as a top enriched pathway following oil exposure. Given the role of cholesterol in maintaining cardiomyocyte integrity and membrane fluidity we predict that changes to cholesterol levels could impact transmembrane ion channel function and contribute to cardiotoxicity. Additional studies are necessary to confirm this hypothesis.

Chapter 3: Effects of phenanthrene exposure on cholesterol homeostasis and cardiotoxicity in zebrafish embryos

3.1 Abstract

Polycyclic aromatic hydrocarbons (PAHs) are pervasive pollutants in aquatic ecosystems and developing fish embryos are especially sensitive to PAH exposure. Exposure to crude oil or phenanthrene (a reference PAH found in oil) produces an array of gross morphological abnormalities in developing fish embryos, including cardiotoxicity. Recently, studies utilizing transcriptomic analyses in several oil-exposed fish embryos found significant changes in the abundance of transcripts involved in cholesterol biosynthesis. Given the vital role of cholesterol availability in embryonic heart development, we hypothesized that cholesterol dysregulation in early development contributes to phenanthrene-induced cardiotoxicity. Within this study, we exposed zebrafish embryos to 12 or 15 μM phenanthrene from 6 to 72 h post-fertilization (hpf) and demonstrated that, in conjunction with pericardial edema and bradycardia, several genes (*fdft1, hmgcra*) in the cholesterol biosynthetic pathway were significantly altered. When embryos were pretreated with a cholesterol solution from 6 to 24 hpf followed by exposure to phenanthrene from 24 to 48 hpf, the effects of phenanthrene on heart rate were partially mitigated. Despite changes in gene expression, whole-mount *in situ* staining of cholesterol was not significantly affected in embryos exposed to phenanthrene ranging in stage from 24 to 72 hpf. However, two-dimensional yolk area was

significantly increased with phenanthrene exposure at 72 hpf, suggesting that lipid transport from the yolk to the developing embryo was impaired.

3.2 Introduction

Polycyclic aromatic hydrocarbons (PAHs) are pervasive environmental pollutants and key contributors to crude oil toxicity in fish (Marty et al., 1997). Early life-stage fish are especially vulnerable to PAH exposure, and fish embryos exposed to sub-lethal concentrations of crude oil or phenanthrene alone (a reference PAH) display a common phenotype characterized by pericardial and yolk sac edema, craniofacial defects, reductions in heart rate (bradycardia), and cardiac arrhythmias in at least 19 fish species (reviewed by Incardona and Scholz 2018). Importantly, impaired development at these early life stages has been linked to functional abnormalities that persist into the juvenile and adult stages (Hicken et al., 2011; Incardona et al., 2015; Mager et al., 2014). Therefore, contamination of spawning habitats can impact recruitment and population growth (Levin and Stunz, 2005). Despite extensive documentation of oil-induced morphological defects, knowledge of the molecular mechanisms that cause these malformations is still limited.

To identify potential mechanisms, several recent studies have employed transcriptomic analysis to assess the mRNA expression profile of fish embryos exposed to crude oil. When multiple studies were compared, cholesterol biosynthesis was consistently found to be one of the top impacted pathways in fish embryos exposed to crude oil. Enhancement of cholesterol-related pathways has been identified in red drum (*Sciaenops ocellatus*; Xu

et al. 2017a), mahi-mahi (*Coryphaena hippurus*; Xu et al. 2017b), Atlantic haddock (*Melanogrammus aeglefinus*; Sørhus et al. 2017), and sheepshead minnow (*Cyprinodon variegatus*; Jones et al. 2020) embryos and larvae exposed to crude oil. Interestingly, a trend towards inhibition of cholesterol-related pathways was observed in Gulf Killifish (*Fundulus grandis*; Jones et al. 2020). While it is difficult to compare studies investigating different developmental stages and exposure regimes, there is evidence of species-specific differences in cholesterol dysregulation following crude oil exposure (Jones et al., 2020).

Altered cholesterol homeostasis – resulting in either an abnormal increase or decrease in cholesterol levels – has been implicated in disease generation in fish and mammals (Campos et al., 2016; Maerz et al., 2019; Maxfield and Tabas, 2005). Zebrafish have often been used as a model organism for the study of cholesterol-related diseases in vertebrates, demonstrating that appropriate regulation of cholesterol is essential for organogenesis during embryonic development (Campos et al., 2016; Maerz et al., 2019). Interestingly, zebrafish embryos exposed to cholesterol-reducing drugs from 10 h post-fertilization (hpf) to 48 hpf display a phenotype similar to that observed when fish embryos are exposed to crude oil, including cardiac looping defects, pericardial edema, bradycardia, body curvature, smaller heads, and smaller eyes by 48 hpf (Maerz et al., 2019). Although the mechanisms by which cholesterol-reducing drugs cause these effects are still being explored, many studies have demonstrated that cholesterol can influence ion-channel function (including those in cardiomyocytes) through specific sterol-protein interactions (reviewed by Levitan et al., 2014). Additionally, cholesterol-enriched

membranes coordinate many cellular processes, including signal transduction, required for embryogenesis (Blassberg and Jacob, 2017; Maerz et al., 2019).

Few studies have investigated the effects of oil exposure on lipid metabolites in early life-stage fish. Laurel et al. (2019) revealed that yolk-sac stage polar cod (*Boreogadus saida*) exposed to a water-soluble fraction of crude oil from oiled gravel columns exhibited increased triacylglycerols, free fatty acids, sterols, and total lipids in pooled homogenates. Additionally, 96-hpf mahi-mahi whole-larval homogenates presented a significant reduction to total cholesterol when exposed to $\sum_{50}$PAH 8.3 μg/L (McGruer et al., 2019). However, because these studies used whole embryo homogenates and did not exclude the unused yolk sac, it is difficult to ascertain the availability of these nutrients to the developing embryo.

This study aims to investigate whether transcriptome-based predictions of cholesterol disruption translate to detectable and relevant changes to cholesterol levels within zebrafish embryos exposed to phenanthrene. To accomplish this, we (1) used a cholesterol reporter molecule (filipin) to visualize free cholesterol distribution within the embryo; (2) pretreated embryos with water-soluble cholesterol to determine whether the presence of excess cholesterol mitigates phenanthrene-induced cardiotoxicity; and (3) assessed yolk-absorption to understand how nutrient transfer is impacted by phenanthrene exposure during embryo development.

3.3 Methods

3.3.1 Animals

Adult wild type (5D) zebrafish were maintained and bred on a recirculating system using procedures described by Mitchell et al. (2018). Adult breeders were handled in accordance with Institutional Animal Care and Use Committee-approved animal use protocol (No. 20150035 and No. 20180063) at the University of California, Riverside.

3.3.2 Embryo exposures

All exposures were conducted in 48-well polystyrene plates (Corning) with 0.667 mL of exposure solution in each well. Fertilized embryos were collected immediately after spawning and reared at 28°C under a 14-h:10-h light:dark cycle in water collected from the recirculating zebrafish rearing system (pH and conductivity of ~7-8 and ~950 µS, respectively) and vacuum-filtered through a 5-µm membrane (Millipore) to remove particulate matter. At shield-stage (~6 hpf) (Kimmel et al., 1995), zebrafish embryos were randomly distributed into wells containing exposure solutions described below, resulting in one embryo per well.

3.3.3 Phenanthrene exposures

Phenanthrene stock solutions were prepared by dissolving phenanthrene (98% purity, Sigma Aldrich) in 100% dimethyl sulfoxide (DMSO) and stored at 4°C. Exposure solutions were produced by spiking filtered system water with 100% DMSO or

phenanthrene stock to produce a vehicle control (0.08% DMSO) or phenanthrene solutions (12 and 15 μM). Shield-stage embryos (~6 hpf) were randomly distributed via forceps into wells containing 0.667 mL exposure solution followed by 75% (0.5 mL) renewals at 24 and 48 hpf. Embryos were exposed from 6 to 72 hpf to 12 and 15 μM phenanthrene without shaking to mimic previous studies which observed effects on heart development in zebrafish following exposure to 10 - 60 μM phenanthrene when exposures were initiated between 4 to 8 hpf (Incardona et al., 2005, 2004). For qPCR analysis, embryos were collected in microcentrifuge tubes with nine embryos per sample, snap-frozen in liquid nitrogen, and stored at -80°C for subsequent total RNA extraction. Before staining with filipin, unhatched embryos were manually dechorionated, pooled (40-48 embryos per sample) in microcentrifuge tubes, and fixed overnight at 4°C with freshly prepared 4% paraformaldehyde (PFA)/1X phosphate-buffered saline (PBS). Following fixation, samples were washed three times each with 1X PBS and then stored in 1X PBS at 4°C until staining.

3.3.4 Atorvastatin exposures

Atorvastatin (Toronto Research Chemicals) was dissolved in 100% DMSO to create the stock solution and stored at 4°C. Filtered water was then spiked with 100% DMSO or atorvastatin stock to produce the vehicle control (0.08% DMSO) or 5 μM atorvastatin solutions. Shield-stage zebrafish embryos (~6 hpf) were exposed in 48-well polystyrene plates (Corning) with 0.667 mL of exposure solution in each well with one embryo per well. To mimic previous studies (Maerz et al., 2019), exposures were conducted without

renewal. At 72 hpf, embryos were collected and fixed with paraformaldehyde as described above before staining with filipin.

3.3.5 Water chemistry analysis

Water concentrations were measured at the beginning and end of the 6- to 72-hpf exposures both in the presence and absence of embryos. Only final concentrations were determined for phenanthrene exposures conducted from 24 to 48 hpf. For determining concentrations at exposure initiation, the initial working solution was sampled directly. To determine final concentrations, the exposure solution was sampled in triplicate by pooling 250 µL for a given sample from every third well. Each replicate was mixed well and then diluted 1:10 with methanol to produce three replicates for analysis. Phenanthrene concentrations were quantified using a Shimadzu Prominence-i LC-2030 HPLC system with fluorescence detection. A Shiseido Capcell Pak C18 column (4.6 x 150 mm) was used for separation equipped with a Phenomenex SecurityGuard column. All mobile phases were degassed by sonication before use. An 11-point calibration curve ranging from 5-200 ng/mL was used for phenanthrene quantification. Excitation and emission wavelengths of 250/365 nm were used for fluorescent detection of phenanthrene based on a previous study (Wheatley and Sadhra, 1998). The mobile phase consisted of 80% methanol and 20% water. The samples (10 µL) were injected in isocratic conditions with a 1.5 mL/min flow rate. The column temperature was maintained at 40°C. The method length was 5.5 min. Reported values are the mean of three replicates for the initial and final concentrations.

3.3.6 Phenotyping

Embryos were arranged laterally in an agarose mold and imaged using a Leica MZ10 F stereoscope equipped with a DMC2900 camera for morphological assessment. Videos were recorded for heart rate analysis. Heartbeats were counted over a 10-s period. Still frames were imported into ImageJ (v1.52p, NIH). Pericardial area was quantified at 72 hpf, and yolk area was quantified at 24, 27, 30, 48, and 72 hpf. Example outlines of areas measured are presented in Appendix B (Fig. B-1).

3.3.7 RNA isolation and real-time PCR (qPCR)

To describe the relative expression of genes in the cholesterol biosynthetic pathway, 3-4 biological replicates, each with nine embryos, were collected for qPCR analysis. Total RNA was extracted using an RNeasy Mini Kit from Qiagen (Valencia, CA). For each sample, RNA quality and quantity were determined using a NanoDrop (model ND-1000), and samples were stored at −80°C until further processing. cDNA synthesis was conducted with the Promega Reverse Transcription System kit (Madison, WI) using 1 μg of RNA following the manufacturer's protocol. cDNA was stored at −20°C until qPCR was performed.

Zebrafish have two paralogous genes encoding a 3-hydroxy-3-methylglutaryl-CoA reductase protein, termed *hmgcra* and *hmgcrb,* both of which were assessed along with farnesyl-diphosphate farnesyltransferase 1 (*fdft1*). qPCR reactions were carried out using the SsoAdvancedTM Universal SYBR® Green Supermix (Bio-Rad, Hercules, CA) on

the BioRad CFX Connect instrument (Hercules, CA). Thermocycling conditions used for the qPCR analysis of all genes were as follows: 95°C for 15 min, followed by 40 cycles of 94°C for 10 s, 60°C for 20 s, and 72°C for 32 s (conditions developed by Mu et al. (2015)). Data were normalized using ef-α as its expression is stable throughout zebrafish development (McCurley and Callard, 2008), and comparisons of mRNA levels were determined according to the $2^{-\Delta\Delta CT}$ method (Livak and Schmittgen, 2001).

Primer sequences for *hmgcra*, *hmgcrb*, and *fdft1* were obtained from Mu et al. (2015) and target-verified by NCBI Primer-BLAST. All primers were tested for specificity using melt curve analysis and 1.2% agarose gel electrophoresis. The primer sequences used are provided in Appendix B (Table B-1).

3.3.8 Filipin staining

Following fixation, embryos were transferred to mesh baskets (20-22 embryos per basket) and depigmented in fresh 3% H_2O_2/0.5% KOH, followed by a 5-min wash in 1X PBS. Embryos were then soaked overnight at room temperature in 0.5 mg filipin/mL PBS (Sigma Aldrich), protected from light. The following day, embryos were washed in 1X PBS containing 0.1% Tween-20 (PBST) five times for 15 min each and protected from light until imaging on the same day. Embryos were arranged laterally in an agarose mold and imaged individually (to prevent photobleaching) under both transmitted and UV light. The mean fluorescence produced by filipin was determined within the larval body

(head and trunk), excluding the yolk, using ImageJ. Example outlines of the region measured are presented in Appendix B (Fig. B-1).

Three background measurements were recorded per image in the area adjacent to the region of interest. A corrected fluorescence value for the area of interest in each image was calculated by subtracting the mean background value from the mean fluorescence value of the region of interest. To reduce variability due to photobleaching, the imaging of controls and respective phenanthrene exposed groups needed to be completed on the same day. Therefore, multiple rounds of staining and imaging were conducted across several days. To control for slight differences in imaging conditions, each sample was normalized to the same stage control that was imaged on the same day. Data are presented as a percent of the corresponding control.

3.3.9 Cholesterol pretreatments

Shield-stage embryos were treated with either filtered system water or a 10-µM water-soluble cholesterol (Sigma Aldrich) solution prior to treatment with phenanthrene (~6-24 hpf). The developing zebrafish heart is sensitive to phenanthrene exposure from 24 to 48 hpf (Incardona et al., 2013). Therefore, embryos were removed from water or cholesterol exposures at 24 hpf, washed three times with fresh filtered system water, and then exposed to either a 0.1% DMSO solution or nominal concentrations of 20 µM or 25 µM phenanthrene. Cholesterol and phenanthrene exposures were conducted in separate 48-well polystyrene plates (Corning) with 0.667 mL of the exposure solution in each well

with one embryo per well. Phenanthrene concentrations were increased to induce cardiac abnormalities within a shortened exposure duration. In the vehicle control, DMSO concentrations were increased to 0.1% DMSO to match the higher DMSO exposure incurred by using higher phenanthrene concentrations. At 48 hpf, exposures were terminated and heart rate was assessed, or embryos were fixed for subsequent staining with filipin as described above.

3.3.10 Statistical analyses

Statistical analyses were performed using the statistical program R. Data were checked for normality and homogeneity of variances. Statistical significance of filipin staining was determined within each stage. The Student's t-test was used when comparisons were made between two treatments. One-way ANOVA was used for comparisons containing more than two treatments. Differences in yolk area between 0.08% DMSO and 12 μM phenanthrene treatment groups were determined by two-way ANOVA. Yolk area at the 72 hpf timepoint was analyzed by a Kruskal-Wallis Rank Sum test. A Tukey's HSD test was performed to assess individual comparisons if statistical differences were determined following a one-way or two-way ANOVA. When parametric assumptions for normality and homoscedasticity of variance were violated, nonparametric comparisons were made using a Kruskal-Wallis Rank Sum Test, followed by a Dunn's Test of Multiple Comparisons. All data are expressed as the mean ± the standard deviation (SD).

3.4 Results

3.4.1 Water chemistry analysis

Phenanthrene concentrations were determined at the end of all exposures and at the beginning of exposures initiated at 6 hpf. Between 6 hpf (initial) and 72 hpf (final), the average measured concentrations of phenanthrene in the presence of embryos declined by 86.9% for samples collected from nominal exposures of 12 μM and 15 μM phenanthrene (Appendix B Table B-2). Phenanthrene concentrations for exposures conducted from 24 to 48 hpf were reduced by an average of 90% by 48 hpf compared with the calculated nominal concentrations of 20 μM and 25 μM phenanthrene (Appendix B Table B-2). In addition to uptake of phenanthrene by the embryo, sorption of phenanthrene to polystyrene wells likely contributed to the decrease in phenanthrene concentrations between the initial and final measurements. This is supported by the measurement of water concentrations for the nominal exposures of 12 μM and 15 μM phenanthrene in the absence of embryos, which declined by an average of 75.9% by 72 h (Appendix B Table B-3).

3.4.2 Morphological abnormalities from phenanthrene exposure

Pericardial edema and bradycardia were used to assess sublethal cardiotoxicity at 72 hpf following phenanthrene exposure. Exposure to 12 and 15 μM phenanthrene significantly decreased heart rate by 39.5% ± 6.8 and 47.5% ± 23.7, respectively (Fig. 3-1B). Pericardial area was significantly increased by 36.4% ± 62.2 and 49% ± 55.0 relative to

the vehicle control following exposure to 12 and 15μM phenanthrene, respectively (Fig. 3-1C). While all phenanthrene treatments produced significant bradycardia and pericardial edema relative to the vehicle control, these metrics were not significantly impacted between treatments. Survival at 72 hpf was >90% in all groups except at the 15 μM phenanthrene concentration, where survival decreased to 79% ± 7.1 (Fig. 3-1A).

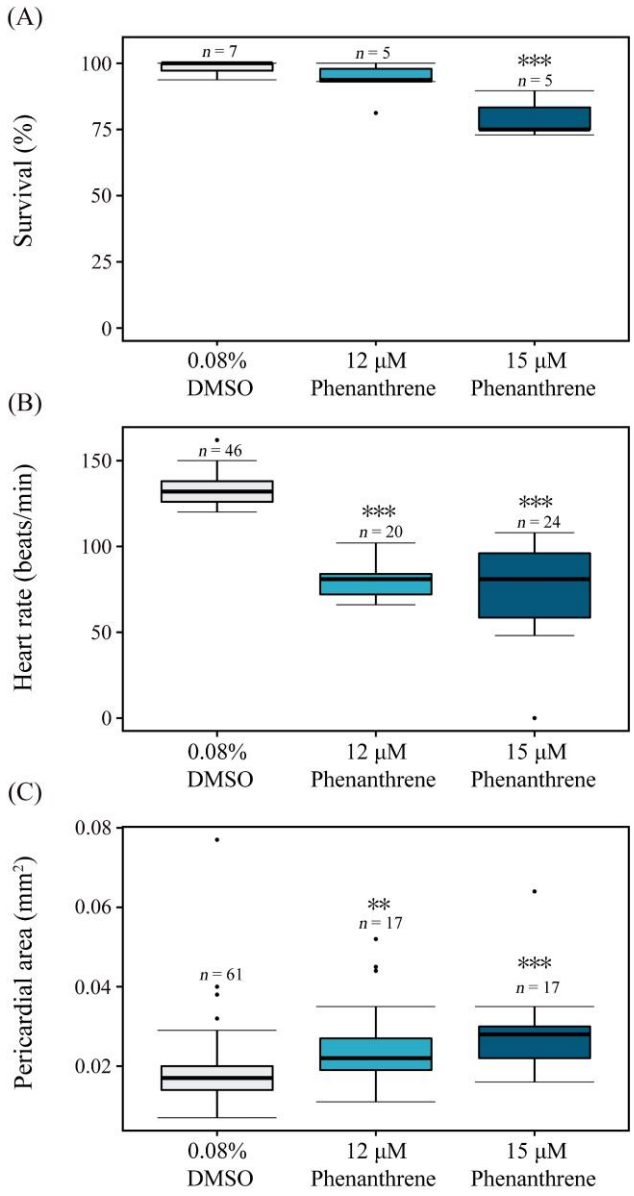

Figure 3-1 Effects of phenanthrene on zebrafish embryos at 72 hpf on (A) Survival (%) calculated from 48 embryos per replicate with 5 or 7 replicates per treatment; (B) heart rate (beats min^{-1}) in individual embryos, and (C) pericardial area (mm^2). Data for pericardial area and heart rate endpoints were analyzed by a Kruskal-Wallis Rank Sum Test, followed by a Dunn's Kruskal-Wallis Test of Multiple Comparisons. Survival data were analyzed by one-way ANOVA, followed by Tukey's HSD multiple comparisons test. **p<0.01, ***p<0.001.

3.4.3 Gene expression (qPCR)

Several genes that encode key enzymes in the cholesterol biosynthetic pathway were assessed by qPCR. At the highest concentration tested (15 µM phenanthrene), transcription of *farnesyl-diphosphate farnesyltransferase 1* (*fdft1*) was significantly increased 2.9-fold (Fig. 3-2A). By contrast, *HMG-CoA Reductase a* (*hmgcra*) was significantly decreased in a concentration-dependent manner across all phenanthrene concentrations (Fig. 3-2B). *HMG-CoA Reductase b* (*hmgcrb*) was not significantly altered but followed a similar decreasing trend to *hmgcra* (Fig. 3-2C). An overview of the cholesterol synthesis pathway (adapted from Sharpe and Brown 2013) is provided in Appendix B (Fig. B-5).

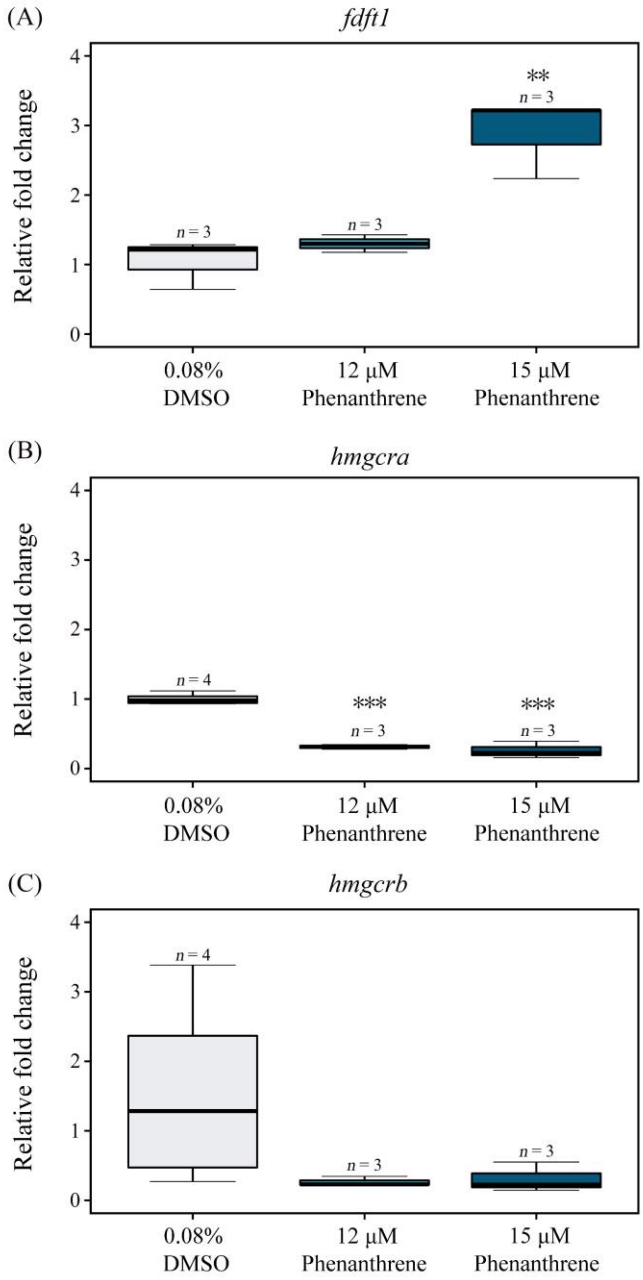

Figure 3-2 Effects of phenanthrene on gene expression in the cholesterol biosynthetic pathway in 72 hpf zebrafish homogenates. Values are presented as relative fold change of (A) *farnesyl-diphosphate farnesyltransferase 1* (*fdft1*) (B) *HMG-CoA Reductase a (hmgcra), (C) HMG-CoA Reductase b* (*hmgcrb*). Data were analyzed by one-way ANOVA, followed by Tukey's HSD multiple comparisons test. $^{**}p<0.01$, $^{***}p<0.001$.

3.4.4 Effects of phenanthrene and atorvastatin on filipin staining

Filipin is a naturally fluorescent polyene macrolide that stains free 3-*β*-hydroxysterols and has been previously used to visualize free cholesterol in fixed cells and tissues (Gimpl and Gehrig-Burger, 2007). Within this study, filipin staining was employed to visualize the distribution of free cholesterol in fixed zebrafish embryos at stages ranging from 24 to 72 hpf. Representative images are presented in Appendix B (Figs. B-2 and B-3).

Filipin staining was evaluated in embryos exposed to vehicle or 12 μM phenanthrene at all stages assessed (24 to 72 hpf). Additionally, filipin staining was evaluated in 72 hpf embryos exposed to 15 μM phenanthrene to link staining measurements to gene expression and morphological assessments at these same concentrations. Atorvastatin was used as a positive control at this time point. No significant differences were observed in the mean fluorescence of filipin in the larval body following exposure to 12 μM phenanthrene (relative to vehicle control) at any stage tested (24 to 72 hpf). Staining in the region of specific organs, including the heart, was not substantial enough to quantify individually. Embryos exposed to the highest phenanthrene concentration (15 μM) until 72 hpf did not significantly differ in staining relative to the vehicle control. However, 72-hpf embryos exposed to 5 μM atorvastatin (as a positive control) displayed a

significant decrease in staining by filipin ($p < 0.001$), demonstrating that changes to cholesterol can be detected by this method (Fig. 3-3).

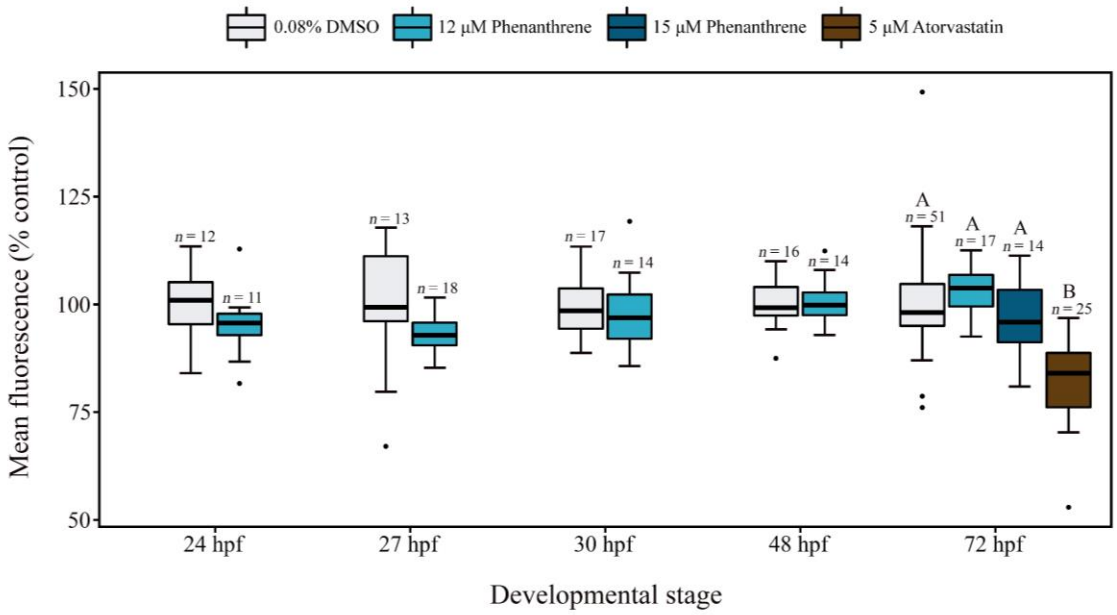

Figure 3-3 Background corrected mean fluorescence of filipin staining in the embryo body (head and trunk) presented as a percent of the same stage control. Statistical significance was determined within each stage. Data for the 24 hpf, 27 hpf, 30 hpf, and 48 hpf time points were analyzed by Student's t-test. Data for the 72 hpf time point were analyzed by a Kruskal-Wallis Rank Sum Test, followed by a Dunn's Test of Multiple Comparisons. Different letters represent a significant difference ($p< 0.05$).

3.4.5 Effects of cholesterol on phenanthrene induced bradycardia

Embryos were pretreated with a 10 µM water-soluble cholesterol solution from 6 to 24 hpf and then exposed to 20 µM or 25 µM phenanthrene to determine whether pretreatment with cholesterol mitigates phenanthrene-induced cardiotoxicity. A higher phenanthrene concentration was used here since the exposure duration was decreased.

A concentration-dependent decrease in heart rate (beat min^{-1}) was observed with increasing phenanthrene exposure. The heart rate of embryos exposed to the vehicle was not significantly affected by cholesterol pretreatment compared with embryos pretreated with water alone. However, in both the 20 µM and 25 µM phenanthrene exposure groups, cholesterol pretreatment from 6 to 24 hpf significantly mitigated the effects of phenanthrene treatment from 24 to 48 hpf, resulting in an increased heart rate relative to the water pretreatment at 48 hpf (p = 0.03) (Fig. 3-4)

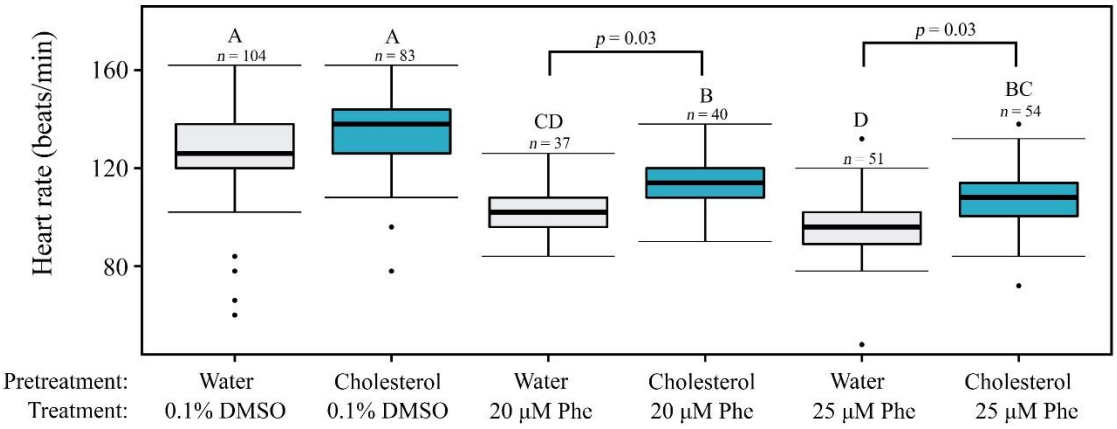

Figure 3-4 Heart rate (beats min^{-1}) in 48 hpf zebrafish embryos pretreated with either a water control or a 10 µM water-soluble cholesterol solution from 6 hpf to 24 hpf followed by treatment from 24 – 48 hpf with either a 0.1% DMSO vehicle control, 20 µM Phenanthrene (Phe) or 25 µM Phe exposure solution. Data were analyzed by a Kruskal-Wallis Rank Sum Test, followed by a Dunn's Test of Multiple Comparisons. Significance letters represent a significant difference (p< 0.05).

3.4.6 Effects of cholesterol and phenanthrene on filipin staining

Interestingly, relative to embryos pretreated with system water and then exposed to the vehicle, filipin staining following phenanthrene treatment revealed a significant decrease in cholesterol within embryos pretreated with cholesterol and then exposed to 25 µM phenanthrene (p= 0.005). However, staining was not altered in embryos pretreated with cholesterol and then exposed to the vehicle, or embryos pretreated with system water and then exposed to 25 µM phenanthrene, compared with the control (system water pretreatment followed by exposure to vehicle) (Fig. 3-5). Representative images are presented in Appendix B (Fig. B-4).

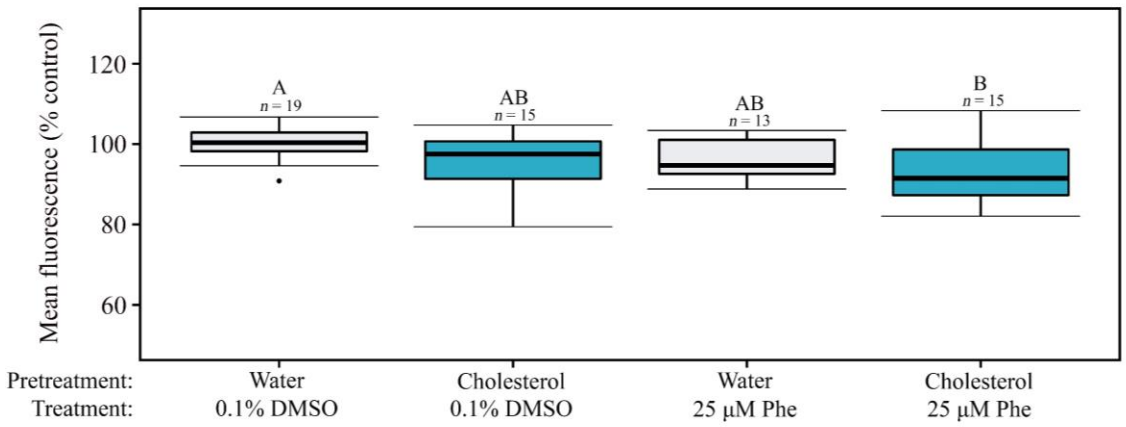

Figure 3-5 Background corrected mean fluorescence of filipin staining in the 48 hpf embryo body (head and trunk) presented as a percent of the Water/ 0.1% DMSO control. Statistical significance was determined by one-way ANOVA, followed by a Tukey's HSD test. Different letters represent a significant difference ($p < 0.05$).

3.4.7 Yolk utilization

Two-dimensional yolk area was quantified to assess whether phenanthrene-exposed embryos utilized the yolk sac and readily accessed nutrients required for development. Yolk area was evaluated in embryos exposed to vehicle or 12 μM phenanthrene at all stages assessed (24 to 72 hpf). Additionally, yolk area was evaluated in 72 hpf embryos exposed to 15 μM phenanthrene to link staining measurements to gene expression and morphological assessments at these same concentrations.

Yolk area remained relatively constant across vehicle control treatments at 24 hpf (0.374 $mm^2 \pm 0.022$), 27 hpf (0.366 $mm^2 \pm 0.022$), and 30 hpf (0.374 $mm^2 \pm 0.027$). However, consistent with the utilization of yolk throughout development, significant decreases in yolk area were observed by 48 hpf (0.301 $mm^2 \pm 0.020$) and 72 hpf (0.263 $mm^2 \pm 0.037$). At 72 hpf, a concentration-dependent increase in the yolk area was observed, with significant increases between the vehicle control and the 12 μM and 15 μM phenanthrene exposure concentrations ($p = 0.01$, $p < 0.0001$, respectively) (Fig. 3-6).

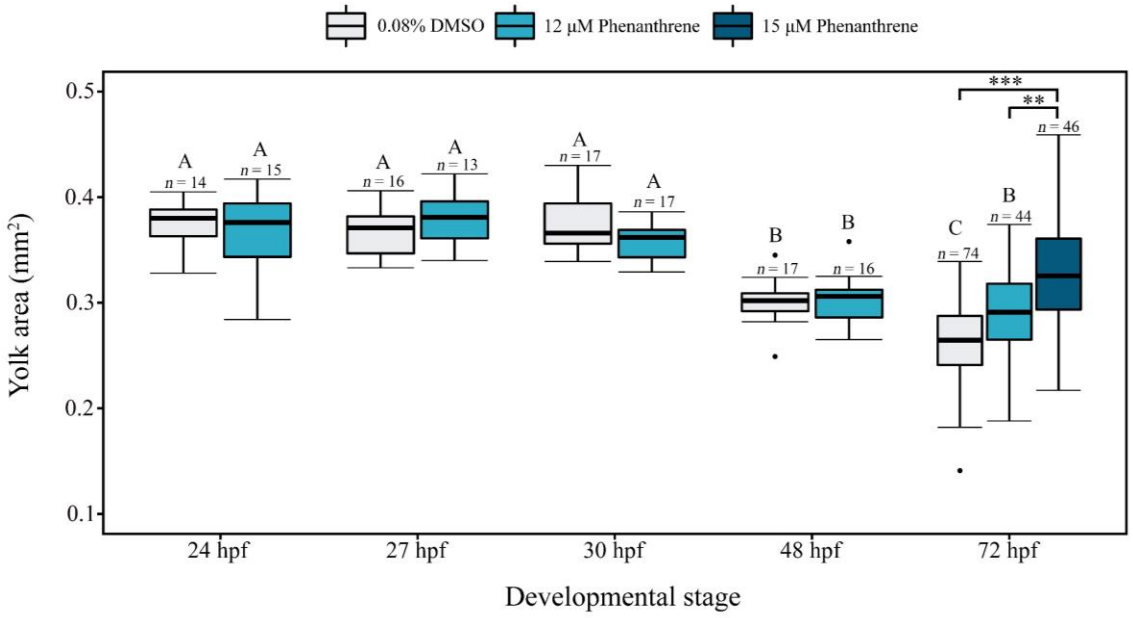

Figure 3-6 Two-dimensional yolk area (mm^2) throughout development. Statistical significance was determined between 0.08% DMSO and 12 µM phenanthrene groups by two-way ANOVA. Data for the 72 hpf time point was analyzed by a Kruskal-Wallis Rank Sum Test, followed by a Dunn's Test of Multiple Comparisons. $^{**}p<0.01$, $^{***}p<0.001$. Different letters represent a significant difference ($p< 0.05$).

3.5 Discussion

Cholesterol biosynthesis plays a vital role in fish embryogenesis (Campos et al., 2016; Maerz et al., 2019), and crude oil has been shown to alter sterol levels in yolk-sac polar cod (Laurel et al., 2019) and total cholesterol in mahi-mahi (McGruer et al., 2019). However, these studies were unable to demonstrate the relevance of these changes to embryo development due to the use of whole-embryo homogenates, which included nutrients in the remaining unused yolk sac. In this study, we investigated the significance of cholesterol dysregulation in producing oil-induced developmental injury.

Zebrafish embryos exposed to 12 or 15 μM phenanthrene from 6 to 72 hpf displayed cardiotoxicity and the dysregulation of *hmgcra* and *fdft1,* which each encode key enzymes in the cholesterol biosynthetic pathway. The enzyme associated with *hmgcr* catalyzes an irreversible and rate-limiting step at the beginning of the cholesterol synthesis pathway (Burg and Espenshade, 2011), while *fdft1* encodes the enzyme which catalyzes the first committed step of cholesterol synthesis (Trapani et al., 2011). Differential expression of these genes suggests that the cholesterol synthesis pathway in zebrafish is altered by phenanthrene exposure, as is seen in embryos of other fish species exposed to crude oil. While other studies have found upregulation or downregulation across the entire pathway with oil exposure, we observed a significant increase in *fdft1* while *hmgcra* was significantly decreased. There is some evidence suggesting that the cholesterol synthesis pathway may be differentially upregulated or downregulated depending on the developmental stage and species (Jones et al., 2020). Thus, our results here could be limited by looking at one developmental stage. There is also the potential for post-transcriptional regulation of mRNA expression by microRNAs (miRNAs). miRNA expression in response to crude oil exposure was recently assessed in red drum (Xu et al., 2019) and mahi-mahi (Diamante et al., 2017). Both studies demonstrated a significant upregulation of miRNA-27b, which is predicted to target *hmgcr*. Overexpression of miRNA-27b has been associated with a trend towards a reduction in *hmgcr* in human hepatocytes (Vickers et al., 2013). Together, this highlights the need to investigate the molecular and physiological changes predicted by transcriptional responses.

To determine whether altered gene expression in the cholesterol biosynthetic pathway coincided with altered cholesterol levels in the developing embryo, the cholesterol reporter molecule filipin was used to visualize cholesterol throughout development. Quantifying mean fluorescence in the embryo body (head and trunk) revealed that cholesterol levels were unchanged at timepoints assessed from 24 to 72 hpf following phenanthrene exposure. Additionally, staining in the heart was not distinctive enough to determine whether overall staining in the organ was altered. As a positive control, embryos exposed to 5 μM atorvastatin demonstrated a decrease in staining by filipin in the larval body, indicating that changes to cholesterol can be detected by this method. While there seems to be a discrepancy between the dysregulation of cholesterol biosynthesis and maintenance of cholesterol levels, there are several possible reasons for this. First, filipin only measures unesterified (free) cholesterol and does not provide the ability to detect the trafficking of cholesterol or the formation of cholesterol esters (Gimpl and Gehrig-Burger, 2007). As maintenance of cholesterol levels is critical for cell function, free cholesterol concentrations in the cell are controlled by additional mechanisms outside of transcriptional controls. Excess cholesterol may be stored in the cell as cholesterol ester droplets (Tabas, 2002). This stored cholesterol can then be mobilized under low cholesterol conditions (Klansek et al., 1996). Alternatively, it is possible that cellular cholesterol levels remain relatively constant or outside of our limit of detection, even as the expression in the synthesis pathway is up- or down-regulated.

Despite not observing changes to cholesterol through whole-mount *in situ* staining, cholesterol is the most abundant lipid in the zebrafish yolk, comprising ~40% of total

lipids in the yolk immediately following fertilization (Fraher et al., 2016). By contrast, cholesterol makes up a much lower percentage of the yolk in many other fish species (3.1 – 11.7 % total lipids for cod (*Gadus morhua*), Atlantic herring (*Clupea harengus*), haddock (*Melanogrammus aeglefinus*), whiting (*Merlangus merlangus*), saithe (*Pollachius viren*), capelin (*Mallotus villosus*), and sand eel (*Ammodytes lancea*) (Tocher and Sargent, 1984)). RNA sequencing has predicted that the cholesterol biosynthesis and lipid metabolism pathways are altered in many species of fish embryos exposed to crude oil. Nevertheless, the variability in yolk composition and exposure regimes could contribute to species-specific sensitivities and responses.

To assess whether altered cholesterol levels are relevant to the development of phenanthrene-induced cardiotoxicity, we pretreated embryos with cholesterol prior to phenanthrene exposure. Interestingly, we found that pretreatment of embryos from 6 to 24 hpf with 10 μM water-soluble cholesterol, followed by phenanthrene exposure from 24 to 48 hpf, significantly increased heart rate relative to phenanthrene-exposed embryos pretreated with a water-only solution. Together, this indicates that cholesterol can partially mitigate the effects of phenanthrene on heart rate and provides evidence that changes to cholesterol during development may play a role in the advancement of cardiotoxicity. Staining for cholesterol following pretreatment (6-24 hpf) and exposure (24-48 hpf) revealed that the influence of cholesterol on heart rate does not correspond with changes to staining. Cholesterol staining was significantly decreased when embryos were pretreated with cholesterol and then exposed to 25 μM phenanthrene (Fig. 3-5), though not altered in other treatment groups. The observed reduction may be due to

elimination or metabolism of excess free cholesterol following cholesterol pretreatment (6-24 hpf). Between 24-48 hpf exposure to high phenanthrene concentrations may further disrupt membrane cholesterol and/or cholesterol synthesis.

Cholesterol pretreatment may be driving changes to heart rate through several mechanisms. First, cholesterol is critical to signaling cascades that drive early development (reviewed by Blassberg and Jacob 2017). If phenanthrene disrupts signaling, the addition of cholesterol could be maintaining or restoring processes important for heart development, resulting in an observed rescue of heart rate perturbation. Alternatively, cholesterol may be acting directly on ion channels in cardiomyocytes. Phenanthrene has been shown to disrupt Ca^{2+} and K^{+} movement in fish cardiomyocytes, leading to arrhythmias and reduced myocyte contractility (Brette et al., 2017). This disturbance is hypothesized to occur through the impairment of multiple ion channels that regulate intracellular Ca^{2+} cycling (i.e., SERCA2 or RYR) and K^{+} movement (i.e., Erg). Extensive research has shown that cholesterol can influence ion channel function either by changing membrane properties or through direct channel interaction (reviewed by Levitan et al., 2010, 2014). Therefore, the addition of cholesterol here could be playing a direct role in ion movement essential to the cardiac cycle. However, follow up work needs to be conducted to elucidate this mechanism.

Before independent feeding commences (~120 hpf in zebrafish), zebrafish are entirely reliant on yolk-derived cholesterol and yolk reserves for cholesterol synthesis. Within this study, by quantifying the two-dimensional yolk area in phenanthrene exposed zebrafish,

we discovered a concentration-dependent increase in yolk area with phenanthrene exposure by 72 hpf (Fig. 3-6). Several previous studies have found disruption of yolk utilization in fish embryos following oil exposure. Carls and Thedinga (2010) described delayed yolk consumption in oil-exposed pink salmon (*Oncorhynchus gorbuscha*) embryos, which they hypothesized was due to developmental delays associated with the exposure. Sørhus et al. (2017) similarly detected diminished yolk absorption in oil exposed Atlantic haddock embryos at 3 d post-hatch, which coincided with the enrichment of transcriptomic pathways related to lipid metabolism. However, in mahi-mahi exposed to crude oil, time to hatch was not impacted, yet 2 days post-fertilization embryos displayed increased yolk utilization, perhaps due to heightened metabolic demand (Pasparakis et al., 2017). These differences between species and life stages may be influenced by changes in metabolic demand and the severity of PAH-induced malformation. However, altered yolk utilization could be a possible driver of transcriptomic predictions related to cholesterol and lipid metabolism at later developmental stages. In our study, reduced yolk utilization may be driven by diminished blood circulation in developing phenanthrene exposed embryos. Blood circulation in fish embryos can be impacted by exposure to phenanthrene (Incardona et al., 2004) or crude oil (Incardona et al., 2005). Because the most substantial effects on yolk area in our study are observed following the onset of circulation, the overall reduction in yolk utilization may be due to diminished circulation, thus downstream of known phenanthrene-induced cardiotoxic effects. However, the measurement of yolk area does not give insight into the lipid content of the yolk or how this may be changed by phenanthrene exposure.

Together, compounds that act by both specific and nonspecific action are capable of producing a phenotype (edema, reduced heart rate, impaired swim bladder inflation, impaired yolk utilization) similar to what we observe with phenanthrene exposure in zebrafish embryos (Horie et al., 2017; Sant and Timme-Laragy, 2018). Additionally, the specificity of the phenanthrene induced phenotype beyond baseline effects has recently been brought into question (Meador and Nahrgang, 2019), and a shared mechanism with other lipophilic compounds cannot be ruled out. However, phenanthrene has been shown to significantly affect excitation-contraction coupling in fish cardiomyocytes, while exposure to other PAHs did not produce the same effects (Brette et al., 2017). More broadly, a metanalysis of 33 RNA sequencing studies investigating 60 different toxicants did not identify cholesterol biosynthesis as a commonly impacted pathway (Schüttler et al., 2017). Therefore, disruption of cholesterol synthesis may be specific to phenanthrene or oil exposure. Our results demonstrate that the addition of cholesterol partially rescues the effects of phenanthrene on heart rate, giving further insight into the mechanism by which phenanthrene may disrupt excitation-contraction coupling in the heart. Perhaps disruption of cholesterol, or more simply phenanthrene disruption of membrane properties, causes malfunction of individual ion channels, which may be restored upon addition of cholesterol. It would be interesting to follow up on this result in future studies using isolated cardiomyocytes.

In conclusion, this study demonstrates that phenanthrene exposure to zebrafish embryos impairs yolk utilization and causes dysregulation of several genes in the cholesterol biosynthetic pathway. Although these changes in gene expression did not alter whole-

mount staining of cholesterol, the pretreatment of cholesterol partially mitigated the effects of phenanthrene on heart rate. Together these data provide evidence that lipid dysregulation could contribute to PAH-induced developmental toxicity. Future studies evaluating yolk composition are needed to better understand nutrient availability to embryos exposed to phenanthrene or crude oil.

Chapter 4: Exposure to *Deepwater Horizon* crude oil increases free cholesterol in larval red drum (*Sciaenops ocellatus*)

4.1 Abstract

The 2010 *Deepwater Horizon* oil spill polluted thousands of miles of shoreline along the northern Gulf of Mexico, coinciding with the spawning season of many fish species living in the region, including red drum (*Sciaenops ocellatus*). Red drum develop rapidly and are sensitive to crude oil exposure during the embryonic and larval periods. This study investigates the predictions from recent transcriptomic studies that processes related to cholesterol synthesis are impacted by oil exposure in fish embryos. We found that red drum embryos exposed for 72-hours to ΣPAH_{50} 3.55 - 15.45 µg L^{-1} exhibited significantly increased pericardial area, a cardiotoxicity metric, but the expression of several genes targeted in the cholesterol synthesis pathway were not affected. However, whole-mount staining revealed significant increases in free cholesterol throughout the larval body (ΣPAH_{50} 4.71 – 16.15 µg L^{-1}), and total cholesterol followed an increasing trend (ΣPAH_{50} 3.55 - 15.45 µg L^{-1}). Cholesterol plays a critical role in fish embryo development and ion channel function. Therefore, the disruption of cholesterol homeostasis, as observed here, could play a role in the oil toxicity phenotype observed across many fish species.

4.2 Introduction

The 2010 *Deepwater Horizon* (*DWH*) oil spill released over 3 million barrels of oil offshore into the Gulf of Mexico, making it the largest marine oil spill in US history

(Trustees, 2016). While pelagic habitats were immediately impacted, with time, crude oil was pushed to the northern shore of the Gulf of Mexico and oiled at least 2113 km of shoreline (Nixon et al., 2016), including nearshore nursery habitats for red drum (*Sciaenops ocellatus*). One year post-spill, moderate to heavy oiling was still observed on 78 km of coastline (Michel et al., 2013), suggesting that nearshore species could have been exposed to oiling in some regions for multiple spawning seasons.

Developing embryos are especially vulnerable to crude oil exposure as they are rapidly forming organ systems that will define organism function for the remainder of the individual's life. While post-metamorphosis fish (juveniles and adults) are also susceptible to oil exposure, they have additional defenses such as a fully developed liver and scales that can provide protection that embryos and larvae do not have (Incardona and Scholz, 2018). The *DWH* oil spill coincided with the spawning season of many gulf fish (Rooker et al., 2013), including red drum, which spawn nearshore in late summer and early fall. Red drum are ecologically and economically valuable and a managed fishery within the gulf region (National Marine Fisheries Service, 2018).

Many fish embryos, including red drum, display a conserved toxicity phenotype following oil exposure characterized by pericardial edema, bradycardia, reduced stroke volume, reduced cardiac output, and craniofacial deformities (Incardona and Scholz, 2018; Khursigara et al., 2017). Impaired embryonic development due to oil exposure has been linked to reduced swimming performance in surviving juvenile and adult fish (Hicken et al., 2011; Incardona et al., 2015; Mager et al., 2014). Understanding the

mechanisms underlying these outcomes can help predict species sensitivity, develop biomarkers, and generate risk assessments. While transmembrane ion transport impairment has been observed (Brette et al., 2014), the specific molecular initiating events underlying oil-induced developmental toxicity are currently unknown.

Transcriptomic analyses allow for a broad look at the organismal response to toxicant exposure that can reduce bias when hypothesizing about potential toxicity mechanisms. Comparing recent transcriptomic studies in embryos exposed to crude oil, cholesterol-related pathways were consistently enhanced across several species, including red drum (*Sciaenops ocellatus*; Xu et al. 2017), mahi-mahi (*Coryphaena hippurus*; Xu et al. 2016), Atlantic haddock (*Melanogrammus aeglefinus*; Sørhus et al. 2017), and sheepshead minnow (*Cyprinodon variegatus*; Jones et al. 2020) embryos and larvae. Cholesterol is known to play a critical role in fish development. Zebrafish embryos exposed to cholesterol-reducing drugs develop a similar phenotype as those exposed to oil, including pericardial edema, bradycardia, smaller heads, and reduced eye area (Maerz et al., 2019). Additionally, bradycardia induced by phenanthrene – a polycyclic aromatic hydrocarbon (PAH) found in crude oil – can be partially rescued by pretreatment with cholesterol, further indicating that cholesterol may contribute to oil-induced toxicity (McGruer et al., 2021). Previous work in mahi-mahi embryos exposed to ΣPAH_{50} 8.3 $\mu g\ L^{-1}$ demonstrated a significant reduction in total cholesterol at 96 hours post-fertilization (hpf) (McGruer et al., 2019). Furthermore, yolk-sac stage polar cod (*Boreogadus saida*) were found to have significant increases in sterols following oil exposure (Laurel et al., 2019). However,

these studies did not account for the unused yolk-sac or different cholesterol pools available to the developing larvae.

In the present study, we investigated whether the predicted transcriptional response translated into the disruption of cholesterol homeostasis in red drum larvae. Using oil collected from the *DWH* surface slick at concentrations that induce visible cardiotoxicity, we assessed the regulation of the cholesterol synthesis pathway, quantified total cholesterol in whole larval homogenates, and visualized the free cholesterol distribution and concentration through whole-mount staining. Using these methods, we evaluated the effects of oil on cholesterol homeostasis in red drum at a stage when the yolk is almost entirely absorbed, but feeding has not yet commenced. Additionally, we provided conclusions concerning the impact of oil on different pools of cholesterol in the larvae, giving insight into the role cholesterol may play in developmental toxicity.

4.3 Methods

4.3.1 Animals

Red drum broodstock were maintained at the Texas Parks and Wildlife-CCA Marine Development Center in Corpus Christi, TX. Following fertilization, red drum embryos were collected and then transferred with aeration to the University of Texas Marine Science Institute. Embryos were handled and visually assessed as described in Khursigara et al. (2017). Briefly, embryos were disinfected with formalin (1ppt) for 1 h. Before oil

exposure, embryo quality and viability were visually assessed, and spawns with minimal fertilization or viability were not used.

4.3.2 *DWH* oil exposure

Red drum embryos were exposed to naturally weathered oil from the surface (OFS) by preparing high-energy water-accommodated fractions (HEWAFs). OFS was collected from the Gulf of Mexico on June 29, 2010, from the hold of barge CT02404 and used to create two sets of exposures, the first on November 12, 2018, and the second on July 19, 2019. HEWAF solutions for both exposures were produced as previously described in Incardona et al. (2013) using a commercial blender. 1 g of oil was loaded per L of seawater (35ppt). Nominal concentrations of 0.625%, 1.25%, and 2.5% HEWAF were produced by diluting the 100% HEWAF with seawater. Exposures were conducted in 1 L beakers with 40 embryos for November 2018 exposures and 30 embryos for July 2019 exposures per beaker with treatments starting at 12 hpf. Each concentration contained six test replicates. Exposures were maintained at 25 °C and 35 ppt salinity with a 14 h:10 h light:dark photoperiod. Larval survival was evaluated daily. All endpoints were assessed at 72 hpf, when red drum larvae have nearly depleted their yolk-sac and transition to exogenous feeding. All experiments were conducted per University of Texas at Austin Institutional Animal Care and Use Committee (IACUC) approved protocols (AUP-2014-00375).

4.3.3 Water chemistry analysis

ΣPAH_{50} concentrations were determined following protocols described by Xu et al. (2017). First, diluted HEWAF solutions were sampled immediately after preparation for PAH analysis. Samples were stored at 4 °C in 250 mL amber bottles until analysis by ALS Environmental (Kelso, WA). Gas chromatography/mass spectrometry-selective ion monitoring (GC/MS-SIM) was used to quantify 76 individual PAHs. A subset of 50 PAH analytes were then totaled to determine the reported ΣPAH_{50} concentrations. Two separate HEWAF mixtures, each with three dilutions, resulted in the six ΣPAH_{50} concentrations reported in this study. PAH concentrations of the 50 analytes measured are graphically represented in Appendix C (Fig. C-3). Temperature, pH, dissolved oxygen, and salinity were measured daily and are reported in Appendix C (Table C-2).

4.3.4 Morphological assessment

Morphological assessments, gene expression, and total cholesterol quantification were conducted on larvae from November 2018 exposures. At 72 hpf, a subset of larvae (5 individuals per test replicate) were anesthetized in 250 mg L^{-1} MS222 (buffered with 500 mg L^{-1} NaHCO3) for imaging. Larvae were oriented laterally in 3% methylcellulose and imaged using a Nikon SMZ800N microscope and a Nikon Digital Sight DS U-3 instrument. Two-dimensional pericardial area was quantified using ImageJ (version 1.53c). Representative images outlining the region measured can be found in Appendix C (Fig. C-1).

4.3.5 RNA isolation and qPCR

The remaining 72 hpf larvae in the test replicates were pooled with another test replicate of the same treatment to create a biological replicate (2 test replicates per biological replicate; n = 3 biological replicate per treatment). Biological replicates were equally divided for quantitative polymerase chain reaction (qPCR) analysis and total cholesterol quantification.

Total RNA was extracted for qPCR from larval homogenates using the RNeasy Mini kit from Qiagen (Valencia, CA) and associated protocols. A NanoDrop (Thermo Fisher Scientific; model ND-1000) was used to assess RNA quality and quantity, and RNA was stored at −80°C. Complementary (c)DNA was reversed transcribed from 1 µg of total RNA using the Promega Reverse Transcription System kit (Madison, WI). cDNA was diluted with nuclease-free water and subsequently stored at −20°C until qPCR was performed.

Primers for 3-hydroxy-3-methylglutaryl-coenzyme A reductase (*hmgcr*), farnesyl-diphosphate farnesyltransferase 1 (*fdft1*), squalene epoxidase (*sqle*), and elongation factor 1 α (*ef-α*) were designed using NCBI Primer-BLAST. Primer sequences and amplicon length are provided in Appendix C (Table C-1). These targets were evaluated based on their critical roles in cholesterol biosynthesis. qPCR analysis of all genes was performed using the thermocycling conditions described in McGruer et al. (2019): 95 °C for 5 min, followed by 40 cycles of 95 °C for 10 s and 60 °C for 30 s. Data were normalized using *ef-α* and analyzed using the $2^{-\Delta\Delta CT}$ method (Livak & Schmittgen, 2001). Melt curves and

1.2% agarose gel electrophoresis were used to assess product formation and primer specificity.

4.3.6 Total cholesterol quantification

Total cholesterol (cholesteryl esters and free cholesterol) was quantified in whole larval homogenates as described in McGruer et al. (2019). The Cell Biolabs, Inc. (San Diego, CA) "Total Cholesterol Assay Kit (Colorimetric)" and associated "tissue lysates" protocol was used for lipid extraction and total cholesterol quantification. Three biological replicates were evaluated per treatment with 30 – 35 embryos per replicate. To summarize, larvae were homogenized in 200 µL chloroform:isopropanol:Triton x-100 (7:11:0.1) to extract lipids. Cholesterol standards provided with the assay kit were used to prepare standard curves and calculate total cholesterol (µg) in each sample. Total cholesterol was normalized to total protein (mg) to account for intersample variability. The total protein of extracted samples was quantified with the Pierce™ BCA Protein Assay Kit (Thermo Scientific, Rockford, IL).

4.3.7 Filipin staining

Filipin staining was conducted on larvae from the July 2019 exposures. Thirty, 72 hpf larvae were pooled per replicate (Control n = 3; Oil exposed n = 5 or 6) and fixed in zinc-based formalin Z-fix for 24 h (Anatech LTD). Larvae were then transferred to 1x phosphate buffer solution (PBS) for storage until staining. Fixed larvae were subsequently stained with the cholesterol reporter molecule filipin using previously

described protocols (McGruer et al., 2021). Fourteen larvae were included in each staining basket. Larvae were imaged immediately following the completion of the staining protocol to prevent signal loss. Precautions were taken to minimize unnecessary light in the room where imaging was conducted, and each larva was mounted in 4% methylcellulose and imaged individually to minimize photobleaching. Images were collected under both transmitted and UV light.

The larval body was outlined in the image taken under transmitted light. Then the outline was overlayed on the fluorescent image to quantify mean fluorescence within the larval body using ImageJ (representative outlines provided in Appendix C Fig. C-2). Background corrected fluorescence values were calculated by subtracting the mean background fluorescence (3 individual measurements) from the mean larval fluorescence.

4.3.8 Statistical analyses

Statistical analyses were conducted in R (R Core Team, 2020). Assumptions of normality were assessed using Shapiro Wilk's test. Homogeneity of variances was determined using Levene's test. Differences in relative gene expression, filipin staining intensity, and total cholesterol were evaluated by one-way analysis of variance (ANOVA). If the ANOVA revealed statistical differences, multiple comparisons were assessed using Tukey's honest significant difference test. Survival and pericardial area data were analyzed by the nonparametric Kruskal-Wallis test followed by Dunn's Test of Multiple Comparisons due to violations of ANOVA assumptions. A significant difference was accepted at $p < 0.05$. All data are presented as means ± standard error of the mean (SEM).

4.4 Results

4.4.1 Oil composition

ΣPAH_{50} concentrations determined from OFS HEWAF dilutions were similar across the two sets of exposures. Analysis of the 2018 HEWAF diluted to 0.625% HEWAF, 1.25% HEWAF, and 2.5% HEWAF revealed ΣPAH_{50} concentrations of 3.55, 7.45, and 15.45 µg L^{-1}, respectively. The same dilutions produced slightly higher concentrations in the 2019 HEWAF, which yielded ΣPAH_{50} concentrations 4.71, 8.15, 16.15 µg L^{-1}, respectively. Across both dates and all dilutions, three-ring PAHs (i.e., phenanthrenes/anthracenes) dominated the quantified PAH component of the HEWAF, comprising ~ 68-80% of total PAHs (Appendix C Fig. C-3).

4.4.2 Embryo survival and cardiotoxicity

Embryo survival at the end of the 72-h exposure ranged from 71.7% ± 4.4 to 97.9% ± 1.2 across all treatments and the two sets of exposures (Fig. 4-1). Survival did not significantly differ between treatments in either the 2018 or 2019 exposures when tested separately by date or when combined.

Pericardial area was quantified as a metric of sublethal cardiotoxicity following 72 h exposure to ΣPAH_{50} 0 – 15.45 µg L^{-1}. HEWAF treatment (ΣPAH_{50} 3.55 – 15.45 µg L^{-1}) significantly increased pericardial area by an average of 121% ± 17.6 relative to the control (Fig. 4-2).

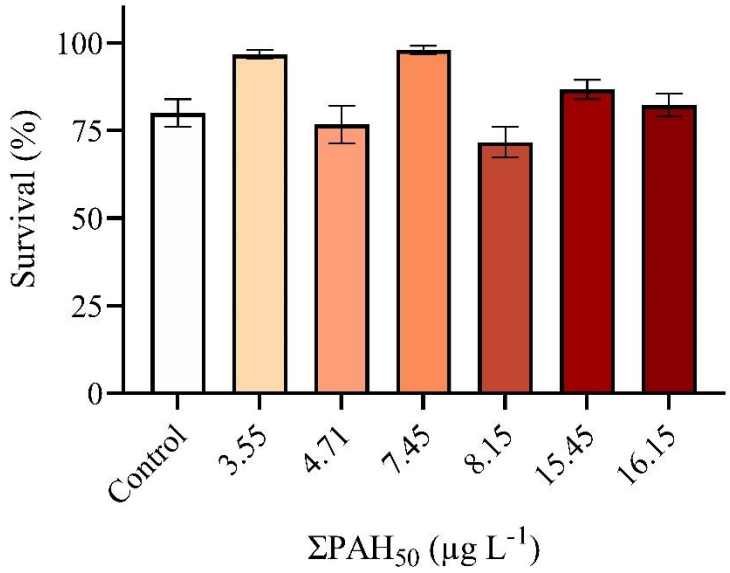

Figure 4-1 Effects of 72 h HEWAF exposure on red drum embryo survival. Survival (%) calculated within each exposure beaker. N = 11 in control treatment; n = 6 in ΣPAH_{50} 3.55 – 16.15 µg L^{-1} treatments. Data were analyzed by a Kruskal-Wallis Rank Sum Test, followed by Dunn's Kruskal-Wallis Test of Multiple Comparisons. Error bars represent ± SEM.

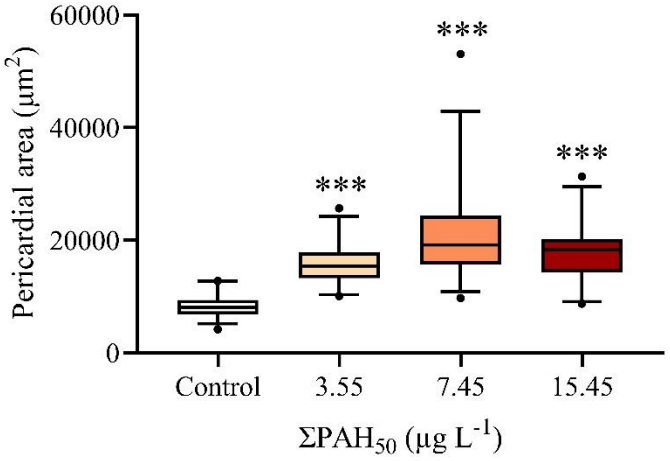

Figure 4-2 Effects of 72 h HEWAF exposure on red drum embryo pericardial area (μm^2) (n = 30 per treatment). Whiskers represent 5th and 95th percentiles. Data were analyzed by a Kruskal-Wallis Rank Sum Test, followed by Dunn's Kruskal-Wallis Test of Multiple Comparisons. ***p<0.001.

4.4.3 Gene expression (qPCR)

The relative mRNA expression of several key genes involved in cholesterol synthesis was assessed in 72 h red drum embryo homogenates exposed to ΣPAH_{50} 0, 3.55, and 15.45 µg L^{-1}. Expression of 3-hydroxy-3-methylglutaryl-coenzyme A reductase (*hmgcr*), farnesyl-diphosphate farnesyltransferase 1 (*fdft1*), squalene epoxidase (*sqle*) all followed a similar decreasing trend. However, mRNA expression was not significantly altered following HEWAF exposure in any genes assessed relative to the control (Fig. 4-3).

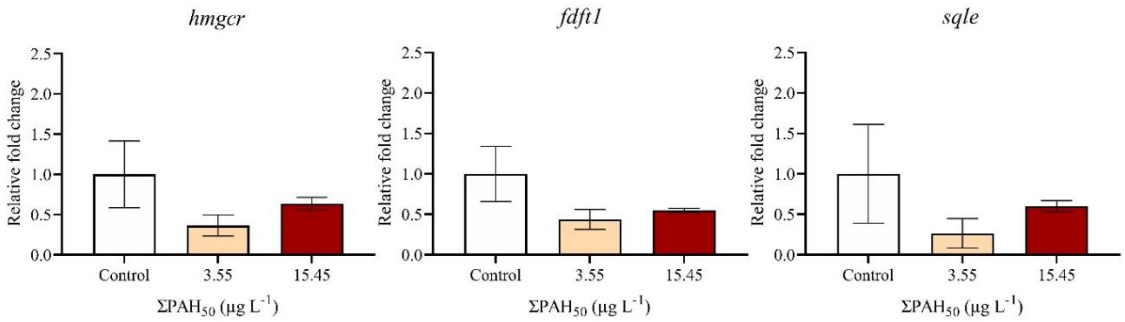

Figure 4-3 Effects of 72 h HEWAF exposure on gene expression in the cholesterol biosynthetic pathway in 72 hpf red drum embryo homogenates (n = 3 per treatment). Values are presented as relative fold change of (A) *HMG-CoA reductase* (*hmgcr*) (B) *farnesyl-diphosphate farnesyltransferase 1* (*fdft1*)*, (C) squalene epoxidase* (*sqle*). Data were analyzed by 1-way ANOVA. Error bars represent ± SEM.

4.4.4 Total cholesterol quantification

Total cholesterol, which encompasses both cholesteryl esters and free cholesterol, normalized to total protein was quantified in control and HEWAF (ΣPAH_{50} 3.55 – 15.45 µg L^{-1}) exposed fish. Normalized total cholesterol displayed an increasing trend in homogenates exposed to HEWAF ΣPAH_{50} 3.55 (37.1 ± 6.0 µg mg^{-1}), 7.45 (33.3 ± 6.5 µg

mg^{-1}), 15.45 (34.9 ± 1.7 µg mg^{-1}), relative to the control (25.8 ± 2.1 µg mg^{-1}), though no significant difference was found ($p = 0.4$) (Fig. 4-4).

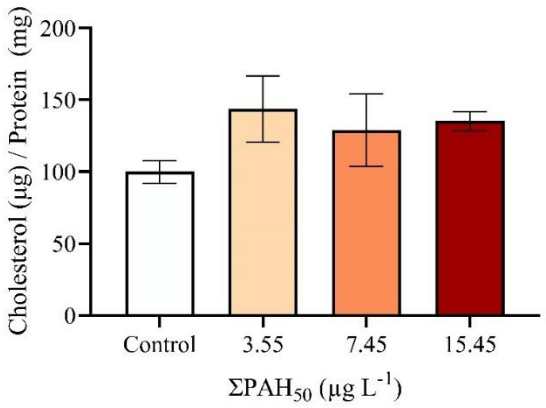

Figure 4-4 Total cholesterol (µg) normalized to total protein (mg) in control and HEWAF treatments (n = 3 per treatment). Data were analyzed by 1-way ANOVA. Error bars represent ± SEM.

4.4.5 Filipin staining

Filipin is a naturally fluorescent polyene macrolide that stains free 3-*β*-hydroxysterols and has been previously used to visualize free cholesterol in fixed cells and tissues (Gimpl and Gehrig-Burger, 2007) and whole-mount zebrafish larvae (McGruer et al., 2021). Here, filipin was used to visualize free cholesterol, separate from cholesterol esters, in 72 hpf larvae. Together, fluorescence from filipin staining was found to be significantly increased in all HEWAF exposed groups (ΣPAH_{50} 4.71 – 16.15 µg L^{-1}) relative to the control (81.4 ± 1.0) ($p \leq 0.007$). However, mean fluorescence did not significantly differ between HEWAF exposures (ΣPAH_{50} 4.71(87.3 ± 0.79), 8.15 (88.6 ± 0.80), 16.15 (87.6 ± 0.86) µg L^{-1}) (Fig. 4-5B). Representative images are presented in Figure 4-5A.

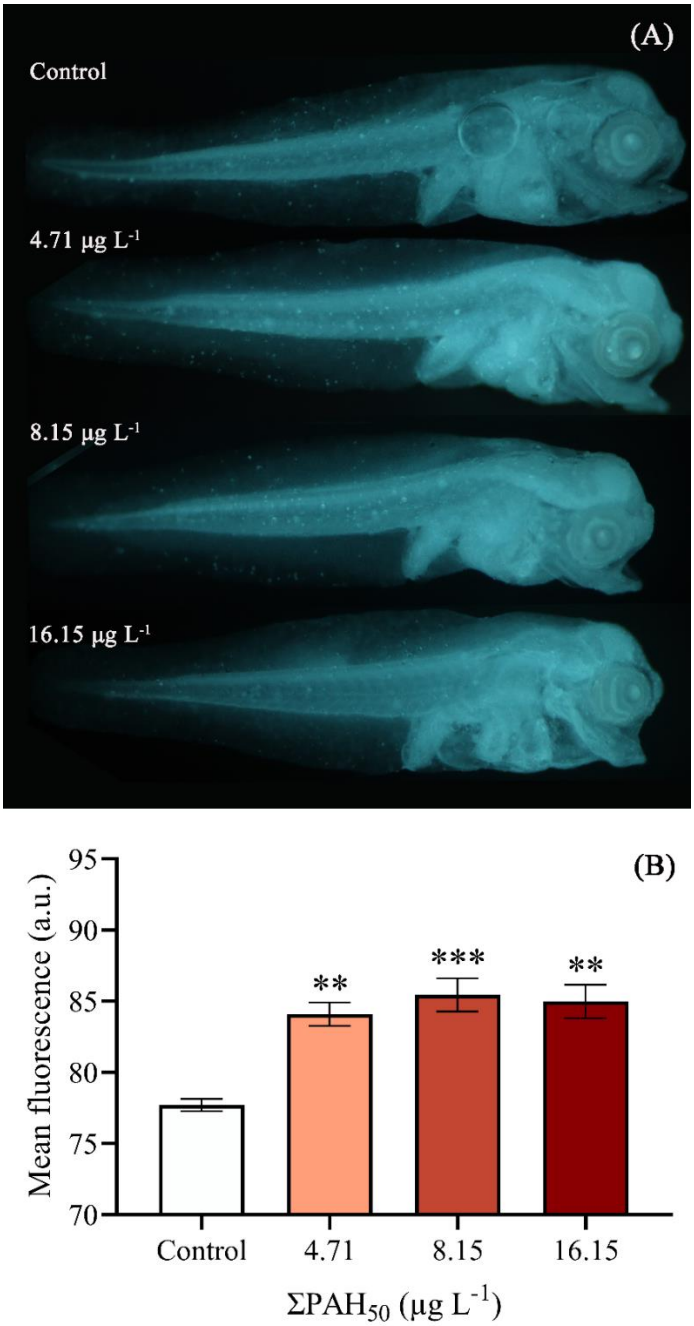

Figure 4-5 (A) Representative images of filipin staining in control and HEWAF exposed 72 hpf red drum embryos. (B) Mean fluorescence intensity of filipin staining in the embryo body (arbitrary units (a.u.)) (n = 3 in control treatment; n = 6 in ΣPAH_{50} 4.71 – 8.15µg L^{-1}; n = 5 ΣPAH_{50} 16.15 µg L^{-1}). Statistical significance was determined by 1-way ANOVA, followed by a Tukey's honestly significant difference test. Error bars represent ± SEM. $^{**}p<0.01$, $^{***}p<0.001$.

4.5 Discussion

Over the past several years, a number of studies have assessed the transcriptomic response of developing fish to crude oil exposure. Many of these studies predicted cholesterol biosynthesis to be one of the top impacted pathways in early life stage fish following oil exposure, including in red drum (Xu et al., 2017, 2019). In the present study, red drum larvae exposed to DWH slick oil displayed elevated free cholesterol levels relative to controls. However, the expression of several genes in the cholesterol biosynthetic pathway was not altered. The discovery of these changes gives evidence that the predicted pathway enhancement in previous transcriptomics studies translates into the disruption of cholesterol, which may contribute to oil-induced maldevelopment of red drum embryos.

Survival of 72 h red drum embryos following OFS HEWAF exposure was greater than 70% across all exposures (ΣPAH_{50} 0 - 16.15 μg L^{-1}) and consistent with the estimated LC_{50} 19.1 μg L^{-1} in 72 h red drum embryos (Khursigara et al., 2017). While survival was not significantly affected, pericardial area was significantly increased at all doses assessed (ΣPAH_{50} 3.55 - 15.45 μg L^{-1}), again consistent with an estimated EC_{50} value of 2.4 μg L^{-1} (Khursigara et al., 2017). Though not measured in this study, pericardial edema incidence likely indicates a concurrent reduction in cardiac output and occurrence of craniofacial deformities as these endpoints were found to be similarly sensitive to OFS HEWAF exposure in red drum (Khursigara et al., 2017). The presence of pericardial edema in embryos exposed to crude oil has been linked to reductions in juvenile or adult

swimming performance in at least pink salmon, pacific herring, and mahi-mahi (Incardona et al., 2015; Mager et al., 2014). Therefore, the doses used in this study may be relevant to effects at later life stages.

Transcriptomic analysis of 72 h red drum embryos predicted the cholesterol biosynthesis pathway was enhanced following exposure to ΣPAH_{50} 4.74 µg L^{-1} (Xu et al., 2017). In the present study, we targeted *hmgcr, fdft1*, and *sqle* with qPCR. Each of these genes encodes key enzymes in the cholesterol synthesis pathway. *Hmgcr* catalyzes a rate-limiting reaction at the beginning of the pathway. Enzymes associated with f*dft1* and s*qle* catalyze successive reactions further along the pathway. Despite previously finding increased expression of *sqle* (log2fold = 1.541; p-value = 2E-07) and *hmgcr* (log2fold = 0.7255; p-value = 8E-06) in 72 h HEWAF exposed red drum (Xu et al., 2017), we did not observe changes in the expression of these genes in this study (ΣPAH_{50} 3.55 - 15.45 µg L^{-1}). Additionally, we targeted *fdft1* because it was significantly altered in zebrafish exposed to phenanthrene (McGruer et al., 2021) and diesel WAF (Mu et al., 2018). However, *fdft1* was not altered in red drum exposed to HEWAF (log2fold = 0.159; p-value = 0.499) (Xu et al., 2017), and we did not observe significant changes to *fdft1* expression in this study. Predictions of pathway enhancement in the previous transcriptomic studies were based on enhanced expression throughout the entire cholesterol synthesis pathway, which includes >20 enzymes (Xu et al., 2017). Here, we are limited to only looking at the expression of a few select genes. Therefore, there may be molecular changes we are not observing. Moreover, there may be variation between experiments due to differences in dose or variability in embryo yolk composition.

Despite a lack of a measurable difference in transcription, measuring both total cholesterol and free cholesterol allowed for a better understanding of how oil exposure may affect cholesterol concentration and distribution. Free cholesterol is unesterified cholesterol that can be readily incorporated into cell membranes, while total cholesterol is the sum of both free cholesterol and cholesteryl esters. Interestingly, we found filipin staining of free cholesterol in whole-mount larvae (whole-body) was significantly increased at all doses tested (ΣPAH_{50} 4.71 – 16.15 μg L^{-1}). By comparison, total cholesterol measured in larval homogenates was not affected by HEWAF exposure (ΣPAH_{50} 3.55 – 15.45 μg L^{-1}) but did follow an increasing trend, adding support to our findings from filipin staining. Together, these results support predictions that cholesterol is impacted by oil exposure and demonstrates that free cholesterol levels are elevated with crude oil exposure.

Previous studies have also measured increases in free cholesterol in the absence of differential expression of enzymes in the synthesis pathway (Qian et al., 2018). Cholesterol biosynthesis is a complex and energetically expensive process requiring more than 20 enzymes. Nearly all genes encoding cholesterol synthesis enzymes are targets of sterol regulatory element-binding protein (SREBP) transcription factors, which allows for coordinated activation of the pathway. However, processes beyond synthesis regulate cellular cholesterol and may explain the increase in free cholesterol that we observed. Outside of the transcriptional response, disturbance to cholesterol homeostasis may be produced by disrupting cholesterol transport (i.e., import and export), disruption to cholesterol metabolism, or post-transcriptional regulation of cholesterol synthesis

enzymes. Future studies would need to be conducted to elucidate the mechanism of cholesterol accumulation.

We know that either an abnormal increase or decrease in cholesterol can cause adverse effects in both fish and mammals (Campos et al., 2016; Maerz et al., 2019; Maxfield and Tabas, 2005). Interestingly, both depletion and excess loading of cholesterol have been implicated in disordered neurodevelopment (Ko et al., 2005), suggesting that sustained excess cholesterol in red drum could impair neurodevelopment. Interestingly, red drum embryos exposed to ΣPAH_{50} 2.72 $\mu g\ L^{-1}$ slick oil displayed a reduced optomotor response (OMR) at 12 days post-hatch relative to controls (Magnuson et al., 2018). Complex neural networks drive OMR, and the resulting behavioral response could be affected by impaired neural development (Naumann et al., 2016). Additionally, larval red drum exposed to *DWH* crude oil displayed increased risk-taking behavior and reduced prey-capture ability, which again could be downstream of impaired cognitive function (Rowsey et al., 2019). Together, these studies suggest a link between neurological development and higher-level behavioral changes which may influence ecological survival.

Additionally, both increases and decreases in free cholesterol have been shown to affect cellular ion movement in cardiomyocytes and other muscle cells by direct or indirect interaction with ion channels (Levitan et al., 2014, 2010). The currently proposed mechanism of cardiac dysfunction in oil-exposed fish is through impairment of Ca^{2+} and K^{+} movement, causing arrhythmias and reduced myocyte contractility (Brette et al.,

2014). Therefore, increased whole-body cholesterol levels are a potential mechanism of cardiac disruption. Ultimately, disruption of heart function can permanently alter morphology and subsequent function (Incardona and Scholz, 2017).

In conclusion, disruption of the nutrient environment, including cholesterol, can have lasting impacts on developing organisms (Sant and Timme-Laragy, 2018). Previous studies have shown species- and stage-dependent impacts of oil on cholesterol/sterols but could not differentiate between nutrients contained in the unused yolk-sac and those utilized by the embryo (Laurel et al., 2019; McGruer et al., 2019). In the present study, we found that free cholesterol levels are elevated in red drum larvae at a stage where the yolk-sac has been largely absorbed, indicating potential developmental consequences. However, the mechanisms by which cholesterol is elevated are unknown, and the downstream effects of elevated cholesterol should be considered further.

Chapter 5: Summary and conclusions

5.1 Summary

The overall goal of the research presented was to progress the understanding of the mechanisms underlying crude oil and polycyclic aromatic hydrocarbon (PAH) induced toxicity in fish. The studies described in chapters 2-4 were based on the hypothesis that compounds in crude oil, particularly PAHs, may alter cholesterol homeostasis in developing fish embryos producing a well-documented developmental toxicity phenotype. Experiments were carried out in the model organism, zebrafish and in mahi-mahi and red drum, two species ecologically relevant to the Gulf of Mexico. By investigating the disruption of cholesterol homeostasis as a potential mechanism of toxicity, we have advanced knowledge of the impacts of petrogenic pollution.

Chapter 2 presents the first study in any species to investigate the multiple predictions that cholesterol biosynthesis is impaired in fish embryos exposed to crude oil. In this experiment, mahi-mahi embryos were exposed to a crude oil water accommodated fraction of ∑PAH 1.31 - 8.3 μg L^{-1}, a lower concentration than that used in the previous transcriptomic study (∑PAH 17.62 μg L^{-1}; Xu et al., 2016). Embryos were exposed shortly after fertilization until 96 hours post-fertilization (hpf), a time point in which mahi-mahi have used most of their yolk but have not begun exogenous feeding. We observed significant increases in the expression of *fdft1*, which encodes a key enzyme in the cholesterol synthesis pathway at ∑PAH concentrations of 2.62 μg L^{-1} and 5.99 μg L^{-1}. Interestingly, we found that exposure to the highest tested HEWAF concentration (∑PAH

8.3 μg L^{-1}) significantly reduced total cholesterol in whole larval homogenates. However, ∑PAH 8.3 μg L^{-1} also caused significant mortality in this experiment, despite a much higher estimated LC_{50} of 19.5 μg L^{-1} predicted in previous studies (Xu et al., 2016). Although it is difficult to ascertain whether the reduction in total cholesterol observed here was influenced by larval mortality, many studies have predicted changes in the cholesterol biosynthetic pathway at sublethal doses. Together, we were intrigued by our findings and decided to pursue our central hypothesis further in the model organism zebrafish.

Zebrafish are an established model organism that lends itself to high throughput experiments and method optimization. Easily cultured in a lab setting, zebrafish spawn year-round, and a wide range of molecular tools have been optimized for the species. By contrast, developmental experiments in marine species such as mahi-mahi and red drum rely on a wild-caught broodstock maintained in dedicated aquaculture facilities, and spawning occurs seasonally, limiting experimental progress. In chapter 3, zebrafish embryos were exposed to the model cardiotoxic PAH, phenanthrene, to further explore the contributions of cholesterol to oil-induced developmental toxicity. In summary, zebrafish embryos exposed from 6 – 72 hpf to 12 or 15 μM phenanthrene (2139 and 2673 μg L^{-1} respectively) displayed bradycardia and pericardial edema, indicators of cardiotoxicity. Similar to our findings in mahi-mahi, the expression of *fdft1* was significantly increased at the 15 μM phenanthrene concentration. However, expression of *hmgcra*, which encodes an enzyme that acts early in the synthesis pathway, was

significantly reduced with exposure to both 12 and 15 µM phenanthrene. The differential expression of *fdft1* and *hmgcra* indicates that the cholesterol synthesis pathway is altered with phenanthrene exposure alone. However, the observation of bidirectional regulation within the pathway is possibly due to post-transcription regulation by microRNAs (Xu et al., 2019) and highlights the limitations of only looking at one developmental stage.

Using zebrafish, we optimized whole-mount staining of 24 – 72 hpf embryos to visualize the localization of free cholesterol in the embryo body. This approach has advantages over using whole-larval homogenates as it offers the ability to focus on specific regions within the larval body. For example, it is possible to exclude the yolk-sac, which contains high concentrations of cholesterol but has not yet been utilized by the developing embryo. Additionally, staining was conducted using the molecule filipin, which stains free cholesterol. This approach allowed us to separate different pools of cholesterol within the larvae, such as free cholesterol versus cholesterol esters, the storage form of cholesterol. However, no significant differences were observed in filipin staining in the embryo body following exposure to 12 µM phenanthrene, relative to vehicle control, at any stage tested (24 to 72 hpf). While this perhaps appears in contrast to our findings from chapter 2, where oil-exposed mahi-mahi embryos displayed a reduction in total cholesterol, there are several key differences between these studies. The first obvious difference is the composition of the solution each species was exposed to. Zebrafish were exposed to a single compound, phenanthrene. Phenanthrene is a tricyclic PAH used to model crude oil exposure as it is thought to be the critical cardiotoxic component of crude

oil. By contrast, in chapter 2, mahi-mahi were exposed to a complex aqueous mixture produced from whole crude oil. While the PAH component of the oil mixture was dominated by tricyclic PAHs (>70%) (Appendix A Figs. A-1 and A-2), there are many other compounds in crude oil, including a sizeable unknown fraction, termed the "unresolved complex mixture." The complexity of this exposure may contribute to differences between the studies. Conducting experiments with single model-PAHs such as phenanthrene allows us to narrow our experimental focus. However, whole-oil exposures allow us to view the biological response to the entire mixture, even if parsing apart individual toxicants is impossible.

Differences in the developmental stages of mahi-mahi in chapter 2 and zebrafish in chapter 3 further complicates our comparisons between these studies. The response of mahi-mahi to oil exposure was assessed at 96 hpf, a stage where the yolk was mostly utilized. By contrast, 72 hpf zebrafish still have a substantial unused yolk-sac, which likely contributes to the nutrient environment of the embryos when sampled. Cholesterol also comprises approximately 40% of all lipids in the zebrafish yolk at fertilization (Fraher et al., 2016), which is much higher than embryos of many other marine fish species (3.1 - 11.7% total lipids; Tocher and Sargent, 1984). Additionally, mahi-mahi exposed to crude oil have been reported to increase yolk utilization compared with seawater controls (Pasparakis et al., 2017). By contrast, phenanthrene exposed zebrafish embryos underutilized the yolk-sac compared with controls in chapter 3. While challenging to compare between different stages and doses, the ability to utilize the yolk

is an intriguing outcome of toxicant exposure, and disruption of yolk usage likely alters the nutrient profile of the developing embryo. The effect of toxicant exposure on yolk utilization, yolk composition, and embryo lipid profile is an interesting avenue of research in developmental toxicology that should be explored further.

Though we did not observe changes in staining for free cholesterol following phenanthrene exposure in zebrafish, we did find that cholesterol could partially mitigate phenanthrene-induced cardiotoxicity. Reduced heart rate (bradycardia) is a common effect of exposure to crude oil or phenanthrene alone in fish embryos (Incardona et al., 2014, 2004). In chapter 3, we assessed the heart rate of 48 hpf zebrafish embryos exposed to either a water-only or cholesterol pretreatment solution from 6 – 24 hpf followed by exposure to a DMSO control or 20 or 25 μM phenanthrene exposure solution from 24 – 48 hpf. Phenanthrene exposure reduced heart rate, as expected, relative to the control. However, cholesterol pretreatment significantly mitigated bradycardia in phenanthrene exposed fish but did not significantly affect the DMSO control. The specificity of this effect within the phenanthrene exposed groups demonstrates that cholesterol may play a role in advancing cardiotoxicity. While here, we assessed an organ-level response, future experiments could evaluate this mitigation on the function of individual cardiomyocytes. Patch-clamp experiments conducted by Brette et al. (2017) demonstrated that phenanthrene is a driver of crude-oil disruption of ion channel function in cardiomyocytes. Attempting to rescue this disruption with cholesterol could provide insight into how cholesterol is affecting heart rate. It remains to be seen whether this

effect occurs through changes to ion channel function or through the rescue of impacts that occur earlier in development, such as through impairment of signaling cascades.

Finally, chapter 4 utilized the techniques optimized in chapter 3 to assess the effects of crude oil on cholesterol in red drum embryos. Red drum are found in bays and estuaries throughout the Gulf of Mexico and were likely exposed to weathered crude oil from the *DWH* spill, which was pushed to the Gulf shoreline with time. Bringing our knowledge gained in chapter 3, we were able to make a more robust assessment of the effects of oil on cholesterol in the ecologically relevant species red drum. Red drum embryos were exposed to crude oil until 72 hpf, a time point where the yolk is almost entirely consumed. In contrast to the reductions in survival observed in oil-exposed mahi-mahi (chapter 2), red drum survival was not significantly affected by crude oil exposure. As such, we were able to assess whether any effects to cholesterol were relevant to sublethal exposure. Additionally, measurement of ΣPAH_{50} concentrations in both chapter 2 and chapter 3 allow us to directly assess interspecies sensitivity to the PAH fraction.

Red drum displayed significant increases in pericardial edema across the range of doses tested, indicating the expected cardiotoxicity. Combining techniques used in chapters 2 and 3, we assessed both total cholesterol in larval homogenates and free cholesterol using whole-mount staining in oil-exposed red drum. In this study, we did not see any significant changes to total cholesterol in red drum homogenates (ΣPAH_{50} 3.55 - 15.45 $\mu g\ L^{-1}$). However, staining for cholesterol was significantly and visibly increased in 72 hpf red drum across all doses tested (ΣPAH_{50} 4.71 – 16.15 $\mu g\ L^{-1}$). In contrast to the

findings of the previous red drum embryo transcriptomic study (Xu et al., 2017), the expression of several key genes in the cholesterol synthesis pathway (*fdft1*, *sqle*, *hmgcr*) were not altered with crude oil exposure.

Putting the results of chapter 4 in the context of previous chapters, we find that free cholesterol is significantly altered in a Gulf relevant species with oil exposure. In chapter 3, we demonstrated that the addition of cholesterol partially mitigated PAH-induced cardiotoxicity. By contrast, in red drum, we observe the simultaneous presentation of cardiotoxicity and elevated free cholesterol levels. These findings leave us wondering how an increase, compared with a decrease, in cholesterol may impact heart function. Studies in mammalian systems have demonstrated that either an increase or decrease in cholesterol can disrupt cardiac function (Maxfield and Tabas, 2005). Thus, disruption of cholesterol homeostasis in either direction could have biological consequences in fish embryos. However, this would need to be investigated further. Additionally, the mechanism through which cholesterol is increased would need to be assessed.

In chapter 2, we observed a decrease in total cholesterol in oil-exposed mahi-mahi, whereas in red drum we observe an increase in free cholesterol and an increasing trend in total cholesterol. Besides being conducted in different species, the differences in these trends could also be driven by the fact that reduced total cholesterol in mahi-mahi was observed at a concentration of oil that caused significant lethality, whereas the concentrations tested in red drum appear to have sublethal consequences. Differences in metabolism and biological processes associated with lethality could explain the

differences in response observed here. However, a directional species-specific response remains possible.

5.2 Hypothetical adverse outcome pathway

Together, the results presented in chapters 2 - 4 focus on molecular, organ, and organismal level responses. However, to understand how a toxicant may impact a population or ecosystem, it is critical to synthesize knowledge across multiple levels of biological organization, ranging from molecular interactions to a population-level response. The adverse outcome pathway (AOP) framework is a conceptual model for visualizing connections between a direct molecular initiating event and apical endpoints. Figure 5-1 presents a potential AOP based on the disruption of cholesterol homeostasis. In this AOP, we make hypothetical links between our observations of reduced total cholesterol (mahi-mahi; chapter 2) and elevated free cholesterol (red drum; chapter 3) and downstream outcomes previously observed in crude oil or phenanthrene exposed fish.

The first potential pathway links altered cholesterol homeostasis to altered heart morphology and function. Disruption to cholesterol homeostasis, resulting in either an abnormal increase or decrease in cholesterol, has been shown in various mammalian models to impact ion channel function through direct or indirect interactions (Levitan et al., 2014, 2010). Alteration of membrane cholesterol is a potential mechanism by which crude oil could impair ion channel function in oil-exposed fish cardiomyocytes.

Cardiomyocytes isolated from several different fish species have demonstrated altered ion channel function and excitation-contraction coupling with oil exposure (Abramochkin et al., 2021; Ainerua et al., 2020; Brette et al., 2017, 2014; Heuer et al., 2019). Heuer et al. (2019) further linked disruption of EC coupling with reduced cardiomyocyte contractility in mahi-mahi, which may account for previously observed reductions in cardiac output and swim performance in oil-exposed mahi (Mager et al., 2014; Nelson et al., 2016; Stieglitz et al., 2016) and other species (Hicken et al., 2011; Incardona et al., 2015; Khursigara et al., 2017). Alternatively, structural and functional defects in the heart can be caused by reduced hedgehog signaling during development, as shown in zebrafish exposed to cholesterol-reducing drugs (Maerz et al., 2019). However, this pathway has less overlap with mechanisms proposed by previous research on oil-induced cardiotoxicity.

Beyond cardiotoxicity, alterations to cholesterol by crude oil may have consequences for nervous system development and function (Grosell and Pasparakis, 2021). In mammalian cells, both cholesterol depletion and loading have been shown to decrease neurite outgrowth (Ko et al., 2005), an essential process in nervous system development (Harrill et al., 2010). Interestingly, zebrafish with deficient neurite outgrowth displayed abnormal swimming behavior (Mullen et al., 2021). Separately, mice with a reduced capacity for cholesterol synthesis had reduced synapse formation resulting in attenuated synaptic transmission, and these outcomes were ultimately linked to impaired cognitive performance (Suzuki et al., 2013). These findings provide insight into how disruption of

cholesterol homeostasis by oil exposure could affect nervous system development and function in oil-exposed fish. For example, larval red drum exposed to crude oil displayed a reduced optomotor response (OMR), relative to controls (Magnuson et al., 2018). Complex neural networks drive OMR; thus, impaired neural development, possibly due to changes in cholesterol, could underly this effect. Additionally, larval fish exposed to oil have displayed increased risk-taking behavior, reduced prey-capture (Rowsey et al., 2019), altered habitat settlement (Johansen et al., 2017), and learning (Geier et al., 2018). Together these responses are possibly a result of impaired cognitive function.

Ultimately, population- and ecosystem health is challenging to measure and is often confounded by variables that are difficult or impossible to quantify. However, through improving our understanding of the mechanisms that underly toxicant effects, impacts on an animal's ability to feed, avoid predation, and find habitat may be attained, enhancing our predictive power and providing a foundation for assessing how oil may impact populations and community health of exposed biota.

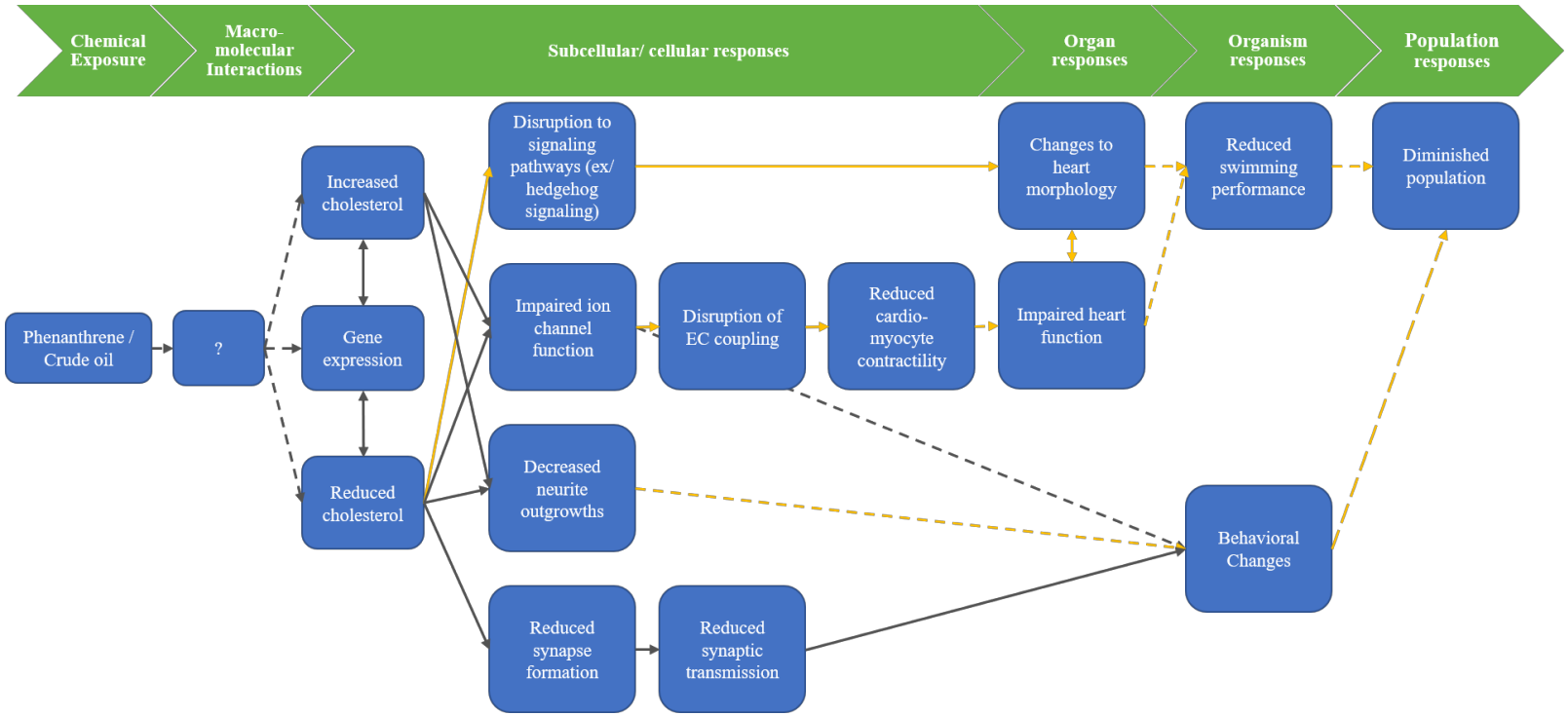

Figure 5-1 Hypothetical adverse outcome pathway for disruption of cholesterol homeostasis by crude oil or phenanthrene exposure. Yellow lines represent a linkage demonstrated in fish. Black lines represent a linkage demonstrated only in a mammalian or mammalian cell model. Dashed lines indicate limited data or a hypothetical linkage. Solid lines indicate a mechanistic or correlational linkage. Abbreviations: EC coupling, Excitation-contraction coupling.

5.3 Concluding remarks

The data and results in this dissertation describe the possible contributions of the disruption of cholesterol homeostasis on known oil-induced toxicity outcomes in fish embryos. However, given the complex nature of crude oil, there are undoubtedly multiple toxicity pathways co-occurring. Future work should follow up on the mechanisms underlying changes to cholesterol homeostasis and expand beyond cholesterol to develop our understanding of the mechanisms underlying these ubiquitous pollutants.

While the focus of this dissertation has been on understanding the consequences of oil exposure on fish, the implications of this work may extend beyond an ecological context. PAH-induced cardiotoxicity exhibits conservation across fish species (Incardona and Scholz, 2018), and depending on the mechanism of action, may be conserved more broadly across vertebrates. Knowledge of PAH-induced cardiotoxicity in fish could additionally give insight into human diseases caused by PAHs (Marris et al., 2020), and overlap between these fields of research should be explored.

To conclude, this dissertation serves to advance our understanding of crude oil and PAH-induced toxicity. When considering the ecological effects of oil pollution, overt mortality has clear ecological consequences. However, a greater mechanistic understanding of oil-induced toxicity is needed to assess the cost of sublethal exposure on exposed fish and how this ultimately impacts fishery output. Overall, our findings demonstrate that crude oil alters cholesterol in the developing marine fish we tested, and these results open avenues for future work to investigate the processes underlying cholesterol alteration.

Ultimately, through this work investigating toxicity mechanisms, we hope to advance predictions of individual species sensitivity, develop biomarkers, and improve the accuracy of ecological risk and damage assessments.

References

Abramochkin, D. V, Kompella, S.N., Shiels, H.A., 2021. Phenanthrene alters the electrical activity of atrial and ventricular myocytes of a polar fish, the Navaga cod. Aquat. Toxicol. 105823. https://doi.org/10.1016/j.aquatox.2021.105823

Ainerua, M.O., Tinwell, J., Kompella, S.N., Sørhus, E., White, K.N., van Dongen, B.E., Shiels, H.A., 2020. Understanding the cardiac toxicity of the anthropogenic pollutant phenanthrene on the freshwater indicator species, the brown trout (Salmo trutta): From whole heart to cardiomyocytes. Chemosphere 239, 124608. https://doi.org/10.1016/j.chemosphere.2019.124608

Ankley, G.T., Bennett, R.S., Erickson, R.J., Hoff, D.J., Hornung, M.W., Johnson, R.D., Mount, D.R., Nichols, J.W., Russom, C.L., Schmieder, P.K., Serrrano, J.A., Tietge, J.E., Villeneuve, D.L., 2010. Adverse outcome pathways: a conceptual framework to support ecotoxicology research and risk assessment. Environ. Toxicol. Chem. 29, 730–41. https://doi.org/10.1002/etc.34

Balijepalli, R.C., Delisle, B.P., Balijepalli, S.Y., Foell, J.D., Slind, J.K., Kamp, T.J., January, C.T., 2007. Kv11.1 (ERG1) K+ channels localize in cholesterol and sphingolipid enriched membranes and are modulated by membrane cholesterol. Channels 1, 263–272. https://doi.org/10.4161/chan.4946

Barros, S., Montes, R., Benito, J., Rodil, R., André, A., Capitão, A., Soares, J., Santos, M.M., Neuparth, T., 2018. Chronic environmentally relevant levels of simvastatin disrupt embryonic development , biochemical and molecular responses in zebra fi sh (Danio rerio). Aquat. Toxicol. 201, 47–57. https://doi.org/10.1016/j.aquatox.2018.05.014

Bayona, J.M., Domínguez, C., Albaigés, J., 2015. Analytical developments for oil spill fingerprinting. Trends Environ. Anal. Chem. https://doi.org/10.1016/j.teac.2015.01.004

Bejarano, A.C., Levine, E., Mearns, A.J., 2013. Effectiveness and potential ecological effects of offshore surface dispersant use during the Deepwater Horizon oil spill: A retrospective analysis of monitoring data. Environ. Monit. Assess. 185, 10281–10295. https://doi.org/10.1007/s10661-013-3332-y

Bers, D.M., 2002. The role of calcium in contraction and flux balance. Nature 415, 198–205. https://doi.org/10.1016/B978-0-12-378630-2.00221-8

Blassberg, R., Jacob, J., 2017. Lipid metabolism fattens up hedgehog signaling. BMC Biol. 15, 1–14. https://doi.org/10.1186/s12915-017-0442-y

Bowles, D.K., Heaps, C.L., Turk, J.R., Maddali, K.K., Price, E.M., 2004.

Hypercholesterolemia inhibits L-type calcium current in coronary macro-, not microcirculation. J. Appl. Physiol. 96, 2240–2248. https://doi.org/10.1152/japplphysiol.01229.2003

Brette, F., Machado, B., Cros, C., Incardona, J.P., Scholz, N.L., Block, B. a, 2014. Crude oil impairs cardiac excitation-contraction coupling in fish. Science (80-.). 1681, 772–776. https://doi.org/10.1126/science.1242747

Brette, F., Orchard, C., 2003. T-tubule function in mammalian cardiac myocytes. Circ. Res. 92, 1182–1192. https://doi.org/10.1161/01.RES.0000074908.17214.FD

Brette, F., Shiels, H.A., Galli, G.L.J., Cros, C., Incardona, J.P., Scholz, N.L., Block, B.A., 2017. A Novel Cardiotoxic Mechanism for a Pervasive Global Pollutant. Sci. Rep. 7, 1–9. https://doi.org/10.1038/srep41476

Brown, M.S., Goldstein, J.L., 2009. Cholesterol feedback: From Schoenheimer's bottle to Scap's MELADL. J. Lipid Res. https://doi.org/10.1194/jlr.R800054-JLR200

Burg, J.S., Espenshade, P.J., 2011. Regulation of HMG-CoA reductase in mammals and yeast. Prog. Lipid Res. 50, 403–410. https://doi.org/10.1016/j.plipres.2011.07.002

Campos, L.M., Rios, E.A., Guapyassu, L., Midlej, V., Atella, G.C., Herculano-Houzel, S., Benchimol, M., Mermelstein, C., Costa, M.L., 2016. Alterations in zebrafish development induced by simvastatin: Comprehensive morphological and physiological study, focusing on muscle. Exp. Biol. Med. 241, 1950–1960. https://doi.org/10.1177/1535370216659944

Carls, M.G., Holland, L., Larsen, M., Collier, T.K., Scholz, N.L., Incardona, J.P., 2008. Fish embryos are damaged by dissolved PAHs, not oil particles. Aquat. Toxicol. 88, 121–127. https://doi.org/10.1016/j.aquatox.2008.03.014

Carls, M.G., Meador, J.P., 2009. A Perspective on the toxicity of petrogenic pahs to developing fish embryos related to environmental chemistry. Hum. Ecol. Risk Assess. 15, 1084–1098. https://doi.org/10.1080/10807030903304708

Carls, M.G., Rice, S.D., Hose, J.E., 1999. Sensitivity of fish embryos to weathered crude oil: Part I. Low-level exposure during incubation causes malformations, genetic damage, and mortality in larval pacific herring (Clupea pallasi). Environ. Toxicol. Chem. 18, 481. https://doi.org/10.1897/1551-5028(1999)018<0481:SOFETW>2.3.CO;2

Carls, M.G., Thedinga, J.F., 2010. Exposure of pink salmon embryos to dissolved polynuclear aromatic hydrocarbons delays development, prolonging vulnerability to mechanical damage. Mar. Environ. Res. 69, 318–325. https://doi.org/10.1016/j.marenvres.2009.12.006

Chun, Y.S., Oh, H.G., Park, M.K., Cho, H., Chung, S., 2013. Cholesterol regulates HERG K+ channel activation by increasing phospholipase C β1 expression. Channels 7, 275–287. https://doi.org/10.4161/chan.25122

Cooper, M.K., Wassif, C.A., Krakowiak, P.A., Taipale, J., Gong, R., Kelley, R.I., Porter, F.D., Beachy, P.A., 2003. A defective response to Hedgehog signaling in disorders of cholesterol biosynthesis. Nat. Genet. 33, 508–513. https://doi.org/10.1038/ng1134

Crockett, E.L., 1998. Cholesterol Function in Plasma Membranes from Ectotherms: Membrane-Specific Roles in Adaptation to Temperature. Integr. Comp. Biol. 38, 291–304. https://doi.org/10.1093/icb/38.2.291

Crone, T.J., Tolstoy, M., 2010. Magnitude of the 2010 gulf of Mexico oil leak. Science (80-.). 330, 634. https://doi.org/10.1109/ICCAD.2004.1382689

Diamante, G., Menjivar-Cervantes, N., Leung, M.S., Volz, D.C., Schlenk, D., 2017a. Contribution of G protein-coupled estrogen receptor 1 (GPER) to 17β-estradiol-induced developmental toxicity in zebrafish. Aquat. Toxicol. 186, 180–187. https://doi.org/10.1016/j.aquatox.2017.02.024

Diamante, G., Xu, E.G., Chen, S., Mager, E., Grosell, M., Schlenk, D., 2017b. Differential Expression of MicroRNAs in Embryos and Larvae of Mahi-Mahi (Coryphaena hippurus) Exposed to Deepwater Horizon Oil. Environ. Sci. Technol. Lett. 4, 523–529. https://doi.org/10.1021/acs.estlett.7b00484

Ditty, J.G., Shaw, R.F., Grimes, C.B., Cope, J.S., 1994. Larval development, distribution, and abundance common dolphin, Coryphaena hippurus, and pompano dolphin, C.equiselis (family: Coryphaenidae), in the northern Gulf of Mexico. Fish. Bull. 92, 275–291.

Esbaugh, A.J., Mager, E.M., Stieglitz, J.D., Hoenig, R., Brown, T.L., French, B.L., Linbo, T.L., Lay, C., Forth, H., Scholz, N.L., Incardona, J.P., Morris, J.M., Benetti, D.D., Grosell, M., 2016. The effects of weathering and chemical dispersion on Deepwater Horizon crude oil toxicity to mahi-mahi (Coryphaena hippurus) early life stages. Sci. Total Environ. 543, 644–651. https://doi.org/10.1016/j.scitotenv.2015.11.068

Farrell, A.P., Smith, F., 2017. Cardiac Form, Function and Physiology, in: Fish Physiology. Elsevier Inc., pp. 155–264. https://doi.org/10.1016/bs.fp.2017.07.001

Fraher, D., Sanigorski, A., Mellett, N.A., Meikle, P.J., Sinclair, A.J., Gibert, Y., 2016. Zebrafish Embryonic Lipidomic Analysis Reveals that the Yolk Cell Is Metabolically Active in Processing Lipid. Cell Rep. 14, 1317–1329. https://doi.org/10.1016/j.celrep.2016.01.016

Geier, M.C., Chlebowski, A.C., Truong, L., Massey Simonich, S.L., Anderson, K.A., Tanguay, R.L., 2018. Comparative developmental toxicity of a comprehensive suite of polycyclic aromatic hydrocarbons. Arch. Toxicol. 92, 571–586. https://doi.org/10.1007/s00204-017-2068-9

Gibbs, R.H., Collette, B.B., 1959. On the Identification, Distribution, and Biology of the Dolphins, Coryphaena hippurus and C. Equiselis. Bull. Mar. Sci. Gulf Caribb. 9, 117–152.

Gimpl, G., Gehrig-Burger, K., 2007. Cholesterol reporter molecules. Biosci. Rep. https://doi.org/10.1007/s10540-007-9060-1

Glickman, N.S., Yelon, D., 2002. Cardiac development in zebrafish: Coordination of form and function. Semin. Cell Dev. Biol. https://doi.org/10.1016/S1084952102001040

Grosell, M., Pasparakis, C., 2021. Physiological Responses of Fish to Oil Spills. Ann. Rev. Mar. Sci. 13, 137–160. https://doi.org/10.1146/annurev-marine-040120-094802

Harrill, J.A., Freudenrich, T.M., Machacek, D.W., Stice, S.L., Mundy, W.R., 2010. Quantitative assessment of neurite outgrowth in human embryonic stem cell-derived hN2^{TM} cells using automated high-content image analysis. Neurotoxicology 31, 277–290. https://doi.org/10.1016/j.neuro.2010.02.003

Heintz, R.A., Rice, S.D., Wertheimer, A.C., Bradshaw, R.F., Thrower, F.P., Joyce, J.E., Short, J.W., 2000. Delayed effects on growth and marine survival of pink salmon Oncorhynchus gorbuscha after exposure to crude oil during embryonic development. Mar. Ecol. Prog. Ser. 208, 205–216. https://doi.org/10.3354/meps208205

Heuer, R.M., Galli, G.L.J., Shiels, H.A., Fieber, L.A., Cox, G.K., Mager, E.M., Stieglitz, J.D., Benetti, D.D., Grosell, M., Crossley, D.A., 2019. Impacts of Deepwater Horizon Crude Oil on Mahi-Mahi (Coryphaena hippurus) Heart Cell Function. Environ. Sci. Technol. 53, 9895–9904. https://doi.org/10.1021/acs.est.9b03798

Hicken, C.E., Linbo, T.L., Baldwin, D.H., Willis, M.L., Myers, M.S., Holland, L., Larsen, M., Stekoll, M.S., Rice, S.D., Collier, T.K., Scholz, N.L., Incardona, J.P., 2011. Sublethal exposure to crude oil during embryonic development alters cardiac morphology and reduces aerobic capacity in adult fish. Proc. Natl. Acad. Sci. 108, 7086–7090. https://doi.org/10.1073/pnas.1019031108

Horie, Y., Yamagishi, T., Takahashi, H., Shintaku, Y., Iguchi, T., Tatarazako, N., 2017. Assessment of the lethal and sublethal effects of 20 environmental chemicals in zebrafish embryos and larvae by using OECD TG 212. J. Appl. Toxicol. 37, 1245–1253. https://doi.org/10.1002/jat.3487

Horton, J.D., Goldstein, J.L., Brown, M.S., 2002. SREBPs: Activators of the complete program of cholesterol and fatty acid synthesis in the liver. J. Clin. Invest. https://doi.org/10.1172/JCI0215593

Hose, J.E., McGurk, M.D., Marty, G.D., Hinton, D.E., Brown, E.D., Baker, T.T., 1996. Sublethal effects of the Exxon Valdez oil spill on herring embryos and larvae: Morphological, cytogenetic, and histopathological assessments, 1989-1991. Can. J. Fish. Aquat. Sci. https://doi.org/10.1139/cjfas-53-10-2355

Incardona, J.P., Carls, M.G., Holland, L., Linbo, T.L., Baldwin, D.H., Myers, M.S., Peck, K.A., Tagal, M., Rice, S.D., Scholz, N.L., 2015. Very low embryonic crude oil exposures cause lasting cardiac defects in salmon and herring. Sci. Rep. 5. https://doi.org/10.1038/srep13499

Incardona, J.P., Carls, M.G., Teraoka, H., Sloan, C.A., Collier, T.K., Scholz, N.L., 2005. Aryl hydrocarbon receptor-independent toxicity of weathered crude oil during fish development. Environ. Health Perspect. 113, 1755–1762. https://doi.org/10.1289/ehp.8230

Incardona, J.P., Collier, T.K., Scholz, N.L., 2011. Oil spills and fish health: Exposing the heart of the matter. J. Expo. Sci. Environ. Epidemiol. 21, 3–4. https://doi.org/10.1038/jes.2010.51

Incardona, J.P., Collier, T.K., Scholz, N.L., 2004. Defects in cardiac function precede morphological abnormalities in fish embryos exposed to polycyclic aromatic hydrocarbons. Toxicol. Appl. Pharmacol. 196, 191–205. https://doi.org/10.1016/j.taap.2003.11.026

Incardona, J.P., Eaton, S., 2000. Cholesterol in signal transduction. Curr. Opin. Cell Biol. https://doi.org/10.1016/S0955-0674(99)00076-9

Incardona, J.P., Gardner, L.D., Linbo, T.L., Brown, T.L., Esbaugh, A.J., Mager, E.M., Stieglitz, J.D., French, B.L., Labenia, J.S., Laetz, C.A., Tagal, M., Sloan, C.A., Elizur, A., Benetti, D.D., Grosell, M., Block, B.A., Scholz, N.L., 2014. Deepwater Horizon crude oil impacts the developing hearts of large predatory pelagic fish. Proc. Natl. Acad. Sci. 111, E1510–E1518. https://doi.org/10.1073/pnas.1320950111

Incardona, J.P., Scholz, N.L., 2018. Case Study: The 2010 Deepwater Horizon Oil Spill and Its Environmental Developmental Impacts, in: Burggren, W., Dubansky, B. (Eds.), Development and Environment. Springer International Publishing, Cham, pp. 235–283. https://doi.org/10.1007/978-3-319-75935-7

Incardona, J.P., Scholz, N.L., 2017. Environmental Pollution and the Fish Heart. Fish Physiol. 36, 373–433. https://doi.org/10.1016/bs.fp.2017.09.006

Incardona, J.P., Swarts, T.L., Edmunds, R.C., Linbo, T.L., Aquilina-Beck, A., Sloan, C.A., Gardner, L.D., Block, B.A., Scholz, N.L., 2013. Exxon Valdez to Deepwater Horizon: Comparable toxicity of both crude oils to fish early life stages. Aquat. Toxicol. 142–143, 303–316. https://doi.org/10.1016/j.aquatox.2013.08.011

Ivančič, I., Degobbis, D., 1984. An Optimal Manual Procedure for Ammonia Analysis in Natural Waters by the Indophenol Blue Method. Water Resour. 18, 1143–1147. https://doi.org/http://dx.doi.org/10.1016/0043-1354(84)90230-6

Jeevaratnam, K., Chadda, K.R., Huang, C.L.H., Camm, A.J., 2018. Cardiac Potassium Channels: Physiological Insights for Targeted Therapy. J. Cardiovasc. Pharmacol. Ther. https://doi.org/10.1177/1074248417729880

Johansen, J.L., Allan, B.J.M., Rummer, J.L., Esbaugh, A.J., 2017. Oil exposure disrupts early life-history stages of coral reef fishes via behavioural impairments. Nat. Ecol. Evol. 1, 1146–1152. https://doi.org/10.1038/s41559-017-0232-5

Jones, E.R., Simning, D., Serafin, J., Sepúlveda, M.S., Griffitt, R.J., 2020. Acute exposure to oil induces age and species-specific transcriptional responses in embryo-larval estuarine fish. Environ. Pollut. 263. https://doi.org/10.1016/j.envpol.2020.114325

Jung, J.H., Hicken, C.E., Boyd, D., Anulacion, B.F., Carls, M.G., Shim, W.J., Incardona, J.P., 2013. Geologically distinct crude oils cause a common cardiotoxicity syndrome in developing zebrafish. Chemosphere 91, 1146–1155. https://doi.org/10.1016/j.chemosphere.2013.01.019

Khursigara, A.J., Perrichon, P., Martinez Bautista, N., Burggren, W.W., Esbaugh, A.J., 2017. Cardiac function and survival are affected by crude oil in larval red drum, Sciaenops ocellatus. Sci. Total Environ. 579, 797–804. https://doi.org/10.1016/j.scitotenv.2016.11.026

Kimmel, C.B., Ballard, W.W., Kimmel, S.R., Ullmann, B., Schilling, T.F., Kimmel, C.B., Ballard, W.W., Ballard, W.W., Kimmel, S.R., Kimmel, S.R., Ullmann, B., Ullmann, B., Schilling, T.F., Schilling, T.F., 1995. Stages of embryonic development of the zebrafish. Dev. Dyn. 203, 253–310. https://doi.org/10.1002/aja.1002030302

Klansek, J.J., Warner, G.J., Johnson, W.J., Glick, J.M., 1996. Compartmental isolation of cholesterol participating in the cytoplasmic cholesteryl ester cycle in Chinese hamster ovary 25-RA cells. J. Biol. Chem. 271, 4923–4929. https://doi.org/10.1074/jbc.271.9.4923

Kloeblen, S., Stieglitz, J.D., Suarez, J.A., Grosell, M., 2018. Characterizing egg quality and larval performance from captive mahi-mahi Coryphaena hippurus (Linnaeus , 1758) spawns over time 282–293. https://doi.org/10.1111/are.13459

Ko, M., Zou, K., Minagawa, H., Yu, W., Gong, J.S., Yanagisawa, K., Michikawa, M., 2005. Cholesterol-mediated neurite outgrowth is differently regulated between cortical and hippocampal neurons. J. Biol. Chem. 280, 42759–42765. https://doi.org/10.1074/jbc.M509164200

Langheinrich, U., Vacun, G., Wagner, T., 2003. Zebrafish embryos express an orthologue of HERG and are sensitive toward a range of QT-prolonging drugs inducing severe arrhythmia. Toxicol. Appl. Pharmacol. 193, 370–382. https://doi.org/10.1016/j.taap.2003.07.012

Laurel, B.J., Copeman, L.A., Iseri, P., Spencer, M.L., Hutchinson, G., Nordtug, T., Donald, C.E., Meier, S., Allan, S.E., Boyd, D.T., Ylitalo, G.M., Cameron, J.R., French, B.L., Linbo, T.L., Scholz, N.L., Incardona, J.P., 2019. Embryonic Crude Oil Exposure Impairs Growth and Lipid Allocation in a Keystone Arctic Forage Fish. iScience 19, 1101–1113. https://doi.org/10.1016/j.isci.2019.08.051

Laurent, P., Holmgren, S., Nilsson, S., 1983. Nervous and humoral control of the fish heart: Structure and function. Comp. Biochem. Physiol. -- Part A Physiol. 76, 525–542. https://doi.org/10.1016/0300-9629(83)90455-3

Law, M.R., Wald, N.J., Rudnicka, A.R., 2003. Quantifying effect of statins on low density lipoprotein cholesterol, ischaemic heart disease, and stroke: Systematic review and meta-analysis. Br. Med. J. 326, 1423–1427. https://doi.org/10.1136/bmj.326.7404.1423

Levin, P.S., Stunz, G.W., 2005. Habitat triage for exploited fishes: Can we identify essential "Essential Fish Habitat?" Estuar. Coast. Shelf Sci. 64, 70–78. https://doi.org/10.1016/j.ecss.2005.02.007

Levitan, I., Fang, Y., Resenhouse-Dantsker, A., Romanenko, V., 2010. Choleterol and Ion Channels, Journal of Chemical Information and Modeling. https://doi.org/10.1007/978-90-481-8622-8

Levitan, I., Singh, D.K., Rosenhouse-Dantsker, A., 2014. Cholesterol binding to ion channels. Front. Physiol. https://doi.org/10.3389/fphys.2014.00065

Livak, K.J., Schmittgen, T.D., 2001. Analysis of relative gene expression data using real-time quantitative PCR and the 2-ΔΔCT method. Methods 25, 402–408. https://doi.org/10.1006/meth.2001.1262

Loughery, J.R., Kidd, K.A., Mercer, A., Martyniuk, C.J., 2018. Part A: Temporal and dose-dependent transcriptional responses in the liver of fathead minnows following short term exposure to the polycyclic aromatic hydrocarbon phenanthrene. Aquat. Toxicol. 199, 90–102. https://doi.org/10.1016/j.aquatox.2018.03.027

Maerz, L.D., Burkhalter, M.D., Schilpp, C., Wittekindt, O.H., Frick, M., Philipp, M., 2019. Pharmacological cholesterol depletion disturbs ciliogenesis and ciliary function in developing zebrafish. Commun. Biol. 2, 1–13. https://doi.org/10.1038/s42003-018-0272-7

Mager, E.M., Esbaugh, A.J., Stieglitz, J.D., Hoenig, R., Bodinier, C., Incardona, J.P., Scholz, N.L., Benetti, D.D., Grosell, M., 2014. Acute embryonic or juvenile exposure to deepwater horizon crude oil impairs the swimming performance of mahi-mahi (Coryphaena hippurus). Environ. Sci. Technol. 48, 7053–7061. https://doi.org/10.1021/es501628k

Magnuson, J.T., Khursigara, A.J., Allmon, E.B., Esbaugh, A.J., Roberts, A.P., 2018. Effects of Deepwater Horizon crude oil on ocular development in two estuarine fish species, red drum (Sciaenops ocellatus) and sheepshead minnow (Cyprinodon variegatus). Ecotoxicol. Environ. Saf. 166, 186–191. https://doi.org/10.1016/j.ecoenv.2018.09.087

Marris, C., Kompella, S., Miller, M., Incardona, J., Brette, F., Hancox, J., Sørhus, E., Shiels, H., 2020. Polyaromatic hydrocarbons in pollution : a heart-breaking matter. J. Physiol. 227–247. https://doi.org/10.1113/JP278885

Marty, G.D., Short, J.W., Dambach, D.M., Willits, N.H., Heintz, R.A., Rice, S.D., Stegeman, J.J., Hinton, D.E., 1997. Ascites, premature emergence, increased gonadal cell apoptosis, and cytochrome P4501A induction in pink salmon larvae continuously exposed to oil-contaminated gravel during development. Can. J. Zool. 75, 989–1007. https://doi.org/10.1139/z97-120

Maxfield, F.R., Tabas, I., 2005. Role of cholesterol and lipid organization in disease. Nature. https://doi.org/10.1038/nature04399

McCurley, A.T., Callard, G. V., 2008. Characterization of housekeeping genes in zebrafish: Male-female differences and effects of tissue type, developmental stage and chemical treatment. BMC Mol. Biol. 9, 1–12. https://doi.org/10.1186/1471-2199-9-102

McGruer, V., Pasparakis, C., Grosell, M., Stieglitz, J.D., Benetti, D.D., Greer, J.B., Schlenk, D., 2019. Deepwater Horizon crude oil exposure alters cholesterol biosynthesis with implications for developmental cardiotoxicity in larval mahi-mahi (Coryphaena hippurus). Comp. Biochem. Physiol. Part - C Toxicol. Pharmacol. 220, 31–35. https://doi.org/10.1016/j.cbpc.2019.03.001

McGruer, V., Tanabe, P., Vliet, S.M.F., Dasgupta, S., Qian, L., Volz, D.C., Schlenk, D., 2021. Effects of phenanthrene exposure on cholesterol homeostasis and cardiotoxicity in zebrafish embryos. Environ. Toxicol. Chem. 00, 1–10. https://doi.org/10.1002/etc.5002

Meador, J.P., Nahrgang, J., 2019. Characterizing Crude Oil Toxicity to Early-Life Stage Fish Based on a Complex Mixture: Are We Making Unsupported Assumptions? Environ. Sci. Technol. 53, 11080–11092. https://doi.org/10.1021/acs.est.9b02889

Megrey, B.A., Rose, K.A., Klumb, R.A., Hay, D.E., Werner, F.E., Eslinger, D.L., Smith, S.L., 2007. A bioenergetics-based population dynamics model of Pacific herring (Clupea harengus pallasi) coupled to a lower trophic level nutrient-phytoplankton-zooplankton model: Description, calibration, and sensitivity analysis. Ecol. Modell. 202, 144–164. https://doi.org/10.1016/j.ecolmodel.2006.08.020

Michel, J., Owens, E.H., Zengel, S., Graham, A., Nixon, Z., Allard, T., Holton, W., Reimer, P.D., Lamarche, A., White, M., Rutherford, N., Childs, C., Mauseth, G., Challenger, G., Taylor, E., 2013. Extent and Degree of Shoreline Oiling: Deepwater Horizon Oil Spill, Gulf of Mexico, USA. PLoS One 8, e65087. https://doi.org/10.1371/journal.pone.0065087

Mitchell, C.A., Dasgupta, S., Zhang, S., Stapleton, H.M., Volz, D.C., 2018. Disruption of nuclear receptor signaling alters triphenyl phosphate-induced cardiotoxicity in zebrafish embryos. Toxicol. Sci. 163, 307–318. https://doi.org/10.1093/toxsci/kfy037

Morris, J.M., Gielazyn, M., Krasnec, M.O., Takeshita, R., Forth, H.P., Labenia, J.S., Linbo, T.L., French, B.L., Gill, J.A., Baldwin, D.H., Scholz, N.L., Incardona, J.P., 2018. Crude oil cardiotoxicity to red drum embryos is independent of oil dispersion energy. Chemosphere 213, 205–214. https://doi.org/10.1016/j.chemosphere.2018.09.015

Mu, X., Liu, J., Yang, K., Huang, Y., Li, X., Yang, W., Qi, S., Tu, W., Shen, G., Li, Y., 2018. 0# Diesel water-accommodated fraction induced lipid homeostasis alteration in zebrafish embryos. Environ. Pollut. 242, 952–961. https://doi.org/10.1016/j.envpol.2018.07.055

Mu, X., Wang, K., Chai, T., Zhu, L., Yang, Y., Zhang, J., Pang, S., Wang, C., Li, X., 2015. Sex specific response in cholesterol level in zebrafish (Danio rerio) after long-term exposure of difenoconazole. Environ. Pollut. 197, 278–286. https://doi.org/10.1016/j.envpol.2014.11.019

Mullen, P., Abbott, J.A., Wellman, T., Aktar, M., Fjeld, C., Demeler, B., Ebert, A.M., Francklyn, C.S., 2021. Neuropathy-associated histidyl-tRNA synthetase variants attenuate protein synthesis in vitro and disrupt axon outgrowth in developing zebrafish. FEBS J. 288, 142–159. https://doi.org/10.1111/febs.15449

National Marine Fisheries, 2018. Fisheries Economics of the US, 2016. p. 249.

Naumann, E.A., Fitzgerald, J.E., Dunn, T.W., Rihel, J., Sompolinsky, H., Engert, F.,

2016. From Whole-Brain Data to Functional Circuit Models: The Zebrafish Optomotor Response. Cell 167, 947-960.e20. https://doi.org/10.1016/j.cell.2016.10.019

Nelson, D., Heuer, R.M., Cox, G.K., Stieglitz, J.D., Hoenig, R., Mager, E.M., Benetti, D.D., Grosell, M., Crossley, D.A., 2016. Effects of crude oil on in situ cardiac function in young adult mahi–mahi (Coryphaena hippurus). Aquat. Toxicol. 180, 274–281. https://doi.org/10.1016/j.aquatox.2016.10.012

Nixon, Z., Zengel, S., Baker, M., Steinhoff, M., Fricano, G., Rouhani, S., Michel, J., 2016. Shoreline oiling from the Deepwater Horizon oil spill. Mar. Pollut. Bull. 107, 170–178. https://doi.org/10.1016/j.marpolbul.2016.04.003

NOAA, 2017. Largest Oil Spills Affecting U.S. Waters Since 1969 | response.restoration.noaa.gov [WWW Document]. URL https://response.restoration.noaa.gov/oil-and-chemical-spills/oil-spills/largest-oil-spills-affecting-us-waters-1969.html (accessed 4.28.21).

Norimatsu, Y., Hasegawa, K., Shimizu, N., Toyoshima, C., 2017. Protein-phospholipid interplay revealed with crystals of a calcium pump. Nature 545, 193–198. https://doi.org/10.1038/nature22357

Olsvik, P.A., Lie, K.K., Nordtug, T., Hansen, B.H., 2012. Is chemically dispersed oil more toxic to Atlantic cod (Gadus morhua) larvae than mechanically dispersed oil? A transcriptional evaluation. BMC Genomics 13. https://doi.org/10.1186/1471-2164-13-702

Osborne, T.F., Espenshade, P.J., 2009. Evolutionary conservation and adaptation in the mechanism that regulates SREBP action: What a long, strange tRIP it's been. Genes Dev. https://doi.org/10.1101/gad.1854309

Palko, B.J., Beardsley, G.L., Richards, W.J., 1982. Synopsis of the biological data on dolphin-fishes, *Coryphaena hippurus* Linnaeus and *Coryphaena equiselis* Linnaeus. FAO Fish. Synopsis Rep 130, 1–34.

Pasparakis, C., Mager, E.M., Stieglitz, J.D., Benetti, D., Grosell, M., 2016. Effects of Deepwater Horizon crude oil exposure, temperature and developmental stage on oxygen consumption of embryonic and larval mahi-mahi (Coryphaena hippurus). Aquat. Toxicol. 181, 113–123. https://doi.org/10.1016/j.aquatox.2016.10.022

Pasparakis, C., Sweet, L.E., Stieglitz, J.D., Benetti, D., Casente, C.T., Roberts, A.P., Grosell, M., 2017. Combined effects of oil exposure, temperature and ultraviolet radiation on buoyancy and oxygen consumption of embryonic mahi-mahi, Coryphaena hippurus. Aquat. Toxicol. 191, 113–121. https://doi.org/10.1016/j.aquatox.2017.07.021

Payne, A.H., Hales, D.B., 2004. Overview of steroidogenic enzymes in the pathway from cholesterol to active steroid hormones. Endocr. Rev. 25, 947–970. https://doi.org/10.1210/er.2003-0030

Perrichon, P., Stieglitz, J.D., Xu, E.G., Magnuson, J.T., Pasparakis, C., Mager, E.M., Wang, Y., Schlenk, D., Benetti, D.D., Roberts, A.P., Grosell, M., Burggren, W.W., 2019. Mahi-mahi (Coryphaena hippurus) life development: morphological, physiological, behavioral and molecular phenotypes. Dev. Dyn. 248, 337–350. https://doi.org/10.1002/dvdy.27

Pouvreau, S., Berthier, C., Blaineau, S., Amsellem, J., Coronado, R., Strube, C., 2004. Membrane cholesterol modulates dihydropyridine receptor function in mice fetal skeletal muscle cells. J. Physiol. https://doi.org/10.1113/jphysiol.2003.055285

Qian, L., Cui, F., Yang, Y., Liu, Y., Qi, S., Wang, C., 2018. Mechanisms of developmental toxicity in zebrafish embryos (Danio rerio) induced by boscalid. Sci. Total Environ. 634, 478–487. https://doi.org/10.1016/j.scitotenv.2018.04.012

R Core Team, 2020. R: A Language and Environment for Statistical Computing.

Reddy, C.M., Arey, J.S., Seewald, J.S., Sylva, S.P., Lemkau, K.L., Nelson, R.K., Carmichael, C.A., McIntyre, C.P., Fenwick, J., Ventura, G.T., Van Mooy, B.A.S., Camilli, R., 2012. Composition and fate of gas and oil released to the water column during the Deepwater Horizon oil spill. Proc. Natl. Acad. Sci. U. S. A. 109, 20229–20234. https://doi.org/10.1073/pnas.1101242108

Rodgers, M.L., Sherwood, T.A., Griffitt, R.J., Wetzel, D.L., 2021. Characterization of transcriptomic responses and transcriptional pathways of southern flounder (Paralichthys lethostigma) chronically exposed to Deepwater Horizon oiled sediments. Chemosphere 230, 105716. https://doi.org/10.1016/j.aquatox.2020.105716

Rooker, J.R., Kitchens, L.L., Dance, M.A., Wells, R.J.D., Falterman, B., Cornic, M., 2013. Spatial, Temporal, and Habitat-Related Variation in Abundance of Pelagic Fishes in the Gulf of Mexico: Potential Implications of the Deepwater Horizon Oil Spill. PLoS One 8, e76080. https://doi.org/10.1371/journal.pone.0076080

Rooker, J.R., Simms, J.R., David Wells, R.J., Holt, S.A., Holt, G.J., Graves, J.E., Furey, N.B., 2012. Distribution and habitat associations of billfish and swordfish larvae across mesoscale features in the gulf of Mexico. PLoS One 7. https://doi.org/10.1371/journal.pone.0034180

Rowsey, L.E., Johansen, J.L., Khursigara, A.J., Esbaugh, A.J., 2019. Oil exposure impairs predator-prey dynamics in larval red drum (Sciaenops ocellatus). Mar. Freshw. Res. 71, 99–106. https://doi.org/10.1071/MF18263

Ryerson, T.B., Camilli, R., Kessler, J.D., Kujawinski, E.B., Reddy, C.M., Valentine, D.L., Atlas, E., Blake, D.R., De Gouw, J., Meinardi, S., Parrish, D.D., Peischl, J., Seewald, J.S., Warneke, C., 2012. Chemical data quantify Deepwater Horizon hydrocarbon flow rate and environmental distribution. Proc. Natl. Acad. Sci. U. S. A. 109, 20246–20253. https://doi.org/10.1073/pnas.1110564109

Sant, K.E., Timme-Laragy, A.R., 2018. Zebrafish as a Model for Toxicological Perturbation of Yolk and Nutrition in the Early Embryo. Curr. Environ. Heal. reports 5, 125–133. https://doi.org/10.1007/s40572-018-0183-2

Schirmer, K., Fischer, B.B., Madureira, D.J., Pillai, S., 2010. Transcriptomics in ecotoxicology. Anal. Bioanal. Chem. 397, 917–923. https://doi.org/10.1007/s00216-010-3662-3

Schüttler, A., Reiche, K., Altenburger, R., Busch, W., 2017. The transcriptome of the zebrafish embryo after chemical exposure: A meta-analysis. Toxicol. Sci. 157, 291–304. https://doi.org/10.1093/toxsci/kfx045

Sharpe, L.J., Brown, A.J., 2013. Controlling cholesterol synthesis beyond 3-hydroxy-3-methylglutaryl-CoA reductase (HMGCR). J. Biol. Chem. 288, 18707–18715. https://doi.org/10.1074/jbc.R113.479808

Shiels, H.A., White, E., 2005. Temporal and spatial properties of cellular Ca2+ flux in trout ventricular myocytes. AJP Regul. Integr. Comp. Physiol. 288, R1756–R1766. https://doi.org/10.1152/ajpregu.00510.2004

Signore, I.A., Jerez, C., Figueroa, D., Suazo, J., Marcelain, K., Cerda, O., Colombo Flores, A., 2016. Inhibition of the 3-hydroxy-3-methyl-glutaryl-CoA reductase induces orofacial defects in zebrafish. Birth Defects Res. Part A - Clin. Mol. Teratol. 106, 814–830. https://doi.org/10.1002/bdra.23546

Singleman, C., Holtzman, N.G., 2012. Analysis of postembryonic heart development and maturation in the zebrafish, Danio rerio. Dev. Dyn. 241, 1993–2004. https://doi.org/10.1002/dvdy.23882

Skogdalen, J.E., Vinnem, J.E., 2012. Quantitative risk analysis of oil and gas drilling, using Deepwater Horizon as case study. Reliab. Eng. Syst. Saf. 100, 58–66. https://doi.org/10.1016/j.ress.2011.12.002

Sørensen, L., Sørhus, E., Nordtug, T., Incardona, J.P., Linbo, T.L., Giovanetti, L., Karlsen, Ø., Meier, S., 2017. Oil droplet fouling and differential toxicokinetics of polycyclic aromatic hydrocarbons in embryos of Atlantic haddock and cod. PLoS One 12, 1–26. https://doi.org/10.1371/journal.pone.0180048

Sørhus, E., Incardona, J.P., Furmanek, T., Goetz, G.W., Scholz, N.L., Meier, S.,

Edvardsen, R.B., Jentoft, S., 2017. Novel adverse outcome pathways revealed by chemical genetics in a developing marine fish. Elife 6, 1–30. https://doi.org/10.7554/eLife.20707

Stieglitz, J.D., Hoenig, R.H., Kloeblen, S., Tudela, C.E., Grosell, M., Benetti, D.D., 2017. Capture, transport, prophylaxis, acclimation, and continuous spawning of Mahi-mahi (Coryphaena hippurus) in captivity. Aquaculture 479, 1–6. https://doi.org/10.1016/j.aquaculture.2017.05.006

Stieglitz, J.D., Mager, E.M., Hoenig, R.H., Benetti, D.D., Grosell, M., 2016. Impacts of Deepwater Horizon crude oil exposure on adult mahi-mahi (Coryphaena hippurus) swim performance. Environ. Toxicol. Chem. 35, 2613–2622. https://doi.org/10.1002/etc.3436

Stoyek, M.R., Croll, R.P., Smith, F.M., 2015. Intrinsic and extrinsic innervation of the heart in zebrafish (Danio rerio). J. Comp. Neurol. 523, 1683–1700. https://doi.org/10.1002/cne.23764

Subczynski, W.K., Pasenkiewicz-Gierula, M., Widomska, J., Mainali, L., Raguz, M., 2017. High Cholesterol/Low Cholesterol: Effects in Biological Membranes: A Review. Cell Biochem. Biophys. 75, 369–385. https://doi.org/10.1007/s12013-017-0792-7

Sundby, S., Kristiansen, T., 2015. The Principles of Buoyancy in Marine Fish Eggs and Their Vertical Distributions across the World Oceans. PLoS One 10, e0138821. https://doi.org/10.1371/journal.pone.0138821

Suzuki, R., Ferris, H.A., Chee, M.J., Maratos-Flier, E., Kahn, C.R., 2013. Reduction of the Cholesterol Sensor SCAP in the Brains of Mice Causes Impaired Synaptic Transmission and Altered Cognitive Function. PLoS Biol. 11, 1001532. https://doi.org/10.1371/journal.pbio.1001532

Tabas, I., 2002. Consequences of cellular cholesterol accumulation: Basic concepts and physiological implications. J. Clin. Invest. 110, 905–911. https://doi.org/10.1172/JCI0216452

Thorpe, J.L., Doitsidou, M., Ho, S.Y., Raz, E., Farber, S.A., 2004. Germ cell migration in zebrafish is dependent on HMGCoA reductase activity and prenylation. Dev. Cell 6, 295–302. https://doi.org/10.1016/S1534-5807(04)00032-2

Tocher, D.R., Sargent, J.R., 1984. Analyses of lipids and fatty acids in ripe roes of some Northwest European marine fish. Lipids 19, 492–499. https://doi.org/10.1007/BF02534481

Trapani, L., Segatto, M., Ascenzi, P., Pallottini, V., 2011. Potential role of nonstatin

cholesterol lowering agents. IUBMB Life. https://doi.org/10.1002/iub.522

Trustees, 2016. Deepwater Horizon Oil Spill Final Programmatic Damage Assessment and Restoration Plan and Final Programmatic Environmental Impact Statement: Front Matter and Chapter 1: Introduction and Executive Summary.

Van Der Wulp, M.Y.M., Verkade, H.J., Groen, A.K., 2013. Regulation of cholesterol homeostasis. Mol. Cell. Endocrinol. 368, 1–16. https://doi.org/10.1016/j.mce.2012.06.007

Vickers, K.C., Shoucri, B.M., Levin, M.G., Wu, H., Pearson, D.S., Osei-Hwedieh, D., Collins, F.S., Remaley, A.T., Sethupathy, P., 2013. MicroRNA-27b is a regulatory hub in lipid metabolism and is altered in dyslipidemia. Hepatology 57, 533–542. https://doi.org/10.1002/hep.25846

Wang, Z., Stout, S.A., Fingas, M., 2006. Forensic Fingerprinting of Biomarkers for Oil Spill Characterization and Source Identification. Environ. Forensics 7, 105–146. https://doi.org/10.1080/15275920600667104

Wheatley, A.D., Sadhra, S., 1998. Use of fluorescence emission spectra for the routine identification of polycyclic aromatic hydrocarbons in liquid chromatography1. Wheatley, A. D. & Sadhra, S. Use of fluorescence emission spectra for the routine identification of polycyclic aromatic hydr. J. Liq. Chromatogr. Relat. Technol. 21, 2509–2521. https://doi.org/10.1080/10826079808003595

Xu, Elvis Genbo;, Khursigara, A.J.., Magnuson, J., Hazard, E.S.S., Hardiman, G., Esbaugh, A.J.., Roberts, A.P., Schlenk, D., 2017. Larval red drum (Sciaenops ocellatus) sublethal exposed to weathered Deepwater Horizon crude oil: Developmental and trscriptomic consequences. Environ. Sci. Technol. 51, 10162–10172. https://doi.org/10.1021/acs.est.7b02037

Xu, E.G., Khursigara, A.J., Li, S., Esbaugh, A.J., Dasgupta, S., Volz, D.C., Schlenk, D., 2019. MRNA-miRNA-Seq Reveals Neuro-Cardio Mechanisms of Crude Oil Toxicity in Red Drum (Sciaenops ocellatus). Environ. Sci. Technol. 53, 3296–3305. https://doi.org/10.1021/acs.est.9b00150

Xu, Elvis Genbo, Mager, E.M., Grosell, M., Hazard, E.S., Hardiman, G., Schlenk, D., 2017. Novel transcriptome assembly and comparative toxicity pathway analysis in mahi-mahi (Coryphaena hippurus) embryos and larvae exposed to Deepwater Horizon oil. Sci. Rep. 7, 44546. https://doi.org/10.1038/srep44546

Xu, E.G., Mager, E.M., Grosell, M., Pasparakis, C., Schlenker, L.S., Stieglitz, J.D., Benetti, D., Hazard, E.S., Courtney, S.M., Diamante, G., Freitas, J., Hardiman, G., Schlenk, D., 2016. Time- and Oil-Dependent Transcriptomic and Physiological Responses to Deepwater Horizon Oil in Mahi-Mahi (Coryphaena hippurus)

Embryos and Larvae. Environ. Sci. Technol. 50, 7842–7851. https://doi.org/10.1021/acs.est.6b02205

Yeagle, P.L., 1985. Cholesterol and the cell membrane. BBA - Rev. Biomembr. 822, 267–287. https://doi.org/10.1016/0304-4157(85)90011-5

Zhao, S., Fernald, R.D., 2005. Comprehensive algorithm for quantitative real-time polymerase chain reaction. J. Comput. Biol. 12, 1047–1064. https://doi.org/10.1089/cmb.2005.12.1047

Zhu, Y., Zhang, C., Chen, B., Chen, R., Guo, A., Hong, J., Song, L.S., 2016. Cholesterol is required for maintaining T-tubule integrity and intercellular connections at intercalated discs in cardiomyocytes. J. Mol. Cell. Cardiol. 97, 204–212. https://doi.org/10.1016/j.yjmcc.2016.05.013

Appendix A – Chapter 2 supplemental information

Table A-1 ∑PAH data and geometric means of initial and final concentrations for total cholesterol exposure

		SUM PAH [50]	Geometric mean			SUM PAH [50]	Geometric mean
S032_Dec 0.5%	Initial	2.468	1.31	S032_Jan 0.5%	Initial	3.413	1.69
	96-hour	0.693			96-hour	0.837	
S032_Dec 1%	Initial	4.770	3.04	S032_Jan 1%	Initial	3.717	2.62
	96-hour	1.936			96-hour	1.849	
S032_Dec 2%	Initial	10.870	8.30	S032_Jan 2%	Initial	8.307	5.99
	96-hour	6.330			96-hour	4.323	

Table A-2 Water quality parameters (mean ± SEM).

Treatment	Water temp. (C)	pH	Dissolved oxygen (mg/L)	Salinity (ppt)
S032_Dec Control	26.40±0.06	8.09±0.002	6.26±0.02	33.48±0.1
S032_Dec 0.5%	26.41±0.06	8.09±0.002	6.25±0.02	33.68±0.1
S032_Dec 1%	26.40±0.05	8.09±0.002	6.25±0.02	33.44±0.1
S032_Dec 2%	26.38±0.05	8.09±0.003	6.19±0.03	33.68±0.1
S032_Jan Control	24.47±0.03	8.09±0.005	6.90±0.03	36.95±0.09
S032_Jan 0.5%	24.39±0.03	8.10±0.005	6.80±0.03	37.05±0.12
S032_Jan 1%	24.43±0.03	8.10±0.004	6.80±0.04	36.98±0.11
S032_Jan 2%	24.39±0.03	8.10±0.004	6.78±0.03	37.1±0.12

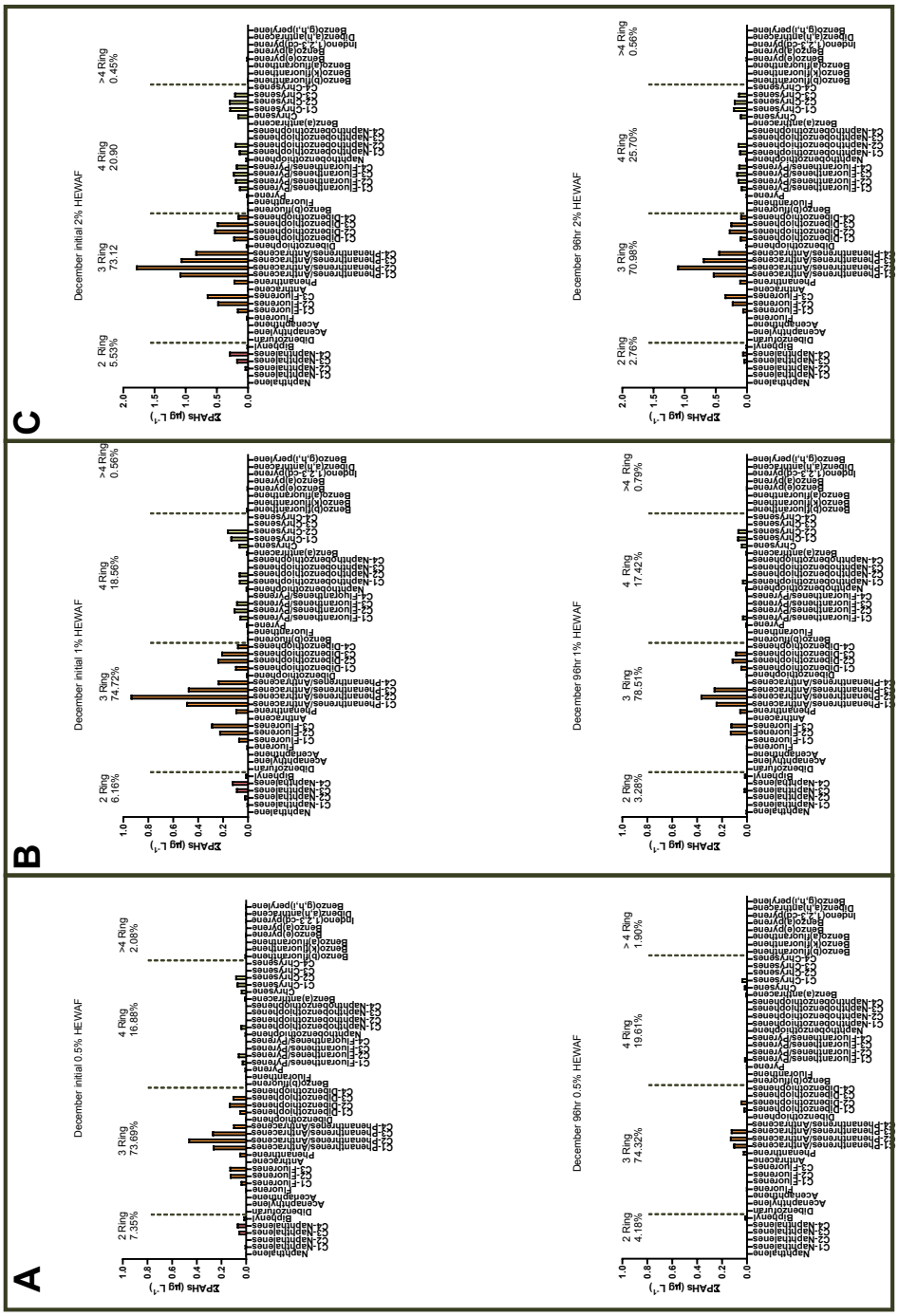

Figure A-1 Percent composition of initial (top) and final 96 hour (bottom) ∑PAH concentrations (µg L-1) of 50 PAH analytes, grouped by number of rings and determined by gas chromatography-mass spectrometry (GC-MS) for (A) 0.5% HEWAF, (B) 1% HEWAF, and (C) 2% HEWAF exposures conducted in December 2017 and held at 26ºC.

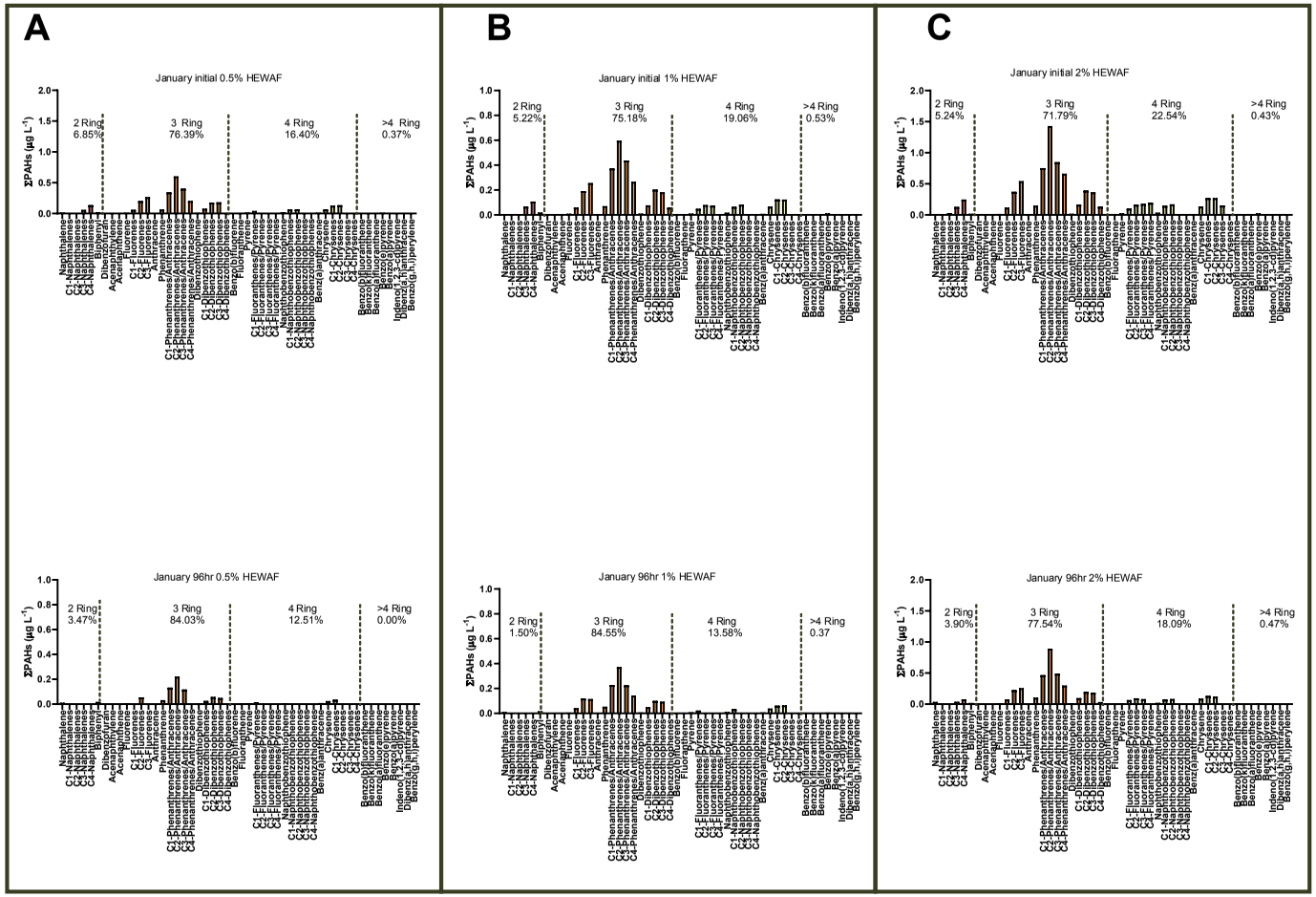

Figure A-2 Percent composition of initial (top) and final 96 hour (bottom) ∑PAH concentrations (µg L^{-1}) of 50 PAH analytes, grouped by number of rings and determined by gas chromatography-mass spectrometry (GC-MS) for (A) 0.5% HEWAF, (B) 1% HEWAF, and (C) 2% HEWAF exposures conducted in January, 2018 and held at 24-25ºC.

Appendix B – Chapter 3 supplemental information

Table B-1 Zebrafish primer sequences

Gene name	Primer sequence
hmgcra forward	5’ TCGTGGAGTGCCTGGTGATTGGT 3’
hmgcra reverse	5' TGGGTCTGCCTTCTCTGCTCTCTC 3'
hmgcrb forward	5’ CTGCCGTTCTTCCTGCTGCTGATT 3’
hmgcrb reverse	5’ GCCGACACCAATGACCAGACACTC 3’
fdft1 forward	5' AGAGGAGGCGTGGAGTCAGTATGC 3'
fdft1 reverse	5’ CATCCGTGACCAGCAGATTCAGACAG 3’
ef-α forward	5’ CTTCTCAGGCTGACTGTGC 3’
ef-α reverse	5' CCGCTAGCATTACCCTCC 3'

Table B-2 Measured phenanthrene concentrations ± SD in exposures solutions containing embryos (n= 3 per treatment, ND = not detected).

Nominal concentration (µg/L)	**Measured initial concentration (µg/L)**	**Percent initial concentration of expected nominal concentration (%)**	**Measured final (48 hpf) concentration (µg/L)**	**Measured final (72 hpf) concentration (µg/L)**	**Percent reduction (final concentration from measured initial concentration)**
0	ND	-	-	ND	-
2139 (12 µM)	1414 ± 14.5	66.1	-	185.2 ± 22.5	86.90
2673 (15 µM)	1502 ± 33.8	56.2	-	196.9 ± 12.6	86.89
3565 (20 µM)	-	-	360.8 ± 8.55	-	
4456 (25 µM)	-	-	432.8 ± 3.36	-	

Table B-3 Measured phenanthrene concentrations ± SD in exposures solutions without embryos (n= 3 per treatment, ND = not detected).

Nominal concentration (µg/L)	Measured initial concentration (µg/L)	Percent initial concentration of expected nominal concentration (%)	Measured final (72 hpf) concentration (µg/L)	Percent reduction (final concentration from measured initial concentration)
0	ND	-	ND	-
2139 (12 µM)	1949 ± 61.8	91.11	427.1 ± 12.1	78.08
2673 (15 µM)	2761 ± 80.1	103.3	723.6 ± 16.5	73.79

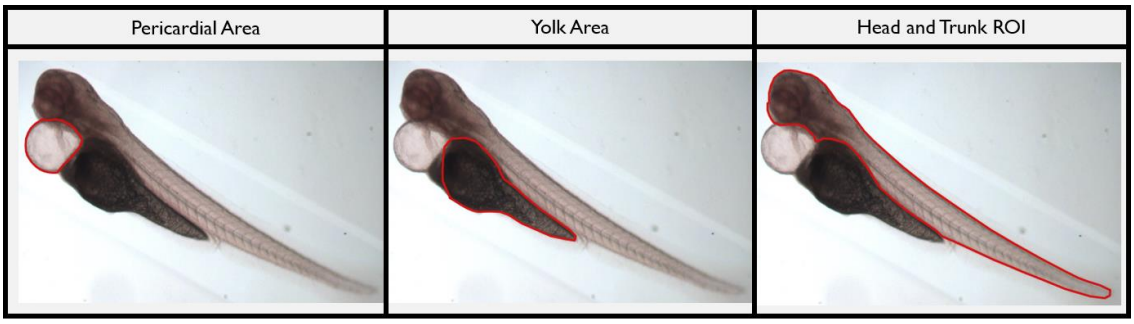

Figure B-1 Representative outlines for measuring pericardial area and yolk area. Outline of head and trunk demonstrates the region of interest (ROI) for quantifying mean fluorescence in filipin stained embryos.

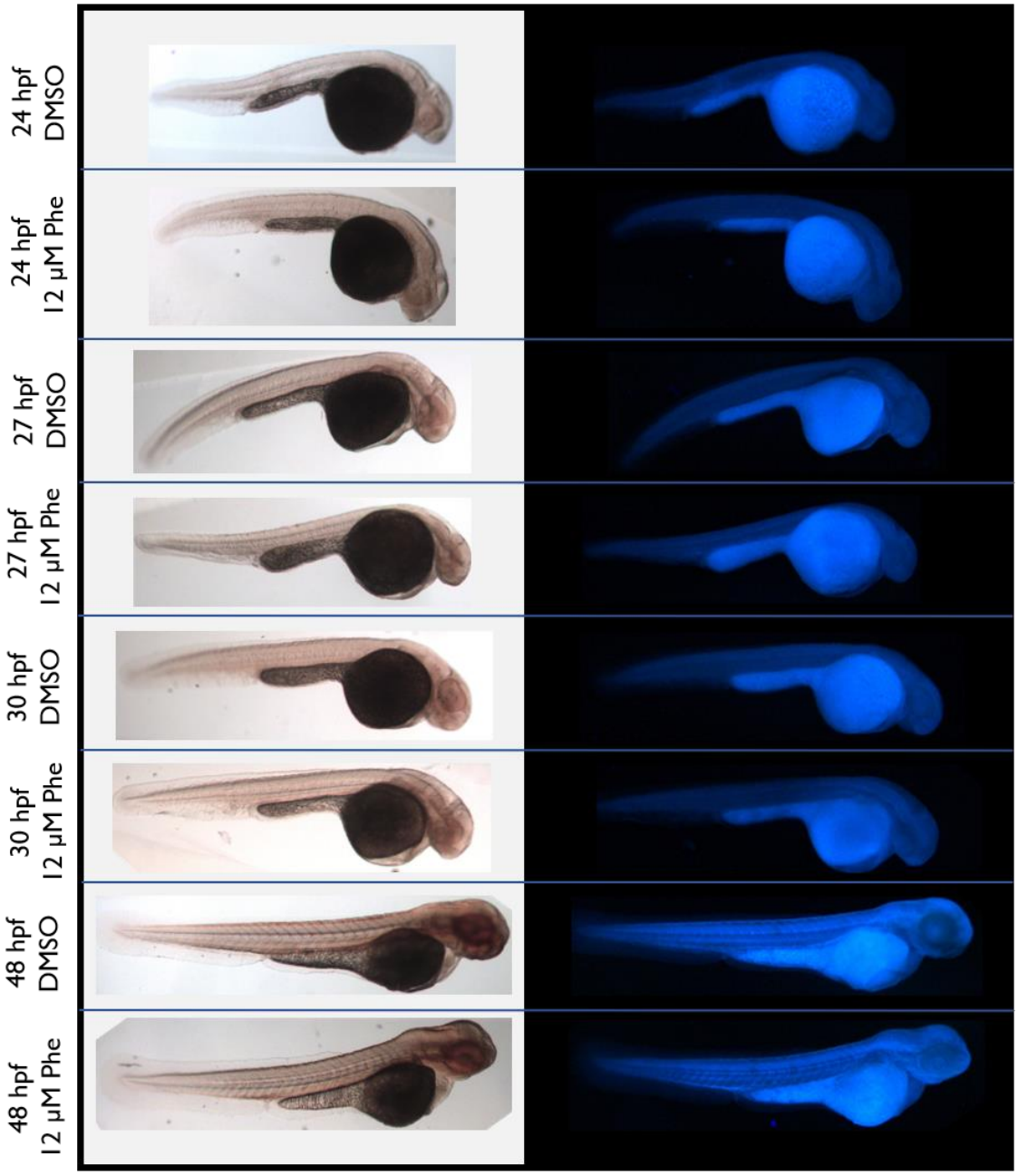

Figure B-2 Images from whole-mount staining with filipin for cholesterol. Images taken under transmitted light are presented in the left column. Images taken under UV fluorescence are presented in the right column. Embryos were exposed to either a 0.08% DMSO control (DMSO) or 12 µM Phenanthrene (Phe) and fixed for staining at 24 hpf, 27 hpf, 30 hpf, and 48 hpf. Images of embryos taken at the same stage are comparable to each other.

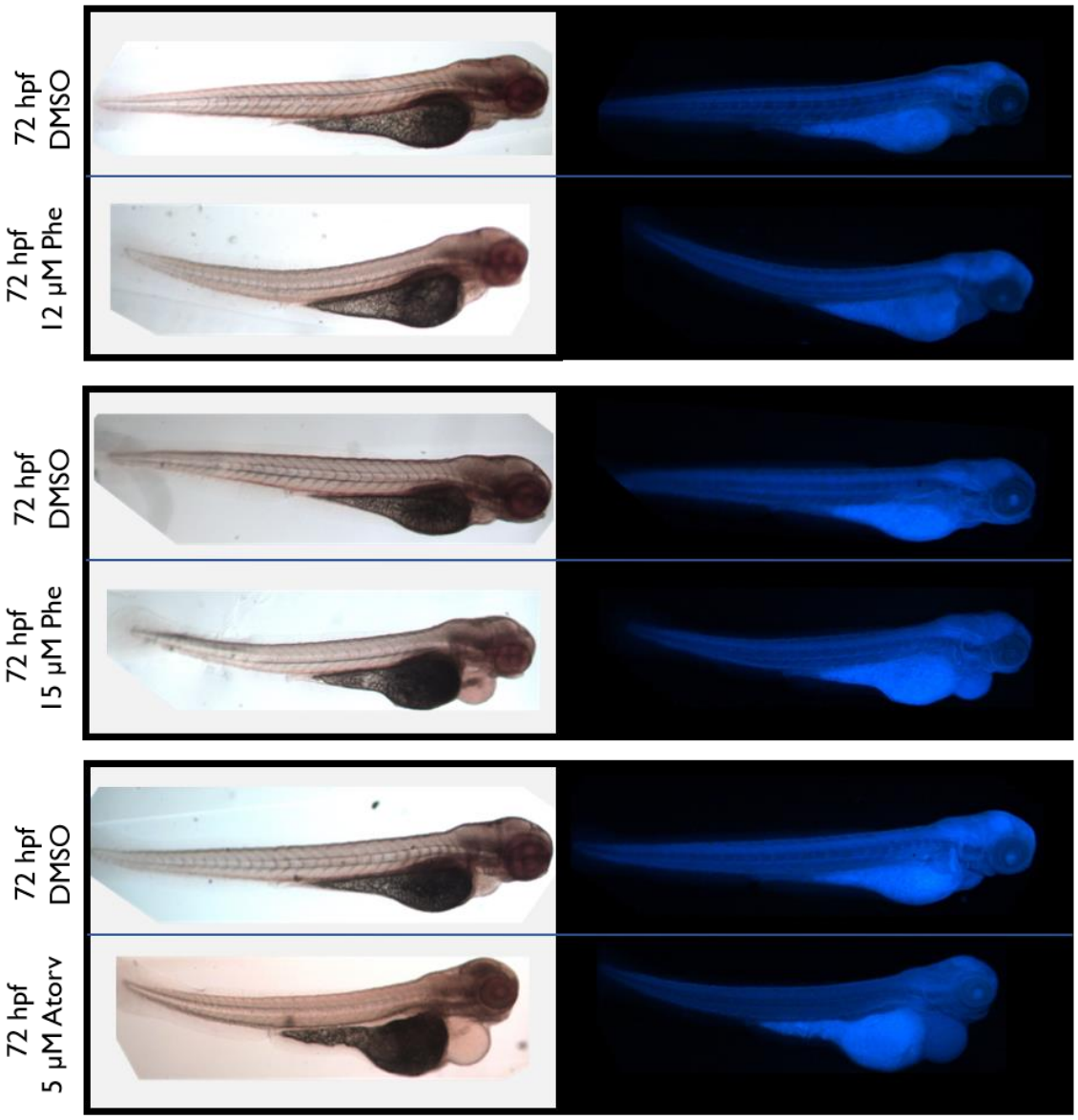

Figure B-3 Images from whole-mount staining with filipin for cholesterol. Images taken under transmitted light are presented in the left column. Images taken under UV fluorescence are presented in the right column. Embryos were exposed to either a 0.08% DMSO control (DMSO), 12 µM Phenanthrene (Phe), 15 µM Phe, or 5 µM Atorvastatin (Atorv) and fixed for staining at 72 hpf. Each set of two images (DMSO control embryo and the respective exposed embryo) are comparable to each other.

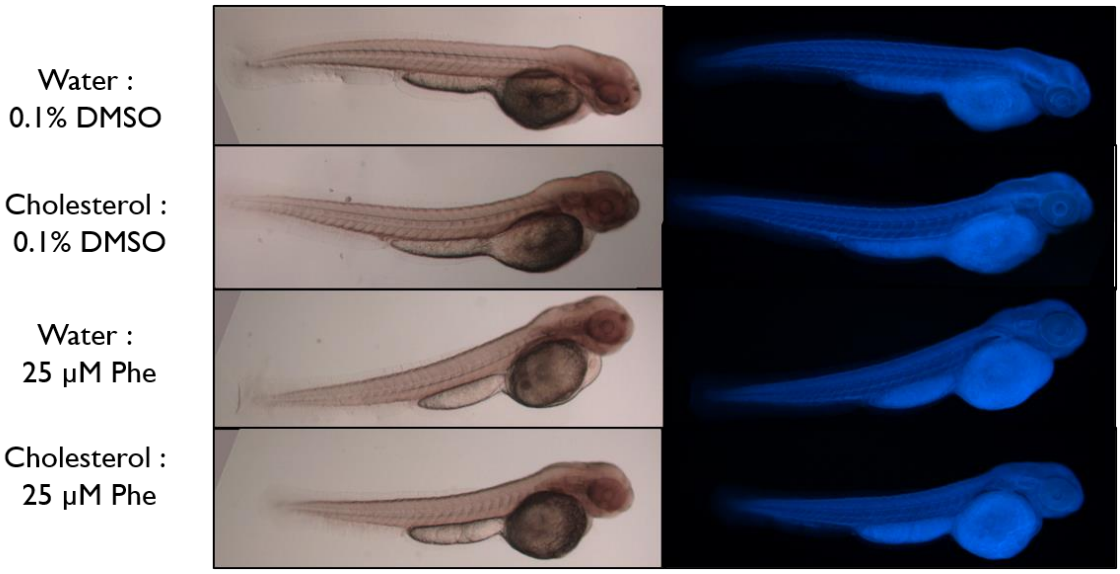

Figure B-4 Images of 48 hpf zebrafish embryos stained with filipin for cholesterol. Images taken under transmitted light are presented in the left column. Images taken under UV fluorescence are presented in the right column. Embryos were pretreated with either a water control or a 10 µM water-soluble cholesterol solution from 6 hpf to 24 hpf followed by treatment from 24 – 48 hpf with 0.1% DMSO vehicle control or 25 µM Phe exposure solution.

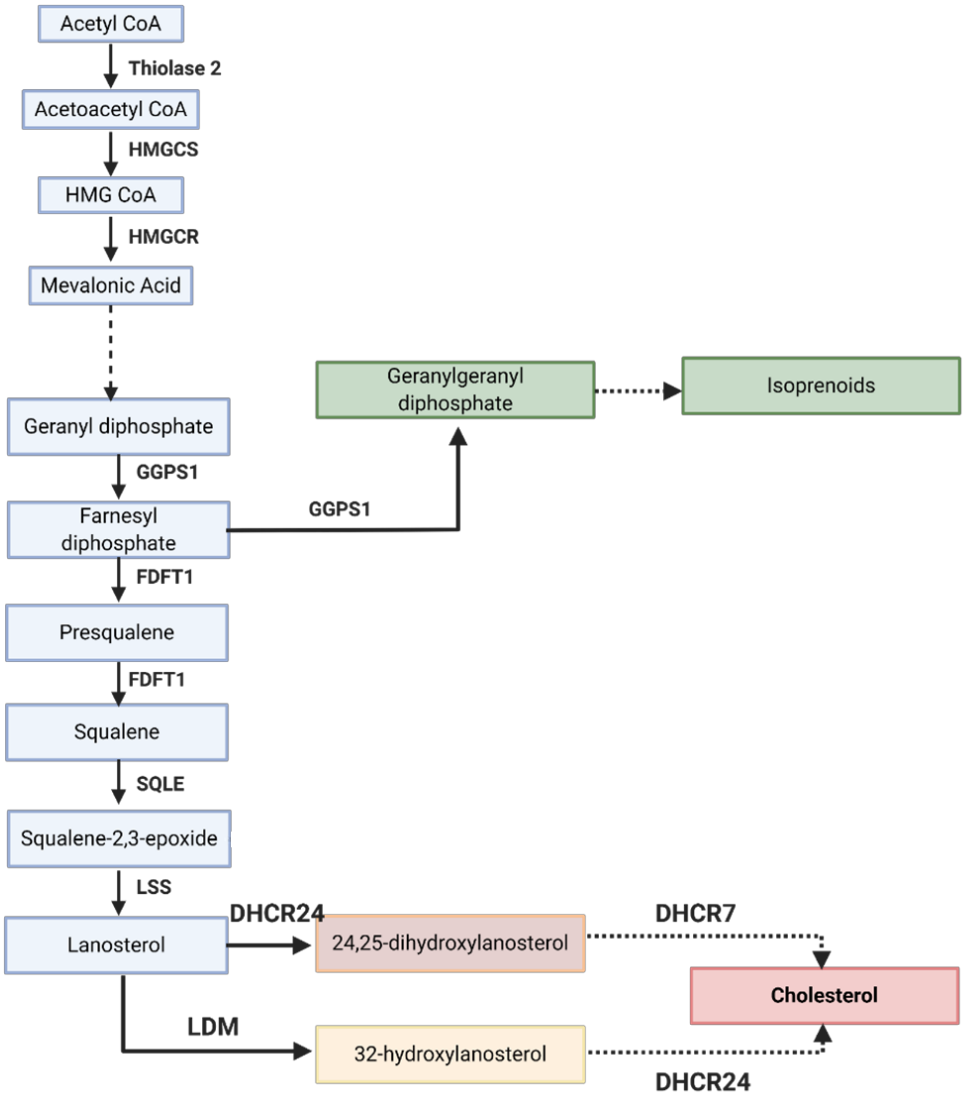

Figure B-5 Cholesterol biosynthesis pathway (adapted from Sharpe and Brown 2013). HMGCS, 3-hydroxy-3-methylglutaryl-CoA synthase; HMGCR, 3-hydroxy-3-methylglutaryl-CoA reductase; GGPS1, geranylgeranyl diphosphate synthase 1; FDFT1, farnesly-diphosphate farnesyltransferase 1; SQLE, squalene epoxidase; LSS, lanosterol synthase; DHCR24, 24-dehydrocholesterol reductase; LDM, lanosterol 14-demethylase; DHCR7, 7-dehydrocholesterol reductase.

Appendix C – Chapter 4 supplemental information

Table C-1 Red drum primer sequences

Gene name	Primer sequence	Amplicon length (base-pairs)
hmgcr forward	5’ TGGGAACCATGTCAGGTGTG 3’	141
hmgcr reverse	5’ CCTGACTCTCACGGGACAAC 3’	
fdft1 forward	5' GGCCTGTTCCTCCAGAAGAC 3'	146
fdft1 reverse	5' AGAGCCGACTCAAGCTTCTC 3'	
sqle forward	5' CGGCGTGGATTTGCTTGATG 3'	150
sqle reverse	5' TCATCATGGGCCTGAGGAGA 3'	
ef-α forward	5' GGTTACGCTCCCGTGCTG 3'	240
ef-α reverse	5' GACAGCCACAGTCTGCCTCA 3'	

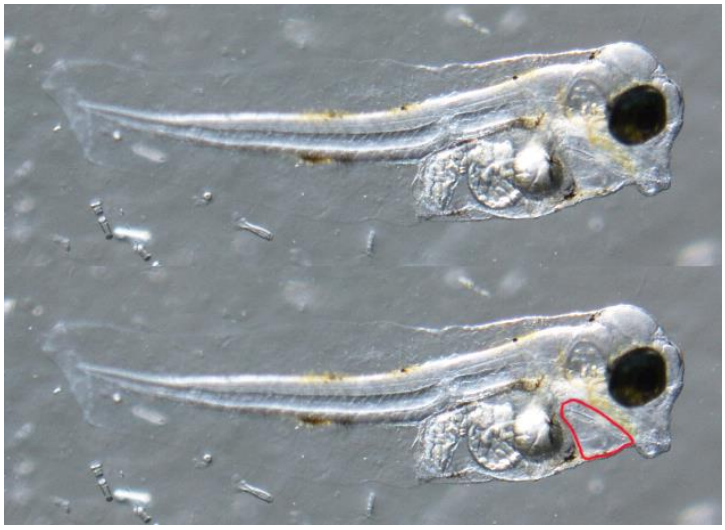

Figure C-1 Representative outlines (red) for measuring pericardial area.

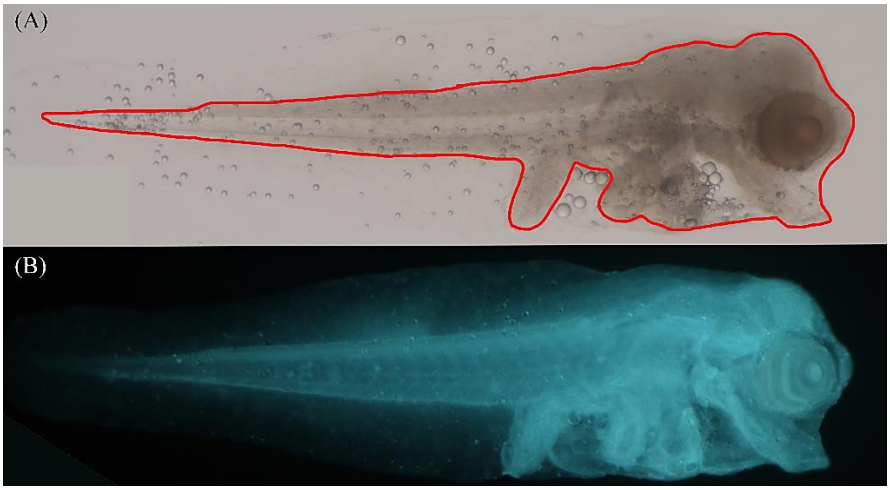

Figure C-2 – Representative outline (red) of the larval body region of interest (ROI) for quantifying mean fluorescence in filipin stained embryos. Image A was taken under transmitted light and used to outline the ROI. The outline was then overlayed on image B, taken under UV light, to quantify mean fluorescence in the ROI.

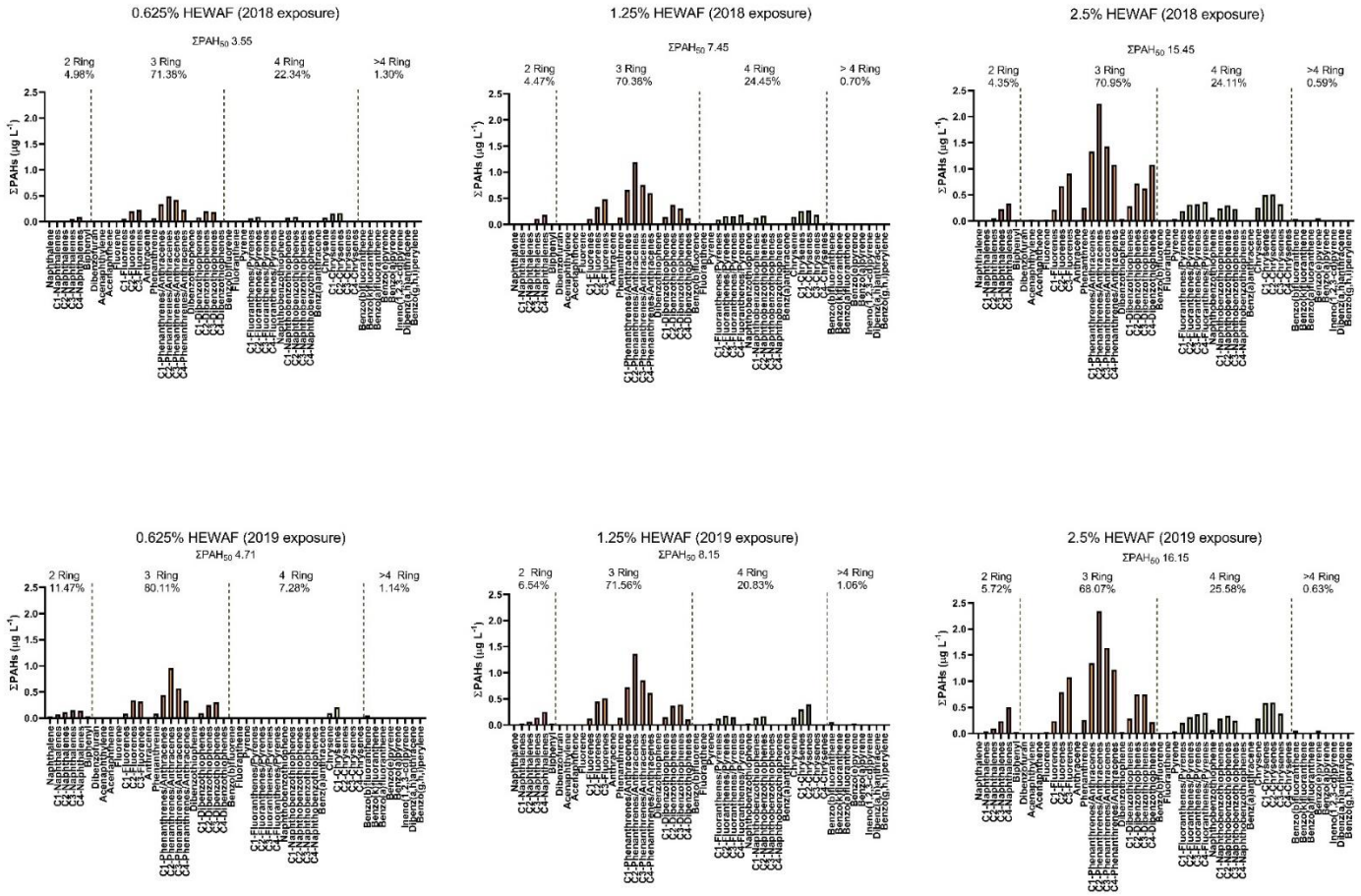

Figure C-3 Percent composition of initial ΣPAH concentrations of 50 PAH analytes, grouped by the number of rings – exposures conducted 2018 and 2019.

Table C-2 Water temperature, pH, dissolved oxygen (D.O), and salinity for each test. All parameters were measured every 24 hrs.

Date	Test	Mean ΣPAH (µg L^{-1})	Period	Water temp. (C)	pH (S.U.)	D.O. (mg L^{-1})	Salinity (ppt)
Nov 2018	OFS 72 hpf	0	0h	25	7.8	5.95	35
Nov 2018	OFS 72 hpf	3.55	0h	26	7.85	6.12	35
Nov 2018	OFS 72 hpf	7.45	0h	25	7.84	6.37	35
Nov 2018	OFS 72 hpf	15.45	0h	25	7.91	6.12	35
Nov 2018	OFS 72 hpf	0	24h	26	8.14	6.68	35
Nov 2018	OFS 72 hpf	3.55	24h	27	8.06	6.33	35
Nov 2018	OFS 72 hpf	7.45	24h	26	8.06	6.67	35
Nov 2018	OFS 72 hpf	15.45	24h	27	8.07	6.54	35
Nov 2018	OFS 72 hpf	0	48h	27	8.2	6.5	35
Nov 2018	OFS 72 hpf	3.55	48h	27	8.15	6.48	35
Nov 2018	OFS 72 hpf	7.45	48h	27	8.16	6.68	35
Nov 2018	OFS 72 hpf	15.45	48h	27	8.17	6.54	35
Nov 2018	OFS 72 hpf	0	72h	26	8.09	6.52	35
Nov 2018	OFS 72 hpf	3.55	72h	27	8.07	6.44	35
Nov 2018	OFS 72 hpf	7.45	72h	26	8.07	6.7	34
Nov 2018	OFS 72 hpf	15.45	72h	27	8.11	6.45	35

Jul 2019	OFS 72 hpf	0	0h	27	8.08	5.87	35
Jul 2019	OFS 72 hpf	4.71	0h	27	8.1	5.88	35
Jul 2019	OFS 72 hpf	8.15	0h	26	8.09	5.89	35
Jul 2019	OFS 72 hpf	16.15	0h	26	8.1	5.92	35
Jul 2019	OFS 72 hpf	0	24h	26	8.13	5.75	35
Jul 2019	OFS 72 hpf	4.71	24h	26	8.12	5.62	35
Jul 2019	OFS 72 hpf	8.15	24h	26	8.11	5.66	35
Jul 2019	OFS 72 hpf	16.15	24h	26	8.12	5.7	35
Jul 2019	OFS 72 hpf	0	48h	26	8.08	5.84	35
Jul 2019	OFS 72 hpf	4.71	48h	26	8.09	5.89	35
Jul 2019	OFS 72 hpf	8.15	48h	26	8.1	5.82	35
Jul 2019	OFS 72 hpf	16.15	48h	26	8.11	5.89	36
Jul 2019	OFS 72 hpf	0	72h	26	8.08	5.87	35
Jul 2019	OFS 72 hpf	4.71	72h	26	8.1	6.01	35
Jul 2019	OFS 72 hpf	8.15	72h	26	8.11	5.94	35
Jul 2019	OFS 72 hpf	16.15	72h	26	8.12	5.88	36